COMPARISON OF DIFFERENT SPATIAL RESOLUTION IMAGES FOR POLYGON-BASED CROP MAPPING

A THESIS SUBMITTED TO
THE GRADUATE SCHOOL OF NATURAL AND APPLIED SCIENCES
OF
MIDDLE EAST TECHNICAL UNIVERSITY

BY

ASLI ÖZDARICI

IN PARTIAL FULFILLMENT OF THE REQUIREMENTS
FOR
THE DEGREE OF MASTER OF SCIENCE
IN
GEODETIC AND GEOGRAPHIC INFORMATION TECHNOLOGIES

SEPTEMBER 2005

Approval of the Graduate School of Natural and Applied Sciences

_____

Prof. Dr. Canan ÖZGEN
Director

I certify that this thesis satisfies all the requirements as a thesis for the degree of Master of Science.

_____

Assist. Prof. Dr. Zuhal AKYÜREK
Head of Department

This is to certify that we have read this thesis and that in our opinion it is fully adequate, in scope and quality, as a thesis for the degree of Master of Science.

_____

Assoc. Prof. Dr. Mustafa TÜRKER
Supervisor

Examining Committee Members

Prof. Dr. Vedat TOPRAK (METU, GEOE) _____

Assoc. Prof. Dr. Mustafa TÜRKER (HU, JDZ) _____

Prof. Dr. Volkan ATALAY (METU, CENG) _____

Assist. Prof. Dr. M. Onur KARSLIOĞLU (METU, CE) _____

Assist. Prof. Dr. Ayşegül AKSOY (METU, ENVE) _____

I hereby declare that all information in this document has been obtained and presented in accordance with academic rules and ethical conduct. I also declare that, as required by these rules and conduct, I have fully cited and referenced all material and results that are not original to this work.

Name, Last name: Aslı ÖZDARICI

Signature :

ABSTRACT

COMPARISON OF DIFFERENT SPATIAL RESOLUTION IMAGES FOR POLYGON-BASED CROP MAPPING

ÖZDARICI, Aslı

M. Sc., Department of Geodetic and Geographic Information Technologies
Supervisor: Assoc. Prof. Dr. Mustafa TÜRKER

September 2005, 133 pages

Polygon-based classification applied on the unitemporal SPOT4 XS, SPOT5 XS, IKONOS XS, QuickBird XS and QuickBird Pansharpaned (PS) images is described. The study site is an agricultural area located near Karacabey, Turkey covering an area of about 95 km^2. The objective was to assess the effect of the spatial resolution on the polygon-based classification of agricultural crops. Both the post-polygon and pre-polygon classifications were carried out. In the post-polygon classification, first, the images were classified on per-pixel basis through a Maximum Likelihood classifier. Then, for each field, the model class was computed and the field was assigned the label of the model class. In the pre-polygon classification, first, the mean values were calculated for each field. Then, the per-pixel Maximum Likelihood Classification was carried out using the mean bands.

The post-polygon classification of the SPOT4 XS and SPOT5 XS images produced an overall accuracy of 76,1% and 81,4%, respectively. The IKONOS XS image provided the highest overall accuracy of 88,6%. On the other hand, the QuickBird XS and QuickBird PS images provided the overall

accuracies of 83,7% and 85,8%, respectively. For the pre-polygon classification, the overall accuracies of the SPOT4 XS and SPOT5 XS images were computed to be 65,2% and 69,8%, respectively. Similar to the post-polygon classification, the IKONOS image provided the highest overall accuracy of 81,8% while the SPOT5 XS image revealed slightly better results than the SPOT4 XS image. The overall accuracies of the QuickBird XS and PS images were found to be 78,6% and 82,1%, respectively.

Keywords: Polygon-based image classification, High resolution, Agricultural crop mapping, SPOT4, SPOT5, IKONOS, QuickBird, Turkey.

ÖZ

PARSEL TABANLI ÜRÜN HARİTALAMASI İÇİN FARKLI ÇÖZÜNÜRLÜKLÜ UYDU GÖRÜNTÜLERİNİN KARŞILAŞTIRILMASI

ÖZDARICI, Aslı

Yüksek Lisans, Jeodezi ve Cografi Bilgi Teknolojileri E.A.B.D.
Tez Yöneticisi: Assoc. Prof. Dr. Mustafa TÜRKER

Eylül 2005, 133 sayfa

Çalışmada, tek tarihte çekilen renkli SPOT 4, SPOT 5, IKONOS, QuickBird uydu görüntüleri ile birleştirilmiş QuickBird görüntüsünün parsel tabanlı sınıflandırma yöntemi ile sınıflandırılması anlatılmaktadır. Çalışma alanı, Türkiye'nin Karacabey yakınlarında yer alan yaklaşık 95 km^2 lik bir tarım alanını kapsamaktadır. Amaç, çözünürlüğün tarımsal ürünler için parsel tabanlı sınıflandırma yöntemi üzerindeki etkisini değerlendirmektir. Yöntem, poligon öncesi ve poligon sonrası olmak üzere parsel tabanlı iki sınıflandırma yöntemine dayanmaktadır. Poligon sonrası sınıflandırmada ilk olarak, En Büyük Olasılık sınıflandırma yöntemi yoluyla görüntüler piksel tabanlı sınıflandırıldı. Ardından, her parselin içine düşen farklı özellikteki pikseller sayılarak sayıca en fazla olan piksel parsele atandı. Poligon öncesi sınıflandırmada, ilk olarak, her parsel için ortalama değerler hesaplandı. Sonra, ortalama değerleri içeren yeni bandlar kullanılarak En Büyük Olasılık sınıflandırması yapıldı.

SPOT4 ve SPOT 5 renkli görüntülerinin poligon sonrası sınıflandırma sonuçları 76,1% ve 81,4% doğruluk üretti. IKONOS renkli görüntüsü 88,6% doğruluk payı ile en yüksek sonucu sağladı. Diğer taraftan,

QuickBird renkli ve birleştirilmiş QuickBird görüntüsü 83,7% and 85,8% doğruluk sağladı. Poligon öncesi sınıflandırma için SPOT 4 ve SPOT 5 görüntülerinin sonuçları 65,2% ve 69,8% olarak hesaplandı. Polygon sonrası sınıflandırmada olduğu gibi, SPOT5 görüntüsü SPOT 4 ten daha iyi sonuçlar sergilerken IKONOS görüntüsü 81,8% ile en yüksek doğruluğu sağladı. QuickBird renkli ve QuickBird birleştirilmiş görüntülerinin doğruluk oranları 78,6% ve 82,1% olarak bulundu.

Anahtar Kelimeler: Parsel tabanlı görüntü sınıflandırma, Yüksek çözünürlük, Tarımsal ürün hatitalama, SPOT4, SPOT5, IKONOS, QuickBird, Türkiye.

To My Family

ACKNOWLEDGEMENT

I would like to express my deepest graditude to my supervisor, Assoc. Prof. Dr. Mustafa TÜRKER for his guidance, valuable advice, encouragement and insight throughout the preparation of this thesis.

I would like to thank Prof. Dr. Vedat TOPRAK, Prof. Dr. Volkan ATALAY, Assist. Prof. Dr. Mahmut O. KARSLIOĞLU and Assist. Prof. Dr. Ayşegül AKSOY for their valuable comments, suggestions and evaluations.

I would like to express my sincere thanks to Ali Özgün OK, Dilek KOÇ, Emre Hamit KÖK, Emre SÜMER and Reşat GEÇEN for their suggestions, assistance and encouragements.

Thanks to my friends, especially Onur SEZER and Nesrin ÇAPRAK, for their motivation and encouragment.

I want to express my gratitude to my friends in GGIT department.

Finally, I would like to thank my father Akil, my mother Fatma and my sisters Öznur and Gül for their motivations, encouragment and patience during my thesis.

TABLE OF CONTENTS

LIST OF TABLES

LIST OF FIGURES

CHAPTER 1

INTRODUCTION

1.1 The Objectives

Remote Sensing (RS) is an effective technology to acquire information about geographic objects. The high spatial resolution satellite images are getting widely used. The images collected by the SPOT 5, IKONOS and QuickBird satellites have become available to extract information about the Earth surface features because detailed spatial information has become a necessity for many applications. Of the many applications, the agricultural activities require a quantitative processing of remote sensing data with high accuracy and reliability. The remotely sensed images are widely used for land cover mapping, environmental modelling and monitoring, yield estimation of agricultural crop production and updating the geographical databases. The result of yield estimation provides the farmers and goverments with significant information for marketing and trading decisions (Lobell and Asner, 2003).

The generation of thematic maps from remotely sensed data is also quite frequently used. The thematic maps are used to extract information from Earth surface for mainly land cover information and to analyse all management applications including crop and irrigation management. Image classification is a commonly used automated operation to extract thematic information from remotely sensed images. Through image classification, all pixels in an image are automatically categorized into land cover classes.

Image classification can be performed using two methods: (i) per-pixel (pixel-based), and (ii) per-field (polygon-based) classification. Per-pixel classification is a conventional way of classification. In per-pixel classification, the pixels are categorized separately into one of the pre-determined classes according to their spectral characteristics. However, in the case of agricultural applications pixel-based classification techniques may cause problems due, for example, to the variations in soil moisture conditions, nutrient limitations or pests and diseases. The other problem may be caused by the mixed pixels that are located at the boundary of two or more land cover types (De Wit and Clevers, 2004). Therefore, when the classification is performed, these factors may lead to assign a combination of the reflectance from two or more land cover types. And, this adversely affect the spectral information of each pixel and as a results in misclassification (Smith and Fuller, 2001).

The basic idea behind a polygon-based classification is that the satellite image is divided into homogenous objects using the knowledge of agricultural field boundaries. With regard to crop classification, this means that the location and the extent of each field is known. During classification, each pixel is assigned to a final class of the entire object according to statistical properties, instead of determining the class label for each pixel separately. Therefore, polygon-based methods eliminate the effect of the spectral variability within the fields and the mixed pixels falling on field boundaries (De Wit and Clevers, 2004). As a result, for the agricultural applications, polygon-based classification techniques produce more reliable results than the per-pixel classification techniques by overcoming the problems of the misclassification.

Polygon-based image classification can be carried out at two moments in the classification procedure: (i) pre-polygon classification, and (ii) post-polygon classification. In pre-polygon classification, the statistical measures such as,

the mean, median and mode values, are calculated per polygon and the pixel values in each polygon are replaced with the computed statistical value. In the post-polygon classification, first, a per-pixel classification is carried out. Then, for each polygon, the frequency of the classified pixels are computed and the polygon is assgned the label of the model class.

Polygon-based image classification is widely used for agricultural areas. By using this method, crop discrimination is mostly achieved using the sequences of images acquired throughout the year along with the knowledge of the growing season for each crop. However, the frequent cloud cover may not permit image avaibility for many agricultural regions. Therefore, creating a need for spectral discrimination within a single multispectral image can be a good approach to overcome this limitation (Lobell and Asner, 2003).

The objective of this study is to compare the classification accuracies of different spatial resolution images on an agricultural land using the polygon-based image classification techniques. For this purpose, both pre- and post-polygon classification techniques were applied on each image. To apply the concept and to evaluate the results, Karacabey (Bursa), Turkey was selected as the study area. The satellite images used to apply the polygon-based classification include SPOT4 XS (20m), SPOT5 XS (10m), IKONOS XS (4m), Quickbird XS (2,44m) and Quickbird Pansharpaned (0,60m). First, each image was geometrically corrected and, the existing vector database was updated using the Quickbird Pansharpaned image. To apply the pre-polygon classification operation, raster and vector data sets were integrated and the mean values were calculated for each agriculture field. Then, the Maximum Likelihood Classification (MLC) was applied on each image. For the post-polygon image classification, first, the MLC was carried out. Then, for each field, the frequency of the classified pixels were computed and the field was assigned the label of the model class. Next, 3*3, 5*5 and 7*7 kernel size low-pass filters were applied on the original bands of each image and

the same classification procedure was repeated using the filtered images. A database was utilized to invoke the queries effectively for assessing the results. Finally, the classified outputs of the images were compared using the reference data. The classification accuracies were computed for finding which spatial resolution and which polygon-based technique provides the most reliable crop map.

1.2 Thesis organization

This thesis consists of five chapters. Chapter 2 provides a literature survey of the image classification on agricultural areas.

The post-polygon image classification is explained in Chapter 3. This chapter also contains the study area, data and the pre-processing stages. In addition, the accuracy assessment and the results of the classifications are also given in this chapter.

In Chapter 4, the information about the pre-polygon classification is described and the results are provided.

Finally, the conclusions and the recommendations for future studies are presented in Chapter 5.

1.3 The Software Used

In order to perform the pre-processing operations that include the digitization, data mosaicing, data fusion, and geometric correction and to perform classification operations, PCI Geomatica v.9.1.5 software was used. The accuracy assessment of the classified outputs was carried out using MS Excel. This program was also used for generating the concidence spectral plots and graphics.

CHAPTER 2

BACKROUND STUDY

In this chapter, the pixel-based and polygon-based image classifications are summarized and the advantages of polygon-based classification are given. A comparison of different spatial resolution images are described and the previous studies about these issues are referenced.

2.1 Polygon-based Image Classification

Conventional image classification algorithms operate on a pixel at a time, in isolation from other pertinent information. The accuracy of per-pixel classification depends largely on the type of the area, type of the image, land cover type, and the image acquisition date. The classification results are affected by the spectral overlaps of land cover classes and the mixed pixels that are present at the boundaries of two or more classes and their spectral reflectance is the mixture of different spectral characteristics of the land cover classes. The features in remotely sensed images contain not only local tone and color, but also contain size, shape, texture, pattern and context. However, these image interpretation elements are not involved in conventional per-pixel image classification. Thus, the conventional per-pixel image classification techniques often fail in discriminating the spectral response patterns and therefore, do not give satisfactory results. The solution could be to perform the classification operation in a polygon-specific manner.

Recently, polygon-based image classification has received considerable attention, especially for agricultural applications. It is known that more

accurate results from the satellite images can be achieved using the spatial context and the land cover data can be acquired for the user defined objects. In polygon-based image classification, the polygon geometry defines the spatial relationships between the pixels falling within the polygon, and the decision by the analysis is taken, for each polygon, based on the coherant processing of the pixels falling within. In addition, the problem of mixed pixels along the boundaries can be eliminated by excluding the boundary pixels in the analysis of the polygon. Therefore, polygon-based image classification generates less noisy and more reliable results.

Polygon-based classification is a kind of post-classification technique. These techniques consist of numerous rule-based re-labelling of image classification results. Janssen et. al (1990) used digital topographic map data to improve the classification accuracy. They treated the map polygons as the objects and defined an object being an area in which only one land cover type was expected. First, a conventional per-pixel image classification was performed by means of a maximum likelihood classifier (MLC) with equal probabilities for each class. Then, a label was determined, for each polygon, based on the majority class. This was followed by assigning the label to the polygon and also to all the pixels that are within the polygon. Accuracy improvement of 12% and 20% over a per-pixel MLC were reported for two agricultural test regions.

Pedley and Curran (1991) compared per-pixel and per-field classifications using SPOT HRV imagery. Their study area covers 10km by 10km with well-drained and virtually flat area. They applied a per-pixel supervised MLC and a per-field classification, however they could not acquire high classification accuracy from these classifications. Therefore, they tried to refine the results by using prior a probabilities and by applying low-pass filters and image texture. At the end of these processes they had nine classification results, a

basic and four refined versions of the per-pixel classification and three refined versions of the per-field classification for 12 classes. They acquired the highest accuracy from the per-field classification as 62.1% using the prior probabilities and image texture.

In a study conducted by Janssen and Molenaar (1995), first, the edges of the subdivisions separating different crop types were extracted within the existing fields by means of complex edge detection routine, and combined with the existing field boundaries to construct the sub-polygons. Then, the field boundaries were overlaid on the satellite imagery and the classification was performed using a conventional supervised per-pixel classifier in a similar way as described in Janssen et al. (1990). Finally, a label was assigned to each polygon, according to the most frequently occurring class, assuming that a sub-polygon contains a unique land cover.

Congalton et al. (1998) proposed a methodology to develop a water model from remotely sensed data by producing an agricultural crop map and other vegetation on the Lower Colorado River Basin. For this purpose, they used a Landsat Thematic Mapper data taken four times per year and integrated them with GIS and detailed ground information to produce accurate map and monitor agricultural crops and other land cover. By this way, they generated a water model. The initial results were not high. Therefore, they increased the accuracy to 93% by using an automated extraction process and data exploration techniques .

Aplin *et al.* (1999) developed a set of classification techniques to detect land cover on a per-parcel basis from high resolution imagery. Of the techniques they developed, the per-field texture filtered classification was reported to provide the best results.

Two field-based image analysis schemes were developed by Turker and Derenyi (2000) for monitoring the changes in land cover conditions within existing land use boundaries stored in a GIS. In the first scheme, a modified parallelepiped image classification was performed, one theme at a time. The results were then assessed on field basis to separate those fields which deviate from the apriori expectations. In the second scheme, only image statistics were generated field-by-field to identify those fields where significant changes occurred.

Aplin and Atkinson (2001) developed a method for classifying land cover at the sub-pixel scale based on pixel segmentation for subsequent per-field classification.

A parcel-based land cover map was generated for Jersey by Smith and Fuller (2001). Their approach used vector land parcel boundaries to subdivide images, aggregated the raster data within the land parcel and classified on a per-parcel basis. The accuracy of the per-parcel approach was increased by using the knowledge-based corrections and they produced a GIS database was produced having an accuracy between 85% and 95% to be used by the other analyses.

Dean and Smith (2003) compared the per-parcel classification approach with a conventional per-pixel classification by examining the maximum likelihood class probabilities. To eliminate the mixed boundary pixels, the per-parcel approach was applied on the core area. They showed that the boundary pixels were more variable than the core pixels. Because of this reason the classification accuracy was improved by the removal of the boundary pixels. To achieve this, first, the mean spectral response was calculated and then, the mean spectral response of the core pixels was extracted through per-parcel classification of the means. In this way, within parcel variation was

removed and classification accuracy was improved according to the per-pixels classification allocation. At the end of the study, they demonstrated that a per-parcel classification provides better result than the per-pixel classification when land cover is homogenous. On the other hand they suggested that the per-pixel classification may be appropriate if land cover has a heterogenous structure. Therefore, if a land cover has both homogenous and heterogenous parcel structures, a hybrid classifier can be more powerful solution.

De Wit and Clevers (2004) developed a methodology by integrating multi-temporal and multi-sensor satellite imagery for producing a crop map of the Netherlands. First, using a Geographical Information System (GIS) they created a crop field database and determined the crop types. At the end of the study they achieved 90% overall accuracy. They concluded that per-field classification was a more effective way to produce crop maps than per-pixel classification. They stated that dynamic crop boundaries can be determined easily by applying the segmentation techniques.

Lloyd *et al.* (2004) classified the land cover of a Mediterranean region using an artificial neural network on per-field basis. In addition to spectral information, geostatistical and texture measures extracted from the co-occurrence matrix were utilized.

Aplin and Atkinson (2004) developed a technique for predicting the missing field boundaries to increase the accuracy of per-field classification. The technique is based on the comparison of the within-field modal land cover proportion and local variance, which provides an indication of the missing boundaries.

In a recent study, Turker and Arikan (In Press), used sequential masking classification of multi-temporal Landsat7 ETM+ images for field-based crop mapping in Karacabey, Turkey. First, the classification of each of the multi-date images was carried out on a standard per pixel basis. Then, the individual class accuracies were examined on each classified data and those classes whose accuracy exceeds a preset threshold were determined. After that, a sequential masking classification procedure was performed using the multi-date images, excluding after each classification the class properly classified. The final classified data were analysed on a field basis to assign each field a class label. It was stated that the proposed sequential masking classification procedure improved the overall accuracy by more than 10%.

2.2 Comparison of Different Spatial Resolution Satellite Images

The resolution of satellite images provides a capability of a Remote Sensing system to resolving adjacent objects. The spatial resolution is defined as the minimum distance between two objects that a sensor can record distinctly (Gao 1999).

Cushine (1987) assessed the effect of spatial resolution on the degree of internal variability within land-cover classes to examine the classification accuracy affected by this within class variance. He used three different spatial resolution images. After classifying the images he found that the classification accuracies within homogenous classes were found to be high at all spatial resolutions. He also improved the classification accuracy by using various spatial filters. He showed that the spatial filters increased the classification accuracy depending on the spatial resolution of the data, the land-cover type being classified and the type of the spatial filter used.

Baker et. al (1991) compared two methods for evaluating the classification accuracy. SPOT HRV imagery was used to produce a map of semi-natural and agricultural land cover type. To evaluate the methodology, two test areas were utilized. The first technique was to use digital terrain information. The aim of this technique was to decrease the effects of topography on spectral information. The second method was to perform a classification of land-cover types using the training data. Low classification results were obtained at the end of the study. They stated that despite the high spectral characteristics of SPOT HRV imagery, classification alone is not capable of discriminating the semi natural land-cover types.

Aplin et al. (1997) present a review about fine spatial resolution satellite sensors within the next decade. They provided the details of various commercial and governmental satellites, such as spatial and spectral characteristics, instruments, satellite orbit and data collection etc.

Green et. al (1998), used different approaches to classify mangrove habitat that are visual interpretation, NDVI image, unsupervised and supervised classifications, band ratios, PCA image and some other methods. Lansat TM, SPOT XS and CASI data were used to classify the mangrove types. At the end of the study, SPOT XS data did not provide satisfactory results to discriminate mangrove and non-mangrove vegetation. On the other hand, CASI data was more accurate than Landsat TM data for all methods. In this study, for mapping the mangroves, an appropriate image processing method was identified.

Gao (1999) aimed to map into lush and stunded mangrove categories in the New Zealand. To do this, SPOT HRV and Landsat TM images at 10m, 20m and 30m resolutions were used. MLC method was used to classify the mangrove categories. Landsat TM was found to be more accurate for lush

mangroves (95%) and for stunded mangroves (87,5%), while the SPOT XS image provided the accuracies of 77,5% and 67,5%, respectively. When the 10m PAN was included in the classification, the accuracies increased to 80%. It was observed that high spectral resolution is more important than the fine spatial resolution for mapping the mangroves.

Langley et. al (2001) compared single date and multitemporal image classification techniques on major vegetation types of the Jornada Experimental Range, New Mexico, USA using Landsat Thematic TM satellite data. It was observed that single date image classification was more accurate than multitemporal images. The advantages of using single date images were less expenditure of time and costs related to data acquisition and preprocessing. Although the multitemporal images improved the classification accuracies for some landscapes, single-date images provide accurate results for vegetation covers in semi-arid regions.

Chen and Stow (2002) compared three training strategies for a supervised MLC. The strategies were applied on five different spatial resolution images. Each image had three multispectral bands. Semi variograms were produced to measure the autocorrelation levels of the selected training sites. The performance of different training technique was evaluated. At the end of the study, they found that, especially for fine resolution images, selection of training strategies was very important for image classification.

Mumby and Edwards (2002) evaluated whether the high spatial resolution of IKONOS multispectral image gives more accurate results than other satellite sensors for supervised classification and mapping coral reef habitat. They compared the accuracy of thematic maps and costs of the IKONOS data with Landsat MSS, Landsat TM, SPOT HRV, SPOT Panchromatic and CASI image. According to analysis, IKONOS data was found to be more accurate

than the other satellites. Although the the best results (75%) were obtained from the IKONOS data, Landsat TM was found to be the most cost-effective to identify the mangrove habitat.

Wang et al. (2004) compared the classification accuracies of IKONOS and QuickBird images. Two images were taken from the same land cover containing mangrove species under the equivalent conditions. They used three test areas to compare the accuracies. The first comparison was applied band by band by examining their spectral statistics. The second method was to apply the MLC technique on each image. Finally, they used textural information together with object-based classification. The results showed that the classification accuracy did not increase when using only the panchromatic channels for each image. On the other hand, when the multispectral bands were examined, IKONOS showed better accuracy than the QuickBird image. The final results showed that object-based classification provides more accurate results for IKONOS (pachromatic band) imagery than the Quickbird image.

CHAPTER 3

POST - POLYGON CLASSIFICATION

3.1 Study Area

The selected study area is located in Marmara region, near Karacabey, Bursa (Figure 3.1) located in Northwest of Turkey. The area is situated between the latitudes 4 444 750.00 N to 4 453 500.00 N and longtitudes 610 750.00 E to 599 850.00 E. The study area is called 'Karacabey Plain', as it is one of the most valuable agricultural regions of Turkey. The area covers an agricultural land of approximately 95 km^2. It contains nine villages: Hotanlı, Küçükkaraağaç, Yolağazı, Sultaniye, Eskisarıbey, Ortasarıbey, Yenisarıbey, Akhisar, and İsmetpaşa.

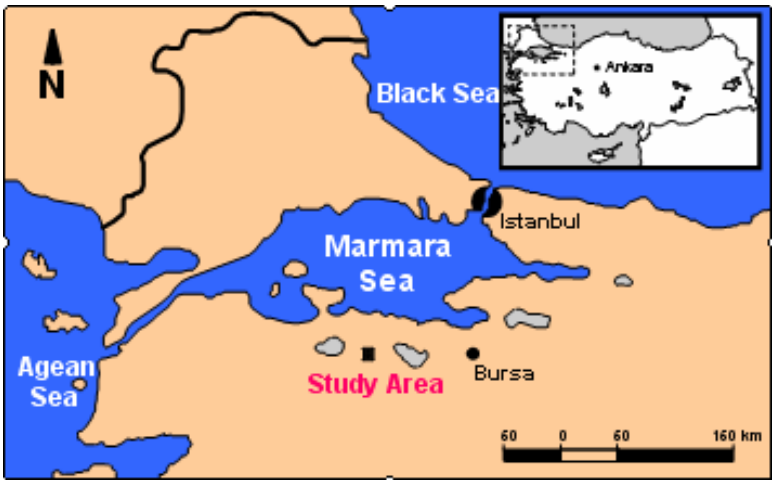

Figure 3.1 The Study Area

The area is characterized by rich, loamy soils, which combined with good weather conditions. This permits to create a prime agricultural land in Karacabey. The area contains numerous crop types and have multiple

growing seasons. The major crops cultivated in the region include tomato, pepper, wheat, corn, sugar beet, rice, and watermelon. The crops pea and onion are of secondary importance in the region. In addition to these crops, a number of pasture, clover and orchyard fields also exist.

3.2 Data Description

In the study area, there are a total of 3401 agricultural fields. The field boundaries of these fields were digitized for a previous graduate study conducted in the department of Geodetic and Geographic Information Technologies at METU (Arikan, 2002). Most of the fields have a rectangular shape.

Five different satellite images that include IKONOS XS (15 July 2004), SPOT4 XS (23 July 2004), SPOT5 XS (22 July 2004), and QuickBird Bundle (13 August 2004) were acquired for this study. Each scene was collected at good wheather conditions, cloud free and of good quality. Therefore, there was no effect for limiting the usefulness of the images. The acquisation dates of the images were kept as close as possible to each other. However, this was very difficult due to different sensor types and the wheather conditions. While the SPOT images were recorded in 8 bits, the IKONOS and Quickbird images were taken as 11 bits. All the images were geocoded to Universal Transverse Mercator (UTM) coordinate system. For SPOT and QuickBird images, level 2A was used as the preprocessing level while the level of IKONOS image was standard geometrically corrected. At these processing levels, the radiometric correction is made to compansate the distortions due to differences in the viewing conditions. The geometric correction is also applied on the images in a standard cartographic projection (UTM WGS 84 by default) without

using the ground control points (Url 1). The technical characteristics of each image are given in Table 3.1

Table 3.1 The technical characteristics of the images used in the study area

	SPOT	IKONOS	QUICKBIRD
Processing Level	Level 2A	Standard Geometrically Corrected	Level 2A
Image Type	Multispectral	Multispectral	Bundle
Datum	WGS84	WGS84	WGS84
Map Projection	Universal Transverse Mercator	Universal Transverse Mercator	Universal Transverse Mercator
Zone Number	35	35	35

SPOT (Systeme Pourl'observation de la Terre), program was arranged as a commertially oriented program by the French Centre National d'Etudes Spatiales (CNES). There are five satellites in the program. These are SPOT 1-2-3, SPOT4 and SPOT 5. In this study, the multispectral images collected by the SPOT 4 and SPOT 5 satellites were used. The multispectral image of SPOT4 satellite has 20 m resolution and contains four bands that are green (G), red (R), near-infrared (NIR), and short wave near-infrared (SWIR). When compared with SPOT 1, 2, and 3, SPOT 4 contains an additional 20 m resolution band in the mid-infrared portion of the spectrum (Table 3.2). This band is capable of monitoring vegetation and mineral discrimination. For the SPOT 4 image, the image size covering the area was 556 pixels by 461 lines.

Table 3.2 The spectral bands of SPOT4 XS image

Spectral band	Wavelength Range (μm)	Spatial Resolution (m)
Band1 (G)	0.50-0.59	20
Band 2 (R)	0.61-0.68	20
Band 3 (NIR)	0.79-0.89	20
Band 4 (SWIR)	1.58-1.75	20

SPOT 5 was launched in May 4, 2002. It is the fifth satellite of the SPOT series and presents a significant number of new and improved features over the previous sensors. Its higher ground resolution is 5m in panchromatic mode. In multispectral mode, it has 10m resolution in the visible and NIR ranges (Table 3.3). The SWIR band in the intermediate infrared is maintained at a resolution of 20 m due to limitations forced by the geometry of the CCD sensors used in this band. The ground width of each instrument is 60 km. The altitude of the satellite at the equator is 822 km and its orbital cycle is 26 days (Url 2). The size of the utilized image area is 1120 pixels by 929 lines for this image.

Table 3.3 The spectral bands of SPOT5 XS image

Spectral band	Wavelength Range (μm)	Spatial Resolution (m)
Band1 (G)	0.50-0.59	10
Band 2 (R)	0.61-0.68	10
Band 3 (NIR)	0.79-0.89	10
Band 4 (SWIR)	1.58-1.75	20

IKONOS satellite is capable of simultaneously collecting 1 m panchromatic and 4 m multispectral images. It was launched in 1999 by Space Imaging. It's spatial resolution provides a significant improvement over previously available satellite images. The satellite orbit has the characteristic of sun-synchronous with 681 km height. It permits global coverage, 3 day access time, and near-nadir viewing angles. It has four multispectral sensors and the radiometric resolution of the sensors is 11 bit on each band. The panchromatic sensor has the range of spectral sensitivity between 450 and 900 nm, while the ranges for the blue, green, red and NIR spectral bands are 445-516 nm, 506-595 nm, 632-698nm, and 757-853 nm, respectively (Table 3.4). The utilized image area contains 2771 pixels and 2324 lines.

Table 3.4 The spectral bands of IKONOS XS image

Spectral band	Wavelength Range (μm)	Spatial Resolution (m)
Band 1 (B)	0.45-0.52	4
Band 2 (G)	0.51-0.60	4
Band 3 (R)	0.63-0.70	4
Band 4 (NIR)	0.76-0.85	4

The last images used in the study were collected by the QuickBird satellite. The Quickbird satellite was launched in 2001 by DigitalGlobe. It is the highest resolution commercial satellite and provides the largest swath width and largest on-board storage of any available satellites. It has 450 km orbital altitude with 16,5 km swath width at nadir and has about 272 km^2 (16,5 km by 16,5 km) at nadir. The spectral and spatial characteristics of the QuickBird satellite are given in Table 3.5 (ASPRS, 2005). While the spectral range of the panchromatic sensor is 450-900 nm, the ranges of blue, green, red and NIR bands are 450-520 nm, 520-600 nm, 630-690 nm, and 760-900 nm, respectively (Table 3.5). In this study, the QuickBird bundle standard product was used. Bundle product means that the panchromatic and multispectral images are commerced together. The size of the utilized image area is 19026 pixels by 15948 lines for the panchromatic image. The number of pixels and lines drop to 4666 and 3873 for the multispectral data.

Table 3.5 The spectral bands of QUICKBIRD Bundle image

Spectral band	Wavelength Range (μm)	Spatial Resolution (m)
Panchromatic	0.45-0.90	0.61
Band 1 (B)	0.45-0.52	2.44
Band 2 (G)	0.52-0.60	2.44
Band 3 (R)	0.63-0.69	2.44
Band 4 (NIR)	0.76-0.90	2.44

3.3 The Methodology

The methodology includes three main steps: (i) pre-processing, (ii) post-polygon classification, and (iii) accuracy assessment. In the pre-processing step, first, the subfield boundaries were digitized and the database was prepared for the vector data. Next, data mosaicing, data fusion, and geometric correction procedures were carried out on the images. After that,
the post-polygon image classification was performed as follows: First, the per-pixel maximum likelihood classfication was carried out using;

(i) the unfiltered common bands (Bands G, R and NIR),
(ii) the filtered (Median 3*3, 5*5 and 7*7) common bands, and
(iii) the all bands of each image.

Then, within each parcel the frequency of the classified pixels was computed and the majority class was assigned to the parcel being considered. Next, the accuracy assessment was carried out. For assesing the results, one third of the reference data collected from the study area during site visit were used. After performing the classification process on each image, the results were assessed by comparing them with the reference data stored in the database.

3.4 Preprocessing

The preprocessing operations were carried out for both the raster and vector data. The preprocessing steps include (i) data mosaicking, (ii) data fusion, (iii) digitizition of sub-field boundaries, and the (iv) geometric correction.

3.4.1 The Preparation of vector data

First, the vector data covering the study area was extracted from existing data using the raster data coordinates (Figure 3.2). Then, the agricultural field boundaries were updated by digitizing them using the polygonal data model of the PCI Geomatica software. The polygonal modal is a simple vector model that is convenient for retrieving the boundaries of the polygons. For the digitization process, the fused QuickBird image was used as it provides the highest spatial resolution (0,62 m) and therefore, high geometric accuracy can be obtained from high resolution images (Aplin. et. al, 1999). During the digitization process it was seen that a single field may contain multiple crops. This may cause heteregonous structures in the fields. Therefore, for each field, subfield boundaries were digitized to obtain reliable classification results (Figure 3.3).

After completing the digitization process, the total number of the fields increased to 4134. A significant number of small fields were observed during the digitization process. The area of the agricultural fields range from 0.0014 ha to 42 ha. The number of the fields and the field sizes are given in table 3.6

Table 3.6 The number of the fields and field sizes in the study area

Number of Fields	Field Size (ha)	Percentage (%)
925	0,0014-0,4999	22,39
1034	0,5000-0,9999	25,03
1910	1,0000-5,9999	46,24
161	6,0000-9,9999	3,89
75	10,0000-19,9999	1,81
20	20,0000-29,9999	0,48
5	30,0000-47,99999	0,12

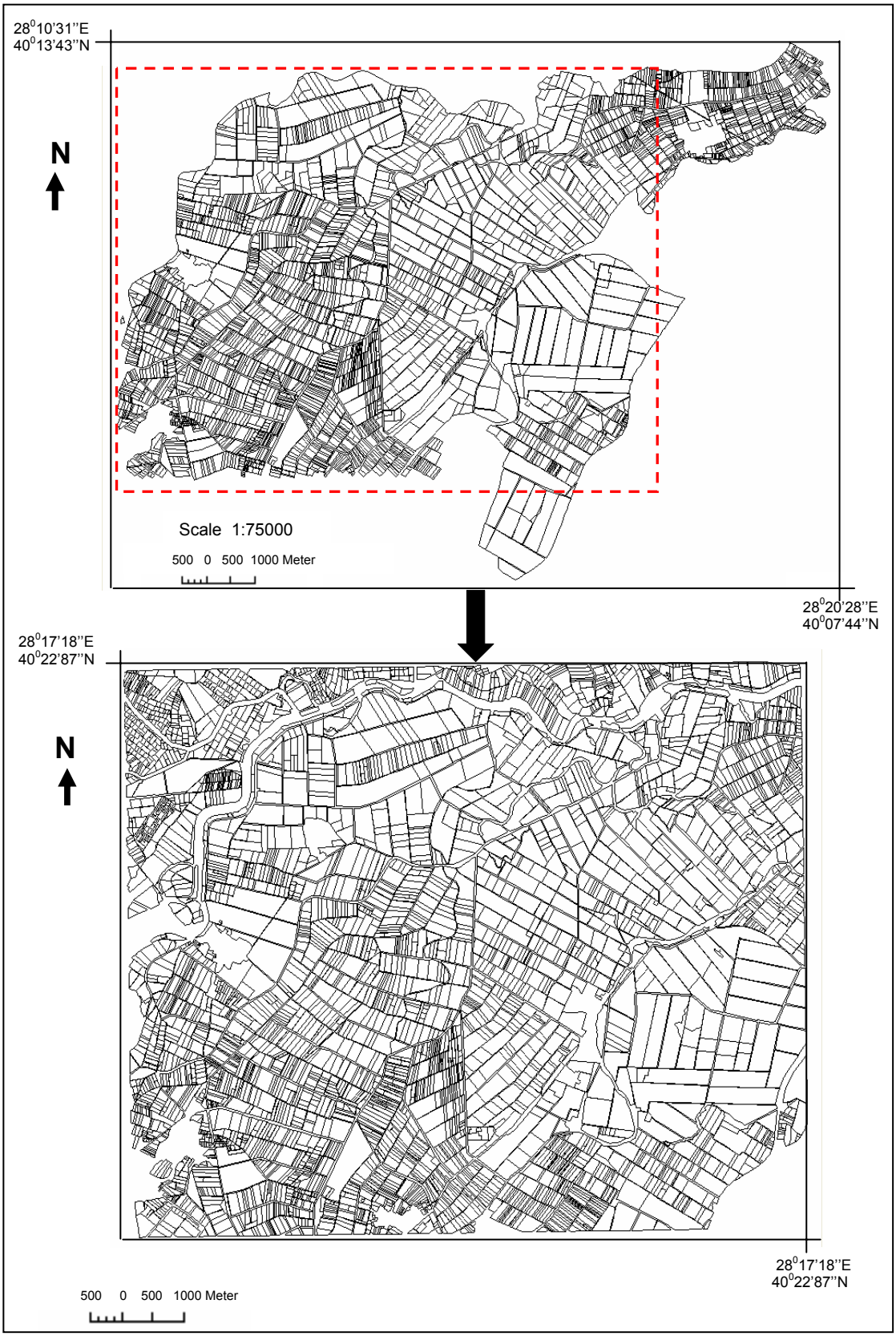

Figure 3.2 The digitized vector data

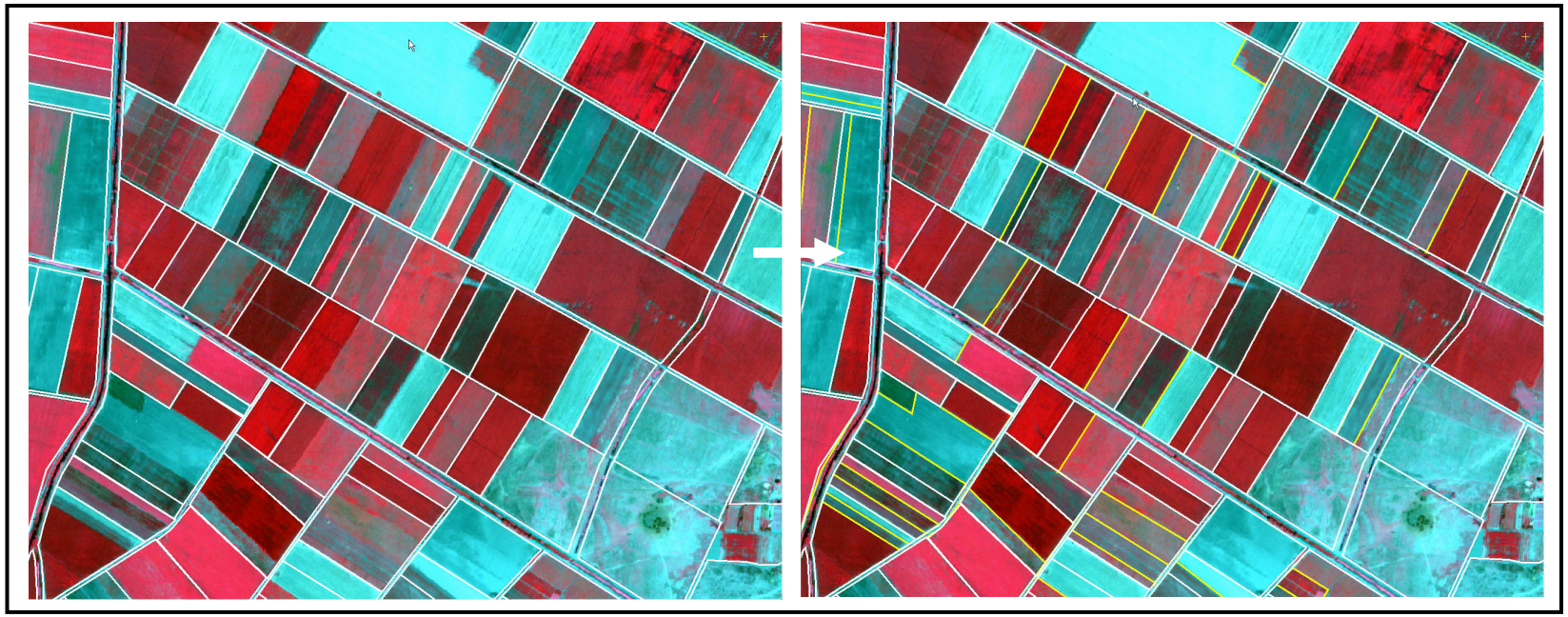

(i) (ii)

Figure 3.3 (i) The original vector, (ii) the updated vector

3.4.2 Database Design

The designed database of vector data consists of the attributes of field boundaries. The attributes include parcel identity number (id), lot number (lno), parcel number (pno), region of the field (region), area of the field (area), perimeter of the field (perimeter), current crop information (current_crop), late crop information (late_crop) and the notes. The region names located in the study area were inserted into the region column. These names were abbreviated using two or three letters of the attributes. The villages were symbolized as hk (Hotanlı), kka (Küçükkaraağaç), yak (Yolağazı), sk (Sultaniye), esk (Eskisarıbey), ysk (Yenisarıbey), ahk (Akhisar) and ipk (İsmetpaşa). Similarly, the crop types were abbreviated as Rs (residue), Sb (sugarbeet), Rc (rice), Cr (corn), and Tm (tomato). The August crops (late_crops) were stated by bringing the prefixes to the crops. For example, while a crop type was recorded as Rs for the July image, if Rs was replaced by another crop type in August, it was labeled as NSCr. Here, the abbreviation NS stands for newly seeded.

For each field, an identity number was designed, based on the last two digits. If the last digit of an id is zero, this means that the parcel is not divided into subfields. If on the other hand, a parcel has several subfields, the last digit was given a number starting from 1. For example, if the id of a parcel is 280 and this parcel is subdivided into two new parcels then, the new fields were renumbered as 281 and 282. Therefore, the number of subfields can be queried through database. After completing the digitization process, the digitized vector data and the database were checked carefully to edit the digitized fields and to correct the errors. A part of the updated attribute data is given in table 3.7

Table 3.7 An example for the updated attribute table

entity	area (sq m)	perimete (m)	id	lno	pno	region	current_crop	late_crop	notes	mod	parsel_id
1047	44659.588	882.49093	6902	117	4	hk	Rs	NSCw		2	690
1048	69915.574	1070.4089	6901	117	4	hk	Tm			1	690
1051	27987.266	701.3581	6870	117	1	hk	Rs			0	687
1052	11512.979	550.84913	6941	119	0	hk	Tm			1	694
1053	28717.814	702.58088	6942	119	0	hk	Cr			2	694
1054	17977.945	648.23021	6943	119	0	hk	Cr			3	694
1055	7301.5313	479.13484	6944	119	0	hk	Rs			4	694
1056	29045.697	709.27902	15320	117	13	sk	Rs	NSCr		0	1532
1058	74505.775	1126.3636	15510	119	8	sk	Tm			0	1551
1059	40078.199	960.29378	15370	117	18	sk	Cr			0	1537
1060	32460.844	1020.1915	15360	117	17	sk	Tm			0	1536
1062	38516.799	1086.9627	15472	119	4	sk	Cr			2	1547
1063	22160.615	612.17541	15471	119	4	sk	Pe	NSCr		1	1547
1064	72923.959	1291.7275	15460	119	3	sk	Rs			0	1546
1066	18930.477	582.30247	15480	119	5	sk	Cr			0	1548
1068	48530.789	1073.4986	15290	117	10	sk	Rs	NSCr		0	1529

3.4.3 Preprocessing of the Images

The preprocessings applied on remotely sensed data include image mosaicing, image fusion, and image-to-map and image-to-image geometric rectifications. Although the images were taken at different times and at different sensor locations, no additional radiometric or atmospheric corrections were applied on the images. This is because, the sun elevation and the azimuth angles of the images were similar for all images: $134{,}60^0$ and $64{,}0^0$ for SPOT4, $131{,}08^0$ and $63{,}05^0$ for SPOT5, $133{,}17^0$ and $65{,}31^0$ for IKONOS, and $141{,}60^0$ and $59{,}60^0$ for QuickBird, respectively (Table 3.8). On the other hand, the aim of this study was to seperate one class from the other classes with the classification. Therefore, radiometrically or atmospherically corrected image values do not dramatically effect the results (De Wit and Clevers, 2004). For this reason, there was no need to correct the images radiometrically or atmospherically.

Table 3.8 The sun azimuth, sun elevation, acquisation date and acquisation time of the images

Sensor Type	Sun Angle Azimuth (^{0})	Solar Elevation (^{0})	Acqst. Date	Acqst. Time
QUICKBIRD	141,60	59,60	13.08.04	08.56
IKONOS (XS)	133,17	65,31	15.07.04	08.56
SPOT5 (XS)	131,08	63,05	22.07.04	08.47
SPOT4 (XS)	134,60	64,00	23.07.04	08.55

3.4.3.1 Data Mosaicking

The standard QuickBird imagery covering the study area was delivered as six separate files. Therefore, the mosaicking process was applied on the QuickBird multispectral and panchromatic sub-images. To do that all the sub-images were selected and the mosaicking operation was carried out using the OrthoEngine module of the PCI Geomatica software (Figure 3.4).

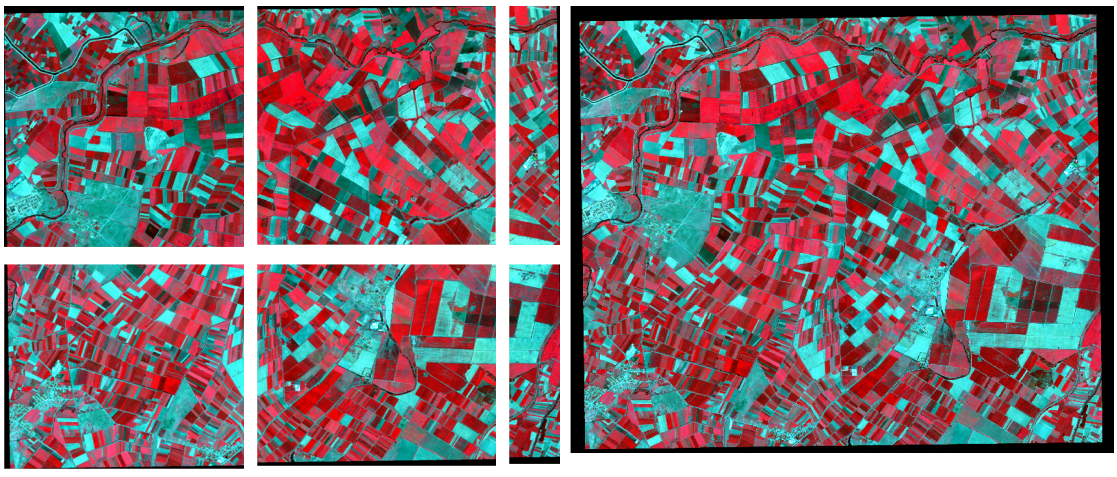

(i) (ii)

Figure 3.4 (i) The separate image files, and (ii) the mosaiced image

3.4.3.2 Data Fusion

To obtain a higher spatial resolution image and to examine more detailed crop information through polygon-based classification, the resolution of the QuickBird multispectral image (2,44m) was enhanced using the QuickBird panchromatic (0,60m) image. To perform this operation, an automatic image fusion algorithm of PCI Geomatica was used (Figure 3.5). There are three types of “pan-sharpening” methods available in the software. The used technique gives good results by means of preserving the spectral characteristics of the data and allowing the fusion process for all bands at the same time (Geomatica OrthoEngine User Guide, 2005).

3.4.3.2 Geometric Correction

The geometric corrections of the images were performed to remove the distortions that occur during the collection of the images. The correction was applied by generating the geometric relationship between the distorted image and the reference data. In fact, the images are geometrically corrected at the ground receiving stations, however, no ground control points (GCPs) are used for this correction process. Therefore, the images still contain, geometric errors and these errors must be removed using the GCPs.

The images were geometrically corrected using the second order polynomial and the nearest neighbour (NN) resampling techniques. The projection system used was UTM (Zone 35). For performing the geometric correction process, the digitized vector data were used as the reference source. After defining the geometric correction parameters, the GCPs were carefully selected from the same locations on both the reference data and the distorted images. GCPs were collected as homogenously as possible distributed throughout the entire

scene. The GCPs were selected from the distinct features, such as the intersections of the roads and the sharp boundaries of the parcels.

First, the fused QuickBird image was geometrically corrected based on the vector data using the image-to-map correction technique. To do that 12 GCPs were selected from the same locations on both the vector data and raster image. After this geometric correction, the total root mean square (RMS) error value was computed as 0,80 pixels in both X and Y directions. Then, image-to-image registration of the SPOT4, SPOT5, IKONOS and Quickbird XS images were carried out based on the corrected Quickbird image using 20 GCPs. The RMS errors were computed as 0,40 pixels for the SPOT4 image, 0,41 pixels for the SPOT5 image, 0,40 pixels for the IKONOS image and 0,40 pixels for the Quickbird XS image (Table 3.9). Next, the geometrically corrected images were visually checked by overlaying the vector field boundaries on the corrected images and displaying them together. It was observed that the results of geometric corrections were quite good to perform the polygon-based image classification procedure.

Table 3.9 The number of GCPs, the order of the polynomial, the resampling method, and the RMS errors for each image

Data	# of GCPs	Polynomial	Resampling Method	RMSE (pixels)
SPOT4 XS	20	2nd	NN	± **0.40**
SPOT5 XS	20	2nd	NN	± **0.41**
IKONOS XS	20	2nd	NN	± **0.40**
Quickbird XS	20	2nd	NN	± **0.40**
Quickbird PS	12	2nd	NN	± **0.80**

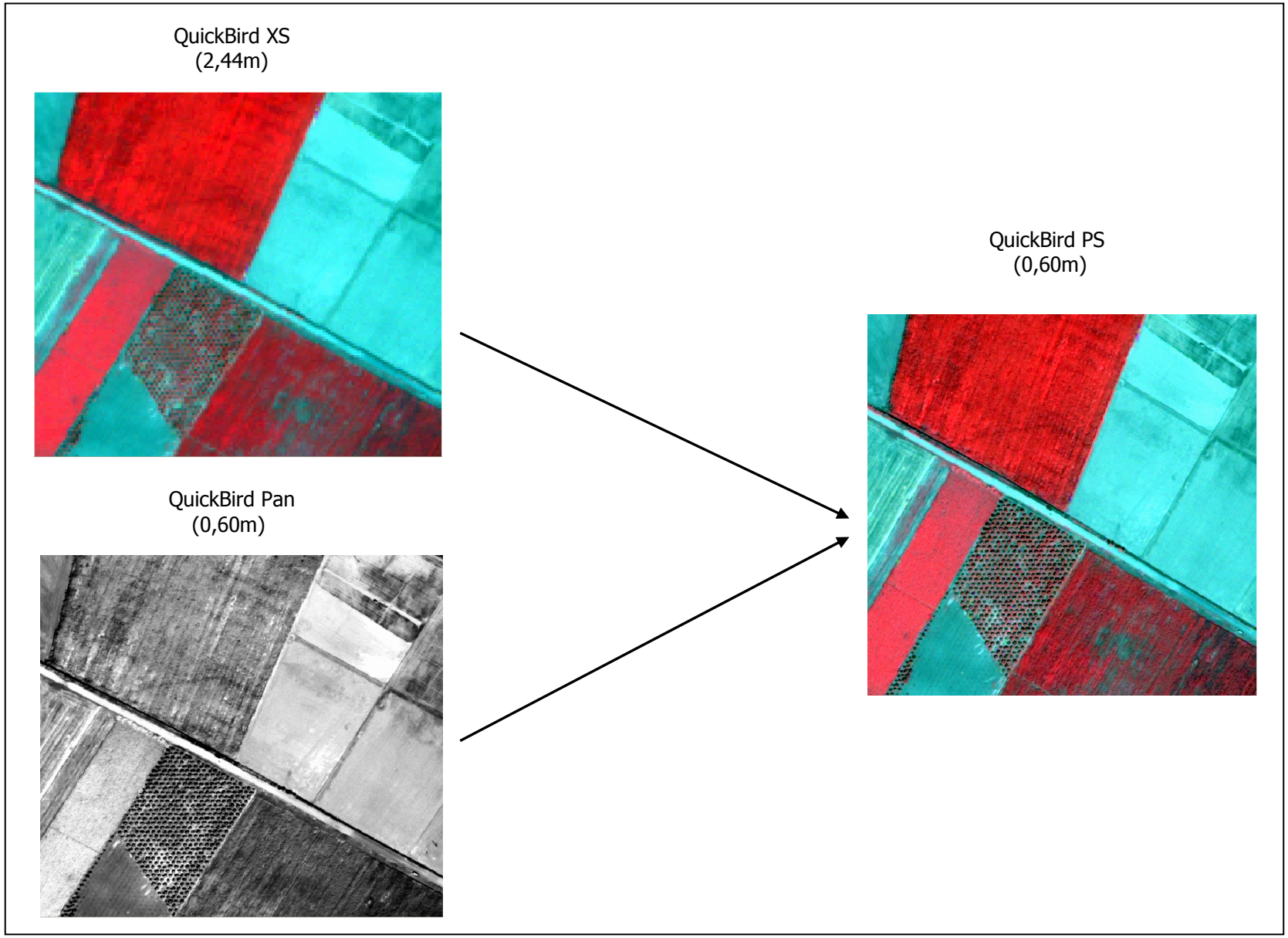

Figure 3.5 Enhancing the spatial resolution of the QuickBird multispectral data by fusing it with the high resolution panchromatic data

3.4 Image Classification

After the pre-processing operations, five different satellite images that have different spatial resolutions were classified. The images used in this study include SPOT4 XS (20m), SPOT5 XS (10m), IKONOS XS (4m), QuickBird XS (2.44m), and QuickBird Pansharpaned (0.60m). The spatial resolution of each image is illustrated in Figure 3.6 and Figure 3.7.

For performing the post-polygon classification procedure, the information of the agricultural fields were collected by visiting them in the study area. The vector map and the raster images were then integrated to divide the images into homogenous segments of the fields and the post-polygon classification was carried out as follows.

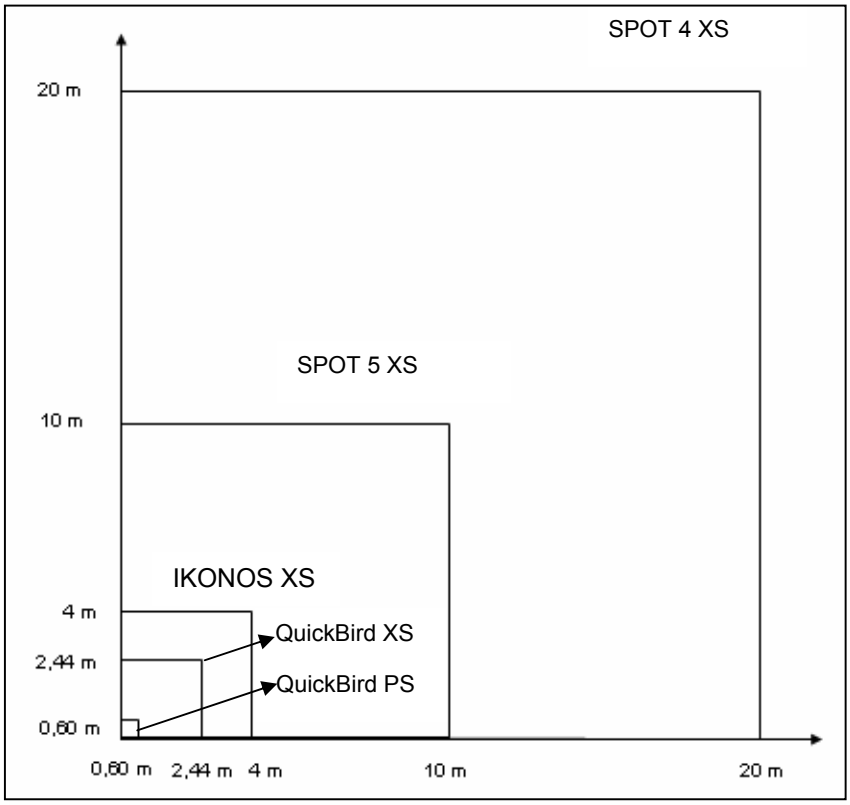

Figure 3.6 The illustration of the spatial resolution of the images

First, pixel-based classification was applied using the common bands of each image through maximum likelihood classifier. Then, the proportions of the polygons covered by each land cover class was calculated and the dominant land cover class was assigned to the entire polygon. The same process was repeated using the filtered (Median 3*3, 5*5, and 7*7) bands. The median filter was used to replaced the central digital number (DN) value of a given kernel size with the mean of that matrix because this filter better preserves the edges.

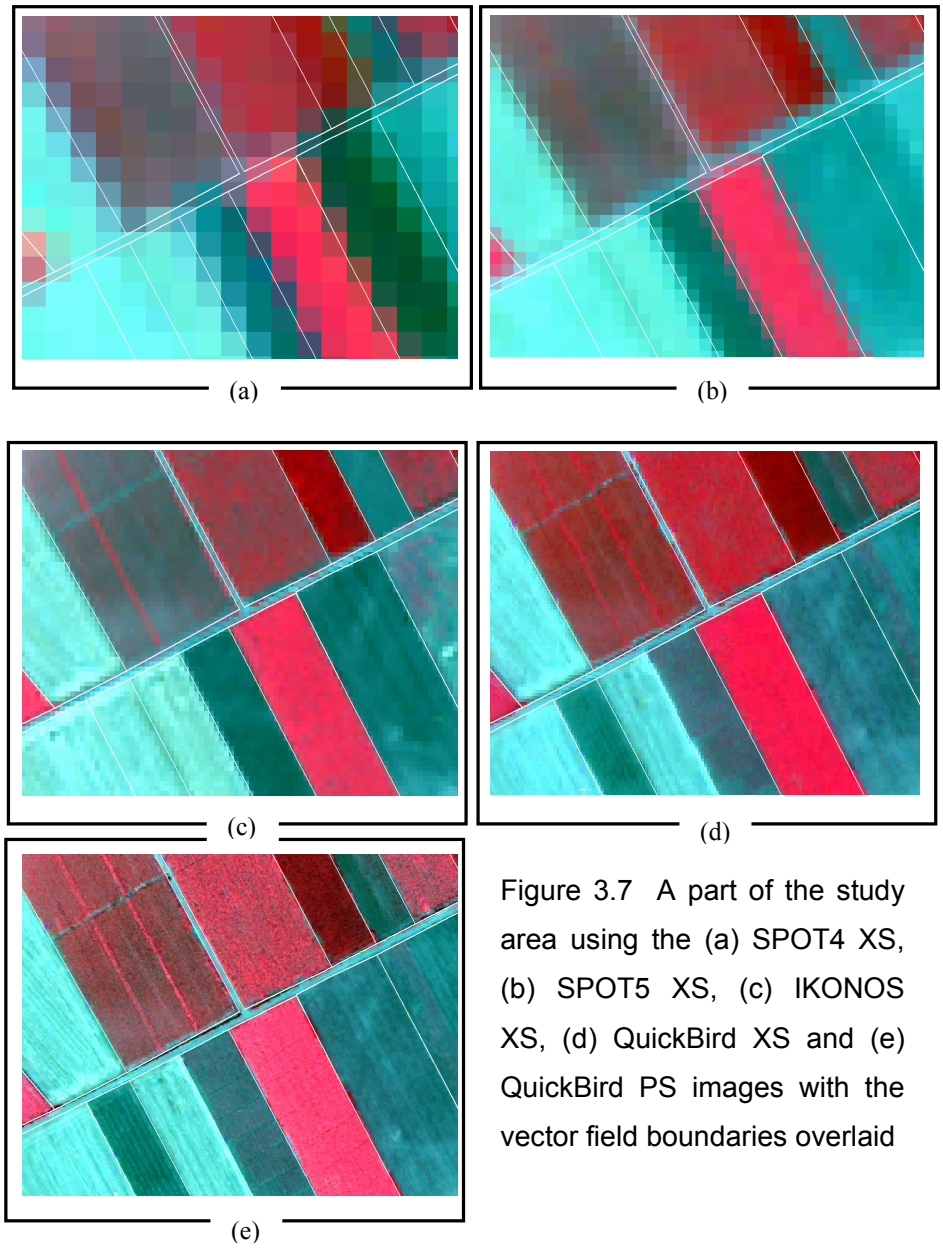

Figure 3.7 A part of the study area using the (a) SPOT4 XS, (b) SPOT5 XS, (c) IKONOS XS, (d) QuickBird XS and (e) QuickBird PS images with the vector field boundaries overlaid

3.5.1 Selection of Training Areas

The accuracy of a classification can be directly affected by the training area selection because it helps to provide the accuracy of the standard deviation produced from the training site statistics for the accuracy of the decision rules in the next stage. Therefore, a great effort was spent during the collection of the training samples.

Different crop types have different spectral characteristics. In addition, the spectral classes could stem from different planting dates, soil moisture conditions, crop management practices, seed variaties, atmospheric conditions, or combinations of these factors that affect the variety of the spectral classes (Lillesand, 2004). Therefore, the subclasses of the agricultural crops were separately characterized as two residue types (Rs1, Rs2), three corn subclasses (Cr1, Cr2, Cr3), two sugarbeet types (Sb1, Sb2) and two tomato (Tm1, Tm2) and pepper (Pp1, Pp2) subclasses to avoid defining the pixel variability in one training set. The subclasses belonging to the same class were then aggregated to make them one class. At the end of the aggregation process, five main crop types (Residue, Corn, Sugarbeet, Tomato/Pepper and Rice) were selected as the classes to perform the classification.

As mentioned before, the images were not able to be taken in the same date due to being collected by different sensors. While the SPOT and IKONOS images were taken in July, the QuickBird images were taken in August. In August, some crops were replaced by a second crop. Because of this reason, when selecting the training samples, the growing dates of each crop was

taken into account. The growing dates of the crops can be seen in Figure 3.8 (Turker and Arikan, (In Press))

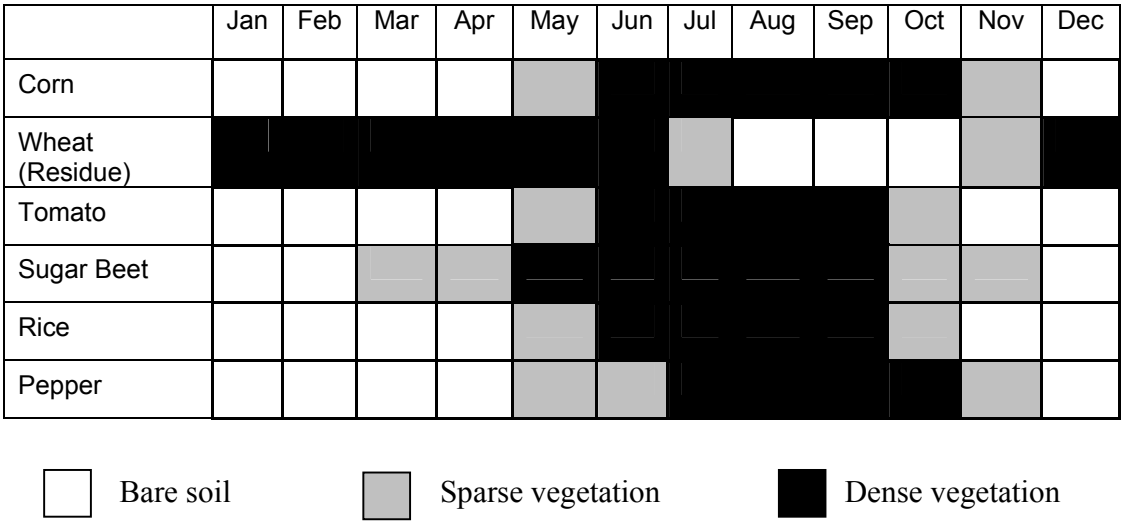

Figure 3.8 The phenological characteristics of the crops

The training samples were selected from the IKONOS image using the colour composite of the bands 4 (NIR), 3 (R), and 2 (G). The false color composite was used because the healty vegetation absorbs most of the green and red incident energy and reflects almost half of the incident NIR energy. Therefore, green vegetation shows up in shades of red. The reason for selecting the training areas from the 4m IKONOS XS image was that the IKONOS data provides more reliable results than the other resolutions. If the training selection was carried out from the SPOT data, due to a rather coarser resolution, some details could be lost. On the other hand, if this selection was carried out from the high resolution QuickBird images, fine details would be highlighted and therefore, the sample collection from the agricultural fields would become rather more difficult.

The training samples were carefully located at the homogenous sites of the polygons. The edge pixels falling on parcel boundaries and the unrepresentative mixed pixels on heterogenous parcels were avoided. While selecting the training pixels, within field statistics were computed and analyzed together with the visual inspection. Therefore, the 4 m IKONOS data was considered to be the optimum image to eliminate the effects of the visual selection procedure.

Next, the scatterplots, histograms, and the coincidence spectral plots were generated from the training samples to see the appropriateness of the training areas. The scatter plots provide significant knowledge about the actual information content of the image and it shows the degree of between-band correlation (Janssen, 1996). The histogram is also a useful graphical representation to understand information content of remotely sensed images. It gives an idea to analyst whether the quality of the data is appropriate. It is especially important for the MLC because it provides a visual check on the normality of the spectral response distributions. Although the histograms illustrate the distribution of individual categories very well, they do not allow to compare two different category types. To see the spectral separation between the classes, the analyses of the coincidence spectral plots are needed. The spectral plots were used to display the mean value and the variance of the distribution at ±3 standard deviations (±3∂) of each class, for each spectral band. A large standard deviation means that the frequency distribution of the training pixels shows more dispersion. On the other hand, a small standard deviation means that the training pixels represent homogenity (Appendix C).

The selected training pixels were then used to compute the statistics of the training areas. When necessary, the training samples were edited to exclude those pixels that significantly deviate from the others. For each subclass, the training statistics of each image are provided in Appendix C. Approximately, one third of the reference fields were used for the training area selection. The remaining reference fields were used for the accuracy assessment process. For making an unbiased comparison between the classified outputs of the images, the same training sites and the checking locations collected from IKONOS were transfered to other images to be used in the classification. Therefore, the same training areas were used for classifying the other images. By using the same training locations for each image, the variation of the classification accuracy could be analyzed. The correlation statistics and the scatterplots were generated from the training samples to show the relations between the spectral variables for each image.

To assess the degree of separability between the training class signatures, the Transformed divergence index (TDI) was used. TDI was computed using the mean and the covariance matrices of the class statistics (Janssen, 1996). It is a commonly used technique and gives information about the signature separabilities. The larger the transformed divergence means the greater the "statistical distance" between the training samples. This provides the higher probability for the correct classification of the classes (Lillesand, 2004). When the distance between the classes increase, the weight of the statistics decrease exponentionally. The divergence values are scaled to lie between 0 and 2000 (Janssen, 1996). While the value of 2000 indicates a complete separation between the classes, a good separation is acquired by 1900. The values below 1700 give poor separation according to this matrix. The matrix was computed using the equation 3.1:

$$TDiver_{cd} = 2000\left(1-\exp\left(\frac{-\ Diver_{cd}}{8}\right)\right)$$ (Equation 3.1)

where; c and d refers to the classes to be included in the classification (Janssen, 1996).

Based on the results of the separability index of the SPOT 4, the minimum separability of 0,9342 was observed between Tm2 and Pp2. However, this low separability values do not affect the accuracy because it was seen that the spectral reflectances of the subclasses tomato and pepper were very close to each other based on the previous selection tests about the training sites. Therefore, the training samples of these two crop types were aggregated under the name of Tm/Pp. In the TDI, the subclasses Sb1 and Rc1 had the separabilities of 1.4740, and Rc2 and Cr1 exhibited the separability value of 1,4920. The separability between the subclasses Rc1 and Sb1 was 1.6943. The other low separability was observed between the subclasses Sb2 and Tm1 as 1.8731. The separability value between the subclasses Rc1 and Tm1 was 1.8050. From this index therefore, the average separability was taken as 1.9476. The spectral confusions between the subclasses can be seen in the coincidence spectral plots in Appendix B.

For the SPOT5 image, the minimum separability value was observed between the subclasses Pp1 and Pp2. The values of 1.6226 and 1.6421 were

the other low separabilities between Cr1 and Rc2 and between Sb2 and Rc1. The average separability value was 1.9593.

For the IKONOS image, the minimum separability value (0.2156) was between Tm2 and Pp1 with. The spectral confusion between the classes can also be seen in the coincidence spectral plots provided in Appendix B.

For the Quickbird XS image, the TDI results show that Tm2-Pp1 pair has the lowest separability of 0.2156. This was followed with a value of 1.2639 between Cr3 and Rc2 and a value of 1.2639 between Cr1 and Rc2. The average separability was computed to be 1.7805 from the separability index.

Based on the separability values of the Quickbird PS image, the Tm2-Pp1 pair has the minimum separability value of 0.1457. The average separability was computed as 1.6675. The separability values for each crop pairs can be seen in Appendix A.

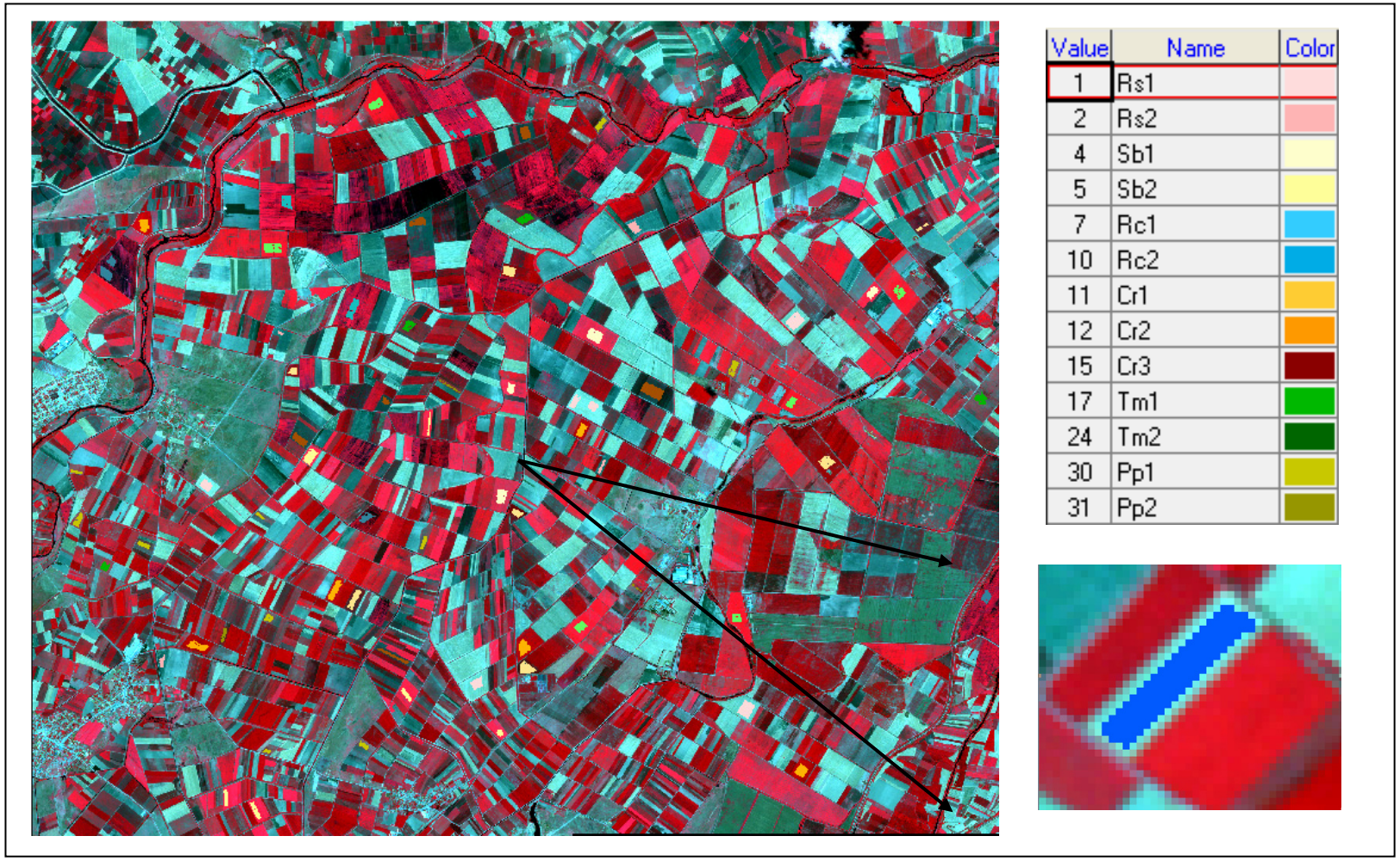

Figure 3.9 The training areas selected from the IKONOS XS (4m) image

3.5.2. Post-Polygon Classification

In post-polygon classification (Figure 3.10), first, a per-pixel MLC was carried out. Then, for each field, the frequency of the classified pixels were computed and the class labels of the polygons were assigned based on the majority class computed for each polygon.

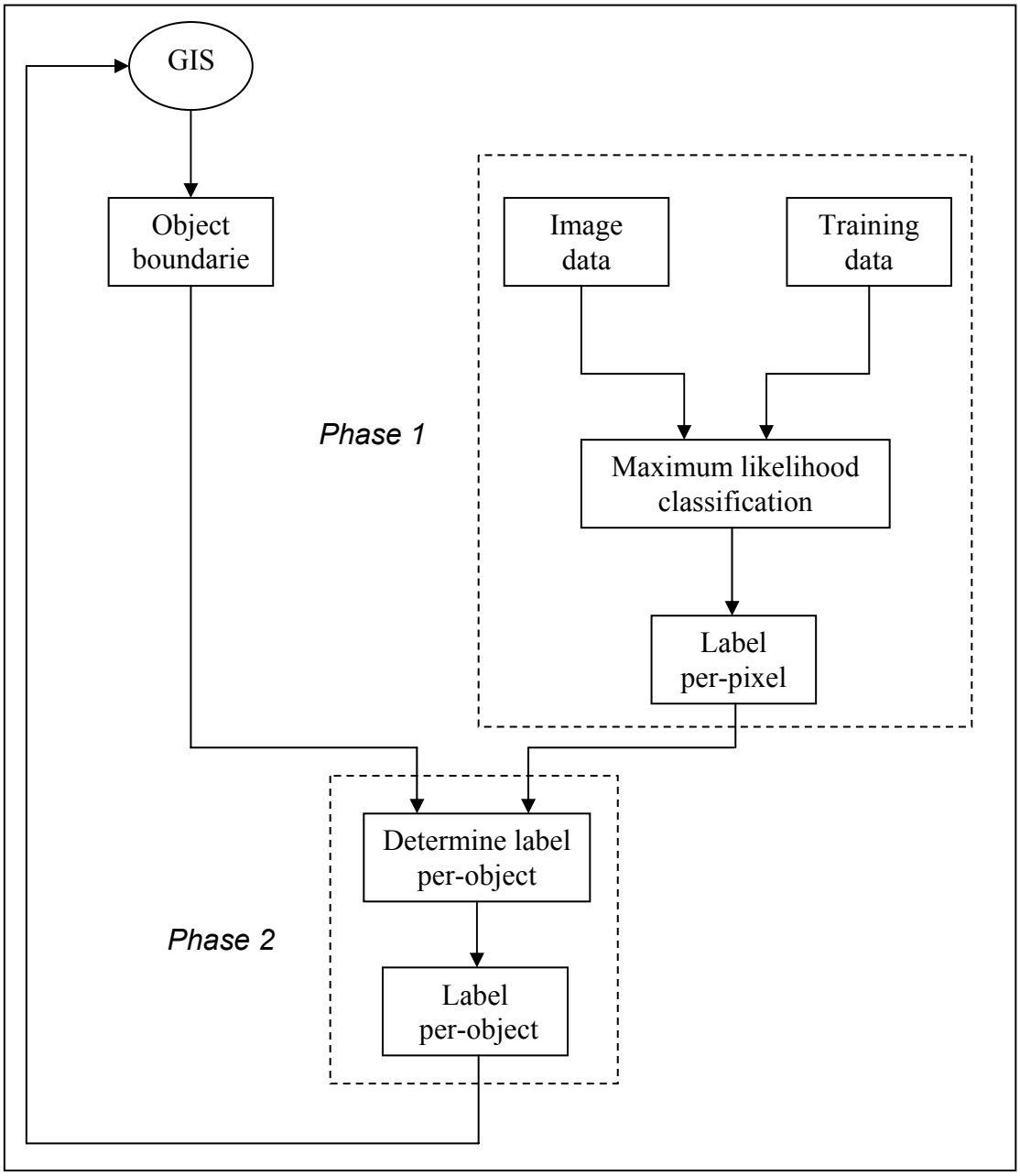

Figure 3.10 Post-polygon classification (Janssen, 1999)

Each of the images used in this study has four spectral bands, three of which (G, R and NIR) are common. While the IKONOS and QuickBird images have blue, green, red and NIR bands, SPOT images have a SWIR band as the fourth band instead of the blue band. The blue band of the IKONOS and the QuickBird images range from 0,45 to 0,52μm and are useful for discriminating soil/vegetation, for coastal mapping and for urban future identification. The green band of the SPOT images, which ranges from 0,52 to 0,60μm, is generally useful for green vegetation mapping and urban future extraction. The red band, which ranges between 0,63 and 0,69μm, is appropriate for the identification of the vegetation types, health and biomas content, water body delination, and soil moisture. The SWIR band of the SPOT satellite images, which has the range between 1,55 and 1,75μm, are sensitive to moisture in soil and vegetation. This band is also useful for discriminating snow and cloud cover areas. The mean value differences of each band for each satellite can be seen in Appendix D.

Of the two polygon-based classification techniques, first, the post-polygon classification was applied using the common bands and the all bands. To do that first, a MLC was applied on each image. Then, for each field, the frequencies of the classified pixels were computed and the majority class was found for the field being considered. Next, the common bands were filtered using the median (3*3, 5*5 and 7*7) smoothing filter and the same post-polygon classification steps were repeated using the filtered images. The classified output of the unfiltered IKONOS image is given in figure 3.11. The classified outputs of the SPOT4, SPOT5, QuickBird XS and QuickBird PS images are provided in Appendix G.

Figure 3.11 The output of the post-polygon classification for the IKONOS XS image using common bands

3.6 Accuracy Assessment

After extracting the information from remotely sensed data through automated classification techniques, the results should be evaluated in order to have knowledge about it's quality. The quality of the information derived from remotely sensed data can be determined using an accuracy assessment technique (Congalton and Green, 1999).

In this study, a total of 1230 fields to be used in accuracy assessment were visited on the ground. Crop information such as; crop type, crop, moisture and bare soil conditions, weeds, etc. were recorded during the site visit, which was conducted on 11-12-13-14 August 2004. In addition, several other information was obtained from the local farmers. A special effort was spent for the distribution of the fields while taking the samples from the study area. The current and late crops (where valid) were recorded on the reference land cover map. The collected reference data were stored in the database to be used for the selection of the training areas and verifying the classified images. The accuracy assessment was carried out using 1021 fields.

To evaluate the results, an error matrix was generated. The error matrix is a widely used accuracy assessment method, in which the relationship between the known reference data (ground truth) and the corresponding results of an automated classification can be compared on category by category basis (Lillesand, 2004). In the present case, approximately one third of the reference data (a total of 1021 sample fields) were used to assess the accuracy and the samples were selected with a homogenous distribution. To compute the accuracies of the classified images, the training fields were extracted from the accuracy assessment using a query function of the database. To make a good comparision between the classified images, the same reference fields were used for the accuracy assessment of each of the classified outputs. However, for the QuickBird images, the number of

reference fields decreased to 967 and therefore, the assessments of the classified QuickBird images were performed using 967 fields. This is because, for 54 fields, the late crop information contained different crop types. Therefore, these fields, which contain different crops, were excluded from the accuracy assessment procedure. The fields were selected through a database and the query results were exported to Microsoft Excel sheet where the error matrices were generated.

For the accuracy assessment, both the overall accuracy and the accuracies of individual classes were computed. The overall accuracy was determined by dividing the total number of correctly classified pixels, which are some of the major diagonal elements of the matrix, by the total number of pixels in the error matrix. The individual class accuracies were estimated by the *producer's accuracies (ommission error)* and the *user's accuracies (commission error)*. The producer's accuracy was computed by dividing the total number of correctly classified pixels by the total number of the reference pixels. This accuracy shows the probability of a reference pixel being correctly classified. By using this statistic, the analyst can determine how well a certain area can be classified. When the total number of the correctly classified pixels in a category is divided by the total number of pixels that were actually classified in that category, the result is a measure of commission error. This measurement is called the *user's accuracy,* which indicates the reliability of a pixel classified on the map actually represents that category on the ground (Janssen, 2005).

In addition to the error matrix, the Kappa statistics were also computed to interpret the results accurately. Kappa analysis yields a statistical measure, k, which is an estimate of Kappa. It is a measure of accuracy between the classification map and the reference data. The overall accuracy includes the data along the major diagonal only and excludes the errors of ommission

and commission. On the other hand the Kappa statistics incorporate the nondiagonal elements of the error matrix as well (Lillesand, 2004).

The Kappa statistics (k) is computed using the formula

$$k = \frac{N\sum_{i=-1}^{r} x_{ii} - \sum_{i=-1}^{r} (x_{i+} \cdot x_{+i})}{N^2 - \sum_{i=-1}^{r} (x_{i+} \cdot x_{+i})}$$

(Equation 3.2)

Where;

r = number of rows in the error matrix

x_{ii} = number of observations in row i and column i (on the major diagonal)

x_{i+} = total of observations in row i

x_{+i} = total of observations in column i

N = total number of observations include in matrix

For each classified output, the computed statistical measures that include overall accuracy and overall kappa are given in Appendix E.

3.7. The Results

The post-polygon classification was applied on the unfiltered common bands, the filtered common bands, and the all bands of each image. For each classified output, an error matrix was computed.

3.7.1 Classification Using the Unfiltered Images

As mentioned earlier, for each image, the polygon-based classification was applied on the common bands of green, red and NIR. The error matrix of the classified SPOT4 image is given in table 3.10. The overall accuracy and overall kappa were obtained as 76,1% and 65,7%, respectively. While the classes Rs, Sb, Rc and Tm/Pp provided similar results, the class Cr had the lowest producer's accuracy of 48,8%, and relatively high user's accuracy of 88,8%.

Table 3.10 The error matrix of the SPOT4 XS image

	Cr	Tm/Pp	Rc	Rs	Sb	RTot
Cr	128	6	1	9	0	144
Tm/Pp	120	322	5	46	7	500
Rc	7	4	21	0	1	33
Rs	6	1	0	277	0	284
Sb	1	28	2	0	29	60
CTot	262	361	29	332	37	1021
Producer's (%)	48,8	89,1	72,4	83,4	78,3	
User's (%)	88,8	64,4	63,6	97,5	48,3	
Overall (%) = 76,1 Kappa (%) = 65,7						

The classified SPOT5 XS image using the common bands provided an overall accuracy of 81,4% and an overall kappa of 73,3% were (Table 3.11). Same as the SPOT 4 image, the class Cr had the lowest producer's accuracy of 59,9% but a significantly high user's accuracy of 94% was computed. It is evident that of the 262 reference polygons, 105 omitted from the class Cr causing low producer's accuracy. Similar to SPOT 4 image, the class Rs was classified with high user's and producer's accuracies.

Table 3.11 The error matrix of the SPOT 5 XS image

	Cr	Tm/Pp	Rc	Rs	Sb	RTot
Cr	157	5	0	5	0	167
Tm/Pp	92	343	3	46	4	488
Rc	7	0	21	0	3	31
Rs	5	2	0	281	0	288
Sb	1	11	5	0	30	47
CTot	262	361	29	332	37	1021
Producer's (%)	59,9	95	72,4	84,6	81	
User's (%)	94	70,2	67,7	97,5	63,8	
Overall (%) = 81,4 Kappa (%) = 73,3						

The overall accuracy and overall kappa of the classified IKONOS image were found to be 88,6% and 83,7%, respectively (Table 3.12). When the producer's accuracies are examined, it is seen that the class Sb gives the highest producer's accuracy of 100%. For this class, the user's accuracy was computed as 75,5%. This means that although all the Sb reference fields were classified correctly as sugarbeet, only 75,5% of the fields actually represent the class Sb on the ground. For all the other classes, the procedure's and user's accuracies were above 75%.

Table 3.12 The error matrix of the IKONOS XS image

	Cr	Tm/Pp	Rc	Rs	Sb	RTot
Cr	206	10	2	6	0	224
Tm/Pp	46	340	1	27	0	414
Rc	4	0	23	0	0	27
Rs	6	2	0	299	0	307
Sb	0	9	3	0	37	49
CTot	262	361	29	332	37	1021
Producer's (%)	78,6	94,1	79,3	90	100	
User's (%)	91,9	82,1	85,1	97,3	75,5	
Overall (%) = 88,6 Kappa (%) = 83,7						

For the QuickBird XS image, the overall accuracy and overall kappa were computed to be 83,7% and 77%, respectively (Table 3.13). While the producer's accuracies of the classes Cr and Rc were 68,7% and 58,6%, their

user's accuracies were found to be 94,8% and 30,3%, respectively. It appears that the significantly low accuracy of the class Rc is caused by the spectral confusion with the class Cr. Of the classes the class Rs provided a remarkably high user's and producer's accuracies. The producer's accuracies of Rs, Sb and Tm/Pp were around 90%. On the other hand, these classes had 87,3%, 66,6% and 84,5% user's accuracies respectively. As can be seen from table 3.13, for the class Rc, the omission and commission errors of Rc were very low.

Table 3.13 The error matrix of the QuickBird XS image

	Cr	Rc	Rs	Sb	Tm/Pp	RTot
Cr	238	0	2	0	11	251
Rc	33	17	1	0	5	56
Rs	26	0	186	0	1	213
Sb	0	7	0	34	10	51
Tm/Pp	49	5	4	3	335	396
CTot	346	29	193	37	362	967
Producer's (%)	68,7	58,6	96,3	91,8	92,5	
User's (%)	94,8	30,3	87,3	66,6	84,5	
Overall (%) = 83,7 Kappa (%) = 77						

The Quickbird PS image was the last image classified. The error matrix of the classified QuickBird pansharpaned image is given in table 3.14. While the producer's accuracy of the classes Rs and Sb were 96,3% and 89,1%, their user's accuracies were found to be 86,1% and 64,7%. The classes Cr and Tm/Pp exhibited 75,1% and 92,2% producer's accuracies and 95,9% and 89,7% user's accuracies. On the other hand, the class Rc gave the worst results for both the producer's and user's accuracies as 58,6% and 29,8%, respectively.

Table 3.14 The error matrix of the QuickBird PS image.

	Cr	Rc	Rs	Sb	Tm/Pp	RTot
Cr	260	1	1	0	9	271
Rc	33	17	1	0	6	57
Rs	28	0	186	0	2	216
Sb	0	7	0	33	11	51
Tm/Pp	25	4	5	4	334	372
CTot	346	29	193	37	362	967
Producer's (%)	75,1	58,6	96,3	89,1	92,2	
User's (%)	95,9	29,8	86,1	64,7	89,7	
Overall (%) = 85,8	Kappa (%) = 79,9					

3.7.2 Classification Using the Filtered Images

3.7.2.1 3*3 Filtering

The results of the 3*3 filtered SPOT 4 image are given in table 3.15. The overall accuracy and overall kappa were computed to be 71,8% and 59,6%, respectively. The individual class accuracies ranged from 45% to 96,8%. The lowest producer's accuracy was obtained for the class Cr although it exhibited remarkably high user's accuracy of 87,8%. The class Sb had the lowest user's accuracy of 45% and relatively high producer's accuracy of 72,9%. It is evident that of the 37 reference fields, ten were omitted from the class Sb causing a low user's accuracy.

Table 3.15 The error matrix of the (3*3) filtered SPOT4 XS image

	Cr	Tm/Pp	Rc	Rs	Sb	RTot
Cr	123	7	1	9	0	140
Tm/Pp	125	318	4	79	8	534
Rc	8	3	22	0	2	35
Rs	6	2	0	244	0	252
Sb	0	31	2	0	27	60
CTot	262	361	29	332	37	1021
Producer's (%)	46,9	88	75,8	73,4	72,9	
User's (%)	87,8	59,5	62,8	96,8	45	
Overall (%) = 71,8	Kappa (%) = 59,6					

For the filtered SPOT5 image, the overall accuracy and overall kappa were found to be 80,2% and 71,4%, respectively (Table 3.16). The classes Rc, Rs and Sb had the producer's accuracies of 72,4%, 82,2% and 78,3%, respectively. For these classes, the user's accuracies were computed to be 77,7%, 97,8% and 64,4%, respectively. The producer's accuracies of the classes Cr and Tm/Pp were 56,4% and 95,8%, while their user's accuracies were found to be 93,6% and 67,8%. The class Cr provided the lowest producer's accuracy of 56,4%. The producer's accuracies of the other classes were relatively high.

Table 3.16 The error matrix of the (3*3) filtered SPOT5 XS image

	Cr	Tm/Pp	Rc	Rs	Sb	RTot
Cr	148	4	2	4	0	158
Tm/Pp	104	346	1	53	6	510
Rc	4	0	21	0	2	27
Rs	5	1	0	275	0	281
Sb	1	10	5	0	29	45
CTot	262	361	29	332	37	1021
Producer's (%)	56,4	95,8	72,4	82,8	78,3	
User's (%)	93,6	67,8	77,7	97,8	64,4	
Overall (%) = 80,2	Kappa (%) = 71,4					

The IKONOS image provided an overall accuracy of 87,9% and an overall kappa of 82,7% (Table 3.17). The class Sb had the highest producer's accuracy of 100%. However, the user's accuracy of this class (74%) was the lowest. The classes Rs and Rc provided 88,5% and 79,3% producer's accuracises and 97,3% and 88,4% user's accuracies, respectively. On the other hand, the producer's accuracy obtained for the classes Cr and Tm/Pp were 79,0% and 93,3%, and the user's accuracies were computed to be 91,5% and 80,8%.

Table 3.17 The error matrix of the (3*3) filtered IKONOS XS image

	Cr	Tm/Pp	Rc	Rs	Sb	RTot
Cr	207	12	2	5	0	226
Tm/Pp	46	337	1	33	0	417
Rc	3	0	23	0	0	26
Rs	6	2	0	294	0	302
Sb	0	10	3	0	37	50
CTot	262	361	29	332	37	1021
Producer's (%)	79	93,3	79,3	88,5	100	
User's (%)	91,5	80,8	88,4	97,3	74	
Overall (%) = 87,9 Kappa (%) = 82,7						

The overall, producer's and user's accuracies of the 3*3 filtered Quickbird XS image are given in table 3.18. For this image, the overall accuracy and overall kappa were computed to be 83,5% and 76,6%, respectively. The individual class accuracies ranged from 58,6% to 96,3% for the producer's accuracy and ranged from 34,0% to 95,8% for the user's accuracy. Of the classes, Rc showed the worst results with the producer's accuracy of 58,6% and the user's accuracy of 34,0%. It is evident that there is spectral confusion between the class Rc and the classes Cr, Sb, and Tm/Pp.

Table 3.18 The error matrix of the (3*3) filtered QuickBird XS image

	Cr	Rc	Rs	Sb	Tm/Pp	RTot
Cr	229	0	2	0	8	239
Rc	30	17	1	0	2	50
Rs	26	0	186	0	1	213
Sb	0	7	0	33	8	48
Tm/Pp	61	5	4	4	343	417
CTot	346	29	193	37	362	967
Producer's (%)	66,1	58,6	96,3	89,1	94,7	
User's (%)	95,8	34	87,3	68,7	82,2	
Overall (%) = 83,5 Kappa (%) = 76,6						

It can be seen in table 3.19 that for the QuickBird PS image, the overall accuracy and overall kappa were computed to be 85,4% and 79,3%, respectively. Similar to the QuickBird XS image, the worst results were

obtained for the class Rc with 58,6% producer's accuracy and 30,9% user's accuracy. On the other hand, the classes Rs and Tm/Pp provided significantly high accuracies.

Table 3.19 The error matrix of the (3*3) filtered QuickBird PS image

	Cr	Rc	Rs	Sb	Tm/Pp	RTot
Cr	258	0	2	0	10	270
Rc	32	17	1	0	5	55
Rs	27	0	186	0	1	214
Sb	0	7	0	33	14	54
Tm/Pp	29	5	4	4	332	374
CTot	346	29	193	37	362	967
Producer's (%)	74,5	58,6	96,3	89,1	91,7	
User's (%)	95,5	30,9	86,9	61,1	88,7	
Overall (%) = 85,4	Kappa (%) = 79,3					

3.7.2.2 5*5 Filtering

The 5*5 filtered SPOT4 image provided 66,6% overall accuracy and 51,3% overall kappa (Table 3.20). As can be seen in the table, the individual class accuracies varied between 32.0% and 91,4%. The classes Rs, Sb and Rc had the producer's accuracies of 68,3%, 51,3% and 72,4% and the user's accuracies of 95,3%, 44,1% and 70,0%, respectively. The low producer's accuracy (32%) of the class Cr indicates that most of the reference fields were omitted from this category. On the other hand, the class Cr exhibited remarkably high user's accuracy of 90,3%. The reverse trend was observed for the class Tm/Pp.

Table 3.20 The error matrix of the (5*5) filtered SPOT4 XS image

	Cr	Tm/Pp	Rc	Rs	Sb	RTot
Cr	84	3	0	6	0	93
Tm/Pp	166	330	6	99	16	617
Rc	4	3	21	0	2	30
Rs	7	4	0	227	0	238
Sb	1	21	2	0	19	43
CTot	262	361	29	332	37	1021
Producer's (%)	32	91,4	72,4	68,3	51,3	
User's (%)	90,3	53,4	70	95,3	44,1	
Overall (%) = 66,6	Kappa (%) = 51,3					

When the error matrix of the SPOT5 image (Table 3.21) is examined, it can be seen that the overall accuracy (78,0%) and the overall kappa (68,2%) are higher than the SPOT 4 image. The lowest producer's accuracy of 55,7% was obtained for the class Cr although the user's accuracy of this class was very high (92,4%) illustrating low commission error. The accuracies of the classes Rc and Rs were similar.

Table 3.21 The error matrix of the (5*5) filtered SPOT5 XS image

	Cr	Tm/Pp	Rc	Rs	Sb	RTot
Cr	146	7	2	3	0	158
Tm/Pp	108	342	1	71	6	528
Rc	2	0	21	0	1	24
Rs	5	1	0	258	0	264
Sb	1	11	5	0	30	47
CTot	262	361	29	332	37	1021
Producer's (%)	55,7	94,7	72,4	77,7	81	
User's (%)	92,4	64,7	87,5	97,7	63,8	
Overall (%) = 78	Kappa (%) = 68,2					

For the IKONOS image, the overall accuracy and overall kappa were computed to be 86,9% and 81,3%, respectively (Table 3.22). Although all the reference Sb fields were correctly classified as sugarbeet, only 72,5% of the Sb fields can be called sugarbeet. Of the 37 Sb fields, 14 were wrongly

included in the other classes. The accuracies of the other classes were around 80%.

Table 3.22 The error matrix of the (5*5) filtered IKONOS XS image

	Cr	Tm/Pp	Rc	Rs	Sb	RTot
Cr	204	15	2	5	0	226
Tm/Pp	49	333	1	36	0	419
Rc	3	0	23	0	0	26
Rs	6	2	0	291	0	299
Sb	0	11	3	0	37	51
CTot	262	361	29	332	37	1021
Producer's (%)	77,8	92,2	79,3	87,6	100	
User's (%)	90,2	79,4	88,4	97,3	72,5	
Overall (%) = 86,9 Kappa (%) = 81,3						

The error matrix of the QuickBird XS image (Table 3.23) shows that the overall accuracy (82,5%) and overall kappa (75%) are reasonably high. While the individual class accuracies varied from 55,1% to 96,3% for producer's, the user's accuracies ranged from 32,0% to 95,7%. The producer's accuracies of the classes Rs and Sb were found to be 96,3% and 78,3%, respectively. For these classes, the user's accuracies (87,3% and 65,9%) were relatively low. The classes Rc, Cr and Tm/Pp exhibited the producer's accuracies of 55,1%, 64,4%, and 95%, respectively.

Table 3.23 The error matrix of the (5*5) filtered QuickBird XS image

	Cr	Rc	Rs	Sb	Tm/Pp	RTot
Cr	223	0	2	0	8	233
Rc	31	16	1	0	2	50
Rs	26	0	186	0	1	213
Sb	0	8	0	29	7	44
Tm/Pp	66	5	4	8	344	427
CTot	346	29	193	37	362	967
Producer's (%)	64,4	55,1	96,3	78,3	95	
User's (%)	95,7	32	87,3	65,9	80,5	
Overall (%) = 82,5 Kappa (%) = 75						

The error matrix of the QuickBird PS image is given in table 3.24. For this image, the overall accuracy and overall kappa were computed to be 86,2% and 80,5%, respectively. The class Rc had the lowest producer's accuracy of 58,6% and a user's accuracy of 31,4%. The classes Rs and Sb provided the producer's accuracies of 96,3% and 91,8%. For these classes, the user's accuracies were 87,3% and 66,6%, respectively. While the producer's accuracies of the classes Cr and Tm/Pp were 74,5% and 93,6%, respectively, their user's accuracies were found to be 95,9% and 89,2%, respectively.

Table 3.24 The error matrix of the (5*5) filtered Quickbird PS image

	Cr	Rc	Rs	Sb	Tm/Pp	RTot
Cr	258	0	2	0	9	269
Rc	33	17	1	0	3	54
Rs	26	0	186	0	1	213
Sb	0	7	0	34	10	51
Tm/Pp	29	5	4	3	339	380
CTot	346	29	193	37	362	967
Producer's (%)	74,5	58,6	96,3	91,8	93,6	
User's (%)	95,9	31,4	87,3	66,6	89,2	
Overall (%) = 86,2	Kappa (%) = 80,5					

3.7.2.3 7*7 Filtering

The overall, producer's and user's accuracies of the 7*7 filtered SPOT4 image are given in table 3.25. As can be seen in the table, the overall accuracy and overall kappa were computed to be 62,3% and 44,7%, respectively. The class Tm/Pp had the highest producer's accuracy of 86.1% and relatively low user's accuracy of 50.4%. The producer's accuracies of the classes Rc, Rs and Sb were moderate but the class Cr exhibited a remarkably low producer's accuracy of 23.2%. The reason for Cr to produce low producer's accuracy is that it exhibits high omission error.

Table 3.25 The error matrix of the (7*7) filtered SPOT4 XS image

	Cr	Tm/Pp	Rc	Rs	Sb	RTot
Cr	61	4	3	3	0	71
Tm/Pp	183	311	7	99	17	617
Rc	3	1	17	0	1	22
Rs	13	23	0	230	1	267
Sb	2	22	2	0	18	44
CTot	262	361	29	332	37	1021
Producer's (%)	23,2	86,1	58,6	69,2	48,6	
User's (%)	85,9	50,4	77,2	86,1	40,9	
Overall (%) = 62,3 Kappa (%) = 44,7						

The SPOT 5 image provided an overall accuracy of 73,1% and an overall kappa of 60,8% (Table 3.26). The lowest producer's accuracy of 42,3% was obtained for the class Cr. But, surprisingly this class had a significantly high user's accuracy of 91,7%. While the classes Tm/Pp and Rc exhibited the producer's accuracies of 95,2% and 65,5%, their user's accuracies were found to be 59,1% and 86,3%, respectively. On the other hand, the producer's accuracies of the classes Rs and Sb were computed to be around 75% and the user's accuracies were computed to be 97,2% and 64,4%, respectively.

Table 3.26 The error matrix of the (7*7) filtered SPOT5 XS image

	Cr	Tm/Pp	Rc	Rs	Sb	RTot
Cr	111	6	3	1	0	121
Tm/Pp	142	344	2	87	7	582
Rc	2	0	19	0	1	22
Rs	6	1	0	244	0	251
Sb	1	10	5	0	29	45
Producer's (%)	42,3	95,2	65,5	73,4	78,3	
User's (%)	91,7	59,1	86,3	97,2	64,4	
Overall (%) = 73,1 Kappa (%) = 60,8						

For the IKONOS image, the overall accuracy and overall kappa were computed to be 86,6% and 80,9%, respectively (Table 3.27). The maximum producer's accuracy of 100% was provided by the class Sb, which provided

relatively lower user's accuracy of 72,5%. The reason for this class providing relatively low accuracy is that 37 fields out of the total 51 were correctly classified as Sb on the ground. The accuracies of the other classes were around 85%, which can be considered remarkably high.

Table 3.27 The error matrix of the (7*7) filtered IKONOS XS image

	Cr	Tm/Pp	Rc	Rs	Sb	RTot
Cr	204	17	2	5	0	228
Tm/Pp	49	332	1	38	0	420
Rc	3	0	23	0	0	26
Rs	6	1	0	289	0	296
Sb	0	11	3	0	37	51
CTot	262	361	29	332	37	1021
Producer's (%)	77,8	91,9	79,3	87	100	
User's (%)	89,4	79	88,4	97,6	72,5	
Overall (%) = 86,6	Kappa (%) = 80,9					

When the results of the QuickBird multispectral image are examined it can be seen that the overall accuracy and overall kappa are 82,7% and kappa 75,3%, respectively (Table 3.28). For Rs and Sb, the producer's accuracies were computed to be 95,8% and 78,3% while the user's accuracies were found to be 87,6% and 69%, respectively. The lowest producer's and user's accuracies were obtained for the class Rc as 55,1% and 32,6%, respectively. While the classes Cr and Tm/Pp yielded 65% and 95,3% producer's accuracies, their user's accuracies were computed to be 95,7% and 80,2%, respectively.

Table 3.28 The error matrix of the (7*7) filtered QuickBird XS image

	Cr	Rc	Rs	Sb	Tm/Pp	RTot
Cr	225	0	2	0	8	235
Rc	30	16	1	0	2	49
Rs	25	0	185	0	1	211
Sb	0	7	0	29	6	42
Tm/Pp	66	6	5	8	345	430
CTot	346	29	193	37	362	967
Producer's (%)	65	55,1	95,8	78,3	95,3	
User's (%)	95,7	32,6	87,6	69	80,2	
Overall (%) = 82,7	Kappa (%) = 75,3					

For the QuickBird PS image, the overall accuracy and overall kappa were computed to be 86,2% and 80,5%, respectively (Table 3.29). While the producer's accuracies of the classes Rs, Sb and Tm/Pp were obtained to be around 90%, their user's accuracies were found to be 87,7%, 66,6% and 89,2%, respectively. The class Rc exhibited the lowest producer's and user's accuracies of 58,6% and 31,4%, respectively.

Table 3.29 The error matrix of the (7*7) filtered QuickBird PS image

	Cr	Rc	Rs	Sb	Tm/Pp	RTot
Cr	257	1	2	0	9	269
Rc	34	17	1	0	2	54
Rs	25	0	186	0	1	212
Sb	0	7	0	34	10	51
Tm/Pp	30	4	4	3	340	381
CTot	346	29	193	37	362	967
Producer's (%)	74,2	58,6	96,3	91,8	93,9	
User's (%)	95,5	31,4	87,7	66,6	89,2	
Overall (%) = 86,2	Kappa (%) = 80,5					

3.7.3 Classification of All Bands

After performing the classification using the common bands, the polygon-based classification of each image was carried out using all the bands to see the effects of the blue and SWIR bands. First, the SPOT4 XS image was classified and the accuracies were obtained. As can be seen in table 3.30, the overall accuracy and overall kappa were computed to be 76,3% and

65,6%, respectively. While the producer's accuracies of the classes Rs and Sb were 79,8% and 72,9%, respectively, their user's accuracies were computed to be 97,4% and 81,8%. The classes Rc, Cr and Tm/Pp exhibited the producer's accuracies of 68,9%, 47,3%, and 95,2% and the user's accuracies of 66,6%, 88,5% and 63%, respectively. The class Cr had the lowest producer's accuracy of 47,3% and relatively high user's accuracy of 88,5%.

Table 3.30 The error matrix of the SPOT4 XS image

	Cr	Tm/Pp	Rc	Rs	Sb	RTot
Cr	124	7	0	9	0	140
Tm/Pp	127	344	7	58	10	546
Rc	5	5	20	0	0	30
Rs	6	1	0	265	0	272
Sb	0	4	2	0	27	33
CTot	262	361	29	332	37	1021
Producer's (%)	47,3	95,2	68,9	79,8	72,9	
User's (%)	88,5	63	66,6	97,4	81,8	
Overall (%) = 76,3	Kappa (%) = 65,6					

The error matrix generated for the SPOT5 XS image is given in table 3.31. As can be seen in the table, the overall accuracy and overall kappa were computed to be 77,9% and 67,8%, respectively. The classes Tm/Pp and Rc produced the producer's accuracies of 97,2% and 79,3% and the user's accuracies of 63,7% and 82,1%, respectively. On the other hand, both the classes Cr, Rs, and Tm/Pp exhibited remarkably high accuracies. The lowest producer's accuracy (41,2%) was obtained for the class Cr. However, despite a low producer's accuracy, the user's accuracy of this class (94,7%) was significantly high. The reason is that a number of 143 fields of 262 were wrongly classified as Tm/Pp.

Table 3.31 The error matrix of the SPOT5 XS image

	Cr	Tm/Pp	Rc	Rs	Sb	RTot
Cr	108	4	0	2	0	114
Tm/Pp	143	351	4	44	9	551
Rc	5	0	23	0	0	28
Rs	6	2	0	286	0	294
Sb	0	4	2	0	28	34
CTot	262	361	29	332	37	1021
Producer's (%)	41,2	97,2	79,3	86,1	75,6	
User's (%)	94,7	63,7	82,1	97,2	82,3	
Overall (%) = 77,9 Kappa (%) = 67,8						

When the error matrix of the IKONOS image are examined, it can be seen that both the overall accuracy (88,9%) and overall kappa (84,1%) are relatively high (Table 3.32). The highest classification accuracy (100%) was obtained for the class Sb. However, despite a high producer's accuracy, the user's accuracy of Sb (75,5%) was relatively low. The classes Rs and Rc provided the producer's accuracies of 90% and 79,3% and the user's accuracies of 97,3% and 85,1%, respectively. Similarly, for the classes Cr and Tm/Pp, the producer's accuracies (79,3% and 94,4%) and the users accuracies (92,4% and 82,5%, respectively) were computed to be remarkably high.

Table 3.32 The error matrix of the IKONOS XS image

	Cr	Tm/Pp	Rc	Rs	Sb	RTot
Cr	208	9	2	6	0	225
Tm/Pp	44	341	1	27	0	413
Rc	4	0	23	0	0	27
Rs	6	2	0	299	0	307
Sb	0	9	3	0	37	49
CTot	262	361	29	332	37	1021
Producer's (%)	79,3	94,4	79,3	90	100	
User's (%)	92,4	82,5	85,1	97,3	75,5	
Overall (%) = 88,9 Kappa (%) = 84,1						

The overall accuracy and overall kappa of the all bands classification of the QuickBird XS image were computed to be 85,0% and 78,7%, respectively (Table 3.33). Although the training representation was marginal for the producer's level, the user's accuracy of the class Rc exhibited the lowest accuracy. On the other hand, the classes Cr, Rs, and Tm/Pp exhibited remarkably high producer's and user's accuracies.

Table 3.33 The error matrix of the QuickBird XS image

	Cr	Rc	Rs	Sb	Tm/Pp	RTot
Cr	249	1	2	0	9	261
Rc	28	18	1	0	4	51
Rs	28	0	187	0	3	218
Sb	0	6	0	34	12	52
Tm/Pp	41	4	3	3	334	385
CTot	346	29	193	37	362	967
Producer's (%)	71,9	62	96,8	91,8	92,2	
User's (%)	95,4	35,2	85,7	65,3	86,7	
Overall (%) = 85	Kappa (%) = 78,7					

Finally, the QuickBird PS image was classified using the all bands. The results are given in table 3.34. As can be seen in the table, the overall accuracy and overall kappa were computed to be 85,5% and 79,5% respectively. Similar to the QuickBird XS image, the class Rc provided the lowest producer's and user's accuracies of 58,6% and 30,3%, respectively. On the other hand, the classes Cr, Rs, and Tm/Pp exhibited remarkably high user's and producer's accuracies.

Table 3.34 The error matrix of the QuickBird PS image

	Cr	Rc	Rs	Sb	Tm/Pp	RTot
Cr	262	1	2	0	10	275
Rc	31	17	1	0	7	56
Rs	28	0	187	0	3	218
Sb	0	7	0	33	14	54
Tm/Pp	25	4	3	4	328	364
CTot	346	29	193	37	362	967
Producer's (%)	75,7	58,6	96,8	89,1	90,6	
User's (%)	95,2	30,3	85,7	61,1	90,1	
Overall (%) = 85,5	Kappa (%) = 79,5					

3.8 Comparing the filtered and unfiltered images

The summary of the accuracies of the classified filtered and unfiltered images is given in Table 3.35. As can be seen in the table that for the SPOT4 XS image, the accuracies decreased when the filtered bands were used for the classification. While, the overall accuracy was computed to be 76,1% when the unfiltered bands were classified, it decreased by about 5% when using the 3*3 filtered bands. On the other hand, the decrease was 10% for the 5*5 filtered image and 15% for the 7*7 filtered image. The lowest producer's accuracy (about 20%) was observed for the class Rc while the class Tm provided the highest producer's accuracy. On the other hand, the lowest user's accuracy was computed for the class Sb, while the highest user's accuracy of about 95% was computed for the class Rs.

Table 3.35 The overall accuracies of the unfiltered bands and the filtered bands of the images

	O.A.of the Unfiltered B.	O.A. of the 3*3 Filtering	O.A. of the 5*5 Filtering	O.A. of the 7*7Filtering
SPOT4 XS	76,1%	71,8%	66,6%	62,3%
SPOT5 XS	81,4%	80,2%	78%	73,1%
IKONOSXS	88,6%	87,9%	86,9%	86,6%
QuickBird XS	83,7%	83,5%	82,5%	82,7%
QuickBird PS	85,8%	85,4%	86,2%	86,2%

O.A : Overall accuracy, B: Bands

The SPOT5 XS image revealed an overall accuracy of 81,4% when the classification was carried out using the unfiltered common bands. It was observed that the accuracy decreased when the filtered bands were used for the classification. The difference between the accuracies of the classified unfiltered bands and the 3*3 and 5*5 filtered bands was not significant. On

the other hand, a decrease of about 8% was observed for the classified 7*7 filtered bands. While the individual class accuracies were high enough for the classified unfiltered bands, the class Sb exhibited the lowest producer's accuracy of about 45%. The lowest user's accuracy was observed for the class Cr.

For the IKONOS image, no significant difference was observed between the results of the classified unfiltered and the filtered bands. For both the filtered and unfiltered bands, the overall accuracy was computed to be approximately 85%. The highest producer's accuracy of 100% was computed to be for the class Sb for each classified output while the user's accuracy (about 73%) of this crop was the lowest. The highest user's accuracy was found to be 97% for the class Rs for each classified output.

Similar to the IKONOS image, the overall accuracies of the QuickBird XS image did not significantly change when the image was filtered using the different kernel sizes. While the lowest producer's and user's accuracies were observed for the class Rc, the highest accuracies were provided for the class Rs.

For the QuickBird PS image, no change was observed for the overall accuracies. For this image, the overall accuracy was computed to be around 85% for both the filtered and unfiltered bands. Similar to the QuickBird XS image, the lowest producer's and user's accuracies were obtained for the class Rc. On the other hand, for each classified output, the highest individual class accuracies were provided by the class Rs.

For each spatial resolution, the overall accuracies of the post-polygon classification are illustrated graphically in figure 3.12.

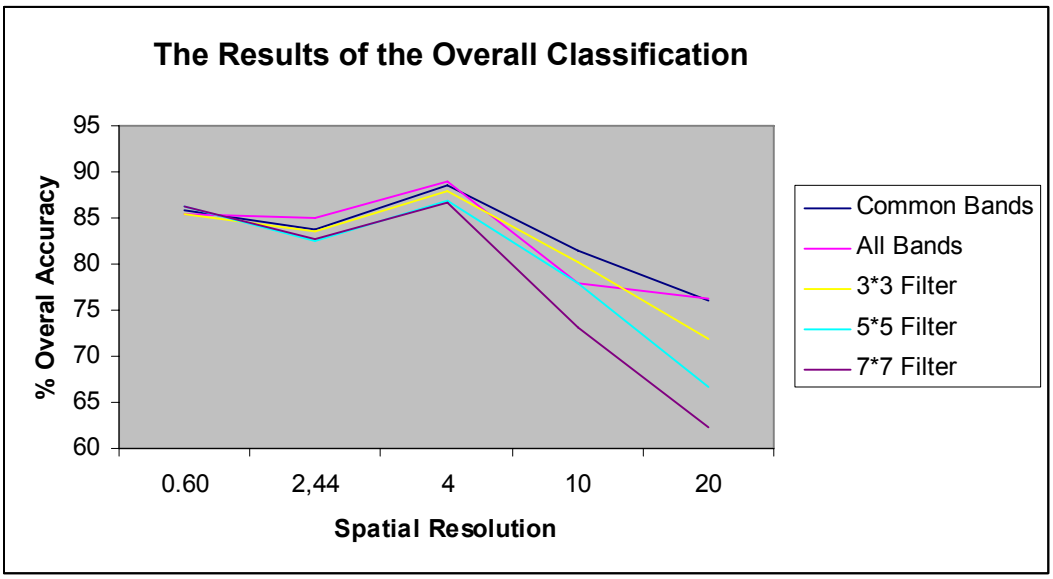

Figure 3.12 The overall accuracies of post-polygon classification for each image

CHAPTER 4

PRE - POLYGON IMAGE CLASSIFICATION

4.1 The Methodology

In this part, the pre-polygon image classification applied to images is explained. The pre-polygon image classification was carried out as follows: First, the mean, median and mode values of the images were computed for each field. Then, the per-pixel Maximum Likelihood Classification was carried out using (i) the unfiltered common bands, (ii) the filtered (Median 3*3, 5*5, and 7*7) common bands of the images. Then, the polygon-based analysis of the classified images was carried out.

4.2 Image Classification

In pre-polygon image classification (Figure 4.1), the statistical measures such as, mean, median and mode, are calculated per polygon and therefore, each field receives a unique spectral value. In this study, the mean values were used as the statistical measure. With this operation, the new bands that contain the mean values were generated for each band of each image. The purpose of computing the mean values in each polygon was to assign unique grey levels to the polygons. Next, the generated new bands were used as the inputs for the per-pixel maximum likelihood classifier.

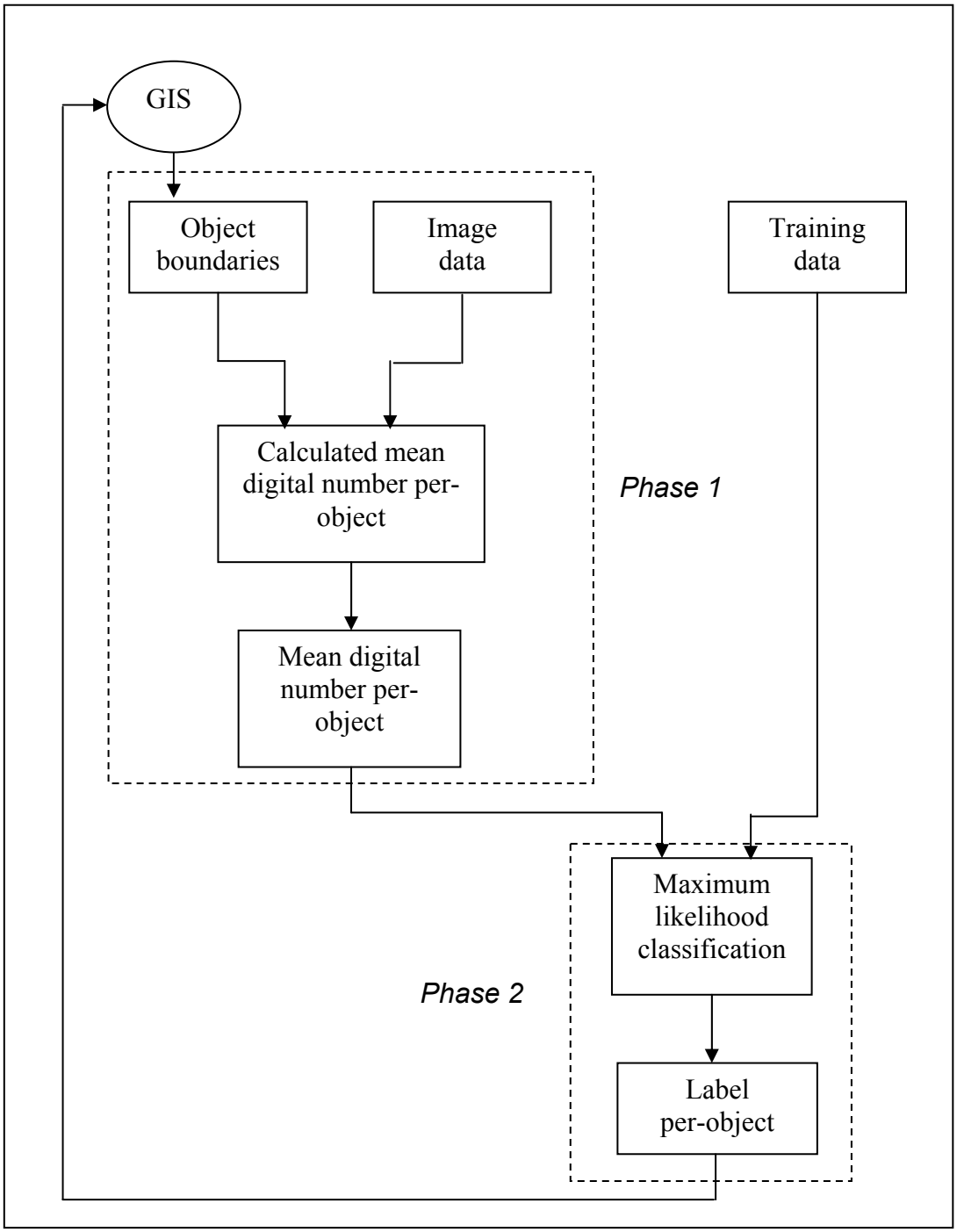

Figure 4.1 Pre-polygon classification (Janssen, 1999)

First, the common bands (green (G), red (R) and near infrared (NIR)) of all the images were used to conduct above explained pre-polygon classification procedure. As mentioned earlier, first, the mean values were computed for each field and assigned to each field. The mean bands (G, R, NIR) of a part of the study area is illustrated in figure 4.2. Then, a MLC was applied using the mean common bands (G, R and NIR) and the class label found for each field was stored in the database. The classified output of the unfiltered IKONOS image is given in figure 4.3. The classified outputs of the SPOT4, SPOT5, QuickBird XS and QuickBird PS images are provided in Appendix H.

Next, the images were filtered using the median filter (3*3, 5*5 and 7*7) prior to polygon-based classification to assess the effect of the filtering on the results of polygon-based classification. Similarly, the supervised maximum likelihood classification was repeated using the filtered common bands. For the filtering procedure, the median filter was chosen because the spectral characteristics of the images can be better preserved with this filter (Cushine, 1987).

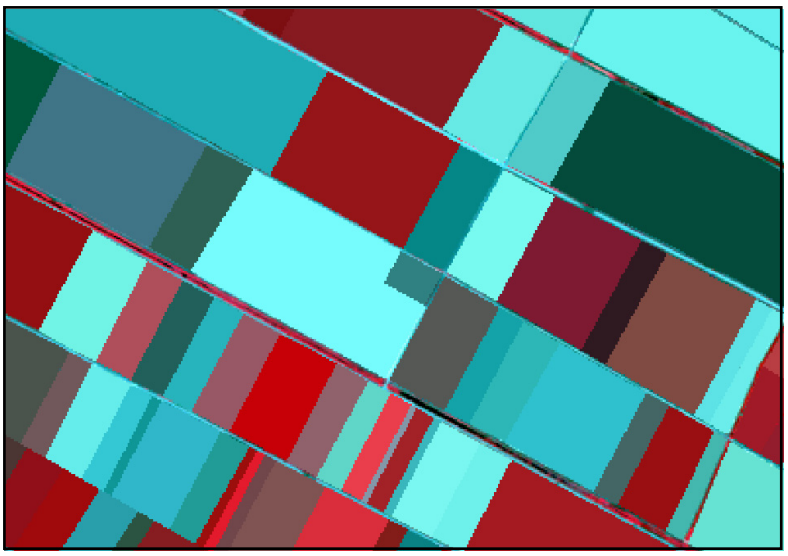

Figure 4.2 The mean bands (G, R, NIR) of IKONOS image

Figure 4.3 The output of the pre-polygon classification for the IKONOS XS image using common bands

4.3 The Results for the Mean Values

To make a more realistic comparison with the results of the post-polygon classification, the pre-polygon classification was carried out using the common bands only. Therefore, below the results of the common bands classification are given only.

4.3.1 Classification Using the Unfiltered Images

As mentioned in the previous chapter, the common bands of the images were G, R and NIR. The purpose of using the three common bands for the classification was to eliminate the spectral effects of the blue band of IKONOS and QuickBird images and the SWIR band of the SPOT images in the classification.

When the error matrix of the SPOT4 image is examined, it can be seen that the overall accuracy and overall kappa were computed to be 65,2% and 50,8%, respectively (Table 4.1). The classes Rs and Sb provided the producer's accuracies of 56,3% and 81% and the user's accuracies of 96,3% and 36,1%, respectively. The lowest producer's accuracy was obtained for the class Rc. This is because most of the Rc fields were classified as Cr and Tm/Pp. On the other hand, Rc provided the highest user's accuracy of 100%. While the producer's accuracies of the classes Cr and Tm/Pp were 78,2% and 66,4%, their user's accuracies were computed to be 69% and 54,1%, respectively.

Table 4.1 The error matrix of the SPOT 4 XS image

	Cr	Tm	Rc	Rs	Sb	RTot
Cr	205	74	14	4	0	297
Tm	49	240	7	140	7	443
Rc	0	0	4	0	0	4
Rs	5	2	0	187	0	194
Sb	3	45	4	1	30	83
CTot	262	361	29	332	37	1021
Producer's (%)	78,2	66,4	13,7	56,3	81	
User's (%)	69	54,1	100	96,3	36,1	
Overall (%) = 65,2 Kappa (%) = 50,8						

For the SPOT 5 image, the overall accuracy and overall kappa were computed to be 69,8% and 56,5%, respectively (Table 4.2). When the individual class accuracies were analyzed, it can be seen that the classes Cr and Rc provided relatively low producer's accuracies. This is due to the fact that several reference fields were not correctly classified for the classes Cr and Rc. The class Rs provided relatively high producer's and user's accuracies.

Table 4.2 The error matrix of the SPOT 5 XS image

	Rs	Tm	Cr	Sb	Rc	RTot
Rs	242	2	5	0	0	249
Tm	88	305	136	3	0	532
Cr	1	32	118	1	5	157
Sb	0	16	1	30	6	53
Rc	1	6	2	3	18	30
CTot	332	361	262	37	29	1021
Producer's (%)	72,8	84,4	45	81	62	
User's (%)	97,1	57,3	75,1	56,6	60	
Overall (%) = 69,8 Kappa (%) = 56,5						

The pre-polyon classification of the IKONOS image provided an overall accuracy of 81,8% and an overall kappa of 74,2% (Table 4.3). While the producer's accuracies of the classes Rs, Sb, and Rc were computed to be 84,9%, 97,2% and 65,5%, their user's accuracies were found to be 97,9%,

69,2% and 82,6%, respectively. The classes Cr and Tm/Pp provided the producer's accuracies in the range between 77% and 82,2% and the user's accuracies in the range between 76,2% and 75,5%. The lowest producer's accuracy was observed for the class Rc, while the other accuracies were close to each other.

Table 4.3 The error matrix of the IKONOS XS image

	Cr	Tm/Pp	Rc	Rs	Sb	RTot
Cr	202	50	7	5	1	265
Tm/Pp	51	297	0	45	0	393
Rc	4	0	19	0	0	23
Rs	5	1	0	282	0	288
Sb	0	13	3	0	36	52
CTot	262	361	29	332	37	1021
Producer's (%)	77	82,2	65,5	84,9	97,2	
User's (%)	76,2	75,5	82,6	97,9	69,2	
Overall (%) = 81,8 Kappa (%) = 74,2						

The overall, producer's and user's accuracies of the QuickBird XS image are given in Table 4.4. As can be seen in the table, the overall accuracy and overall kappa were computed to be 78,6% and 68,6%, respectively. The lowest producer's accuracies were obtained for the classes Rc and Sb. It is evident from the table that only 8 fields out of 29 were correctly classified as Rs. On the other hand, due to high commission error, the lowest user's accuracy of 53,3% was also observed for the class Rc.

Table 4.4 The error matrix of the QuickBird XS image

	Rs	Cr	Tm/Pp	Sb	Rc	RTot
Rs	180	21	1	0	0	202
Cr	1	216	14	0	5	236
Tm/Pp	12	102	341	21	13	489
Sb	0	0	6	16	3	25
Rc	0	7	0	0	8	15
CTot	193	346	362	37	29	967
Producer's(%)	93,2	62,4	94,1	43,2	27,5	
User's (%)	89,1	91,5	69,7	64	53,3	
Overall (%) = 78,6 Kappa (%) = 68,6						

The overall accuracy and overall kappa of the classified QuickBird PS image were computed to be 82,1% and 74%, respectively (Table 4.5). While the class Rs exhibited the highest accuracies, the class Rc provided the lowest producer's and user's accuracies of 34,4% and 27%, respectively. The producer's and user's accuracies of the classes Cr and Tm/Pp were high enough while the accuracies of the class Sb were marginal.

Table 4.5 The error matrix of the QuickBird PS image

	Rs	Cr	Tm/Pp	Sb	Rc	RTot
Rs	183	20	0	0	0	203
Cr	2	249	23	0	4	278
Tm	7	52	332	17	12	420
Tm/Pp	0	0	6	20	3	29
Rc	1	25	1	0	10	37
CTot	193	346	362	37	29	967
Producer's (%)	94,8	71,9	91,7	54	34,4	
User's (%)	90.1	89.5	79	68.3	27	
Overall (%) = 82,1 Kappa (%) = 74						

4.3.2 Classification Using the Filtered Images

In order to see the effect of filtering on the pre-polygon classification of the common bands, each image was filtered using the kernel sizes of 3*3, 5*5 and 7*7 and the classification operation was carried out using the filtered

images. The median filter was chosen because the original spectral values are better preserved by the median filter when compared with the mean filter.

4.3.2.1 3*3 Filtering

The accuracies of the classified 3*3 filtered SPOT4 image are given in table 4.6. It can be seen in the table that the overall accuracy and overall kappa were found to be 64,8% and 49,9%, respectively. The class Rc provided the lowest producer's accuracy of 17,2%. The low producer's accuracy of Rc is due to the fact that only five reference fields out of 29 were correctly classified. Although 78,3% of the reference fields were correctly identified as Sb, only 32,5% fields that were labeled Sb are actually sugarbeet on the ground. The class Cr exhibited moderate producer's and user's accuracies.

Table 4.6 The error matrix of the (3*3) filtered SPOT 4 XS image

	Cr	Tm/Pp	Rc	Rs	Sb	RTot
Cr	163	38	9	8	1	219
Tm/Pp	85	274	9	131	7	506
Rc	1	1	5	0	0	7
Rs	6	2	0	192	0	200
Sb	7	46	6	1	29	89
CTot	262	361	29	332	37	1021
Producer's (%)	62,2	75,9	17,2	57,5	78,3	
User's (%)	74,4	54	71,4	95,9	32,5	
Overall (%) = 64,8 Kappa (%) = 49,9						

For the classified filtered SPOT 5 image, the overall accuracy and overall kappa were found to be 78,6% and 69,4%, respectively (Table 4.7). For this image, the lowest producer's accuracy was obtained for the class Rc, which exhibited relatively high user's accuracy. The producer's accuracies of the other classes were above 75%. When the user's accuracies were examined, it was observed that the class Rs provided the highest value of 97%.

Table 4.7 The error matrix of the (3*3) filtered SPOT 5 XS image

	Cr	Tm/Pp	Rc	Rs	Sb	RTot
Cr	205	64	10	2	1	282
Tm/Pp	48	288	0	64	5	405
Rc	3	0	14	0	0	17
Rs	6	2	0	265	0	273
Sb	0	7	5	1	31	44
CTot	262	361	29	332	37	1021
Producer's (%)	78,2	79,7	48,2	79,8	83,7	
User's (%)	72,6	71,1	82,3	97	70,4	
Overall (%) = 78,6 Kappa (%) = 69,4						

After classifying the filtered IKONOS image, it was found that the overall accuracy and overall kappa were 81% and 73%, respectively (Table 4.8). The lowest producer's accuracy of 65,5% was obtained for the class Rc. It appears that ten rice pixels were omitted from this class. On the other hand, 86,3% of the rice fields classified as Rc actually represent the Rc category on the ground. The procedure's and user's accuracies of the other classes were relatively high.

Table 4.8 The error matrix of the (3*3) filtered IKONOS XS image

	Cr	Tm	Rc	Rs	Sb	RTot
Cr	203	47	7	5	1	263
Tm	50	301	0	57	0	408
Rc	3	0	19	0	0	22
Rs	6	1	0	270	0	277
Sb	0	12	3	0	36	51
CTot	262	361	29	332	37	1021
Producer's(%)	77,4	83,3	65,5	81	97,2	
User's (%)	77,1	73,5	86,3	97,4	70,5	
Overall (%) = 81 Kappa (%) = 73						

The results of the classified filtered QuickBird XS image are given in table 4.9. For this image, the overall accuracy and overall kappa were computed to be 78,5% and 68,6%, respectively. The classes Sb and Rc provided relatively low producer's and user's accuracies. It appears that, for these classes, a number of fields were not classified correctly and therefore, they

revealed low accuracies. Of the classes, Rs provided the highest producer's and user's accuracies.

Table 4.9 The error matrix of the (3*3) filtered QuickBird XS image

	Rs	Cr	Tm/Pp	Sb	Rc	RTot
Rs	180	21	1	0	0	202
Cr	1	215	15	0	5	236
Tm/Pp	12	100	339	20	11	482
Sb	0	0	7	17	4	28
Rc	0	10	0	0	9	19
CTot	193	346	362	37	29	967
Producer's (%)	93,2	62,1	93,6	45,9	31	
User's (%)	89,1	91,1	70,3	60,7	47,3	
Overall (%) = 78,5		Kappa (%) = 68,6				

For the QuickBird PS image, the classification of the filtered bands provided an overall accuracy of 82,1% and an overall kappa of 74% (Table 4.10). The lowest accuracies were obtained for the class Rc. The reason for Rc to produce low accuracies is that it demonstrates high omission and commission errors. While the class Sb exhibited marginal accuracies, the accuracies of the other classes were significantly high.

Table 4.10 The error matrix of the (3*3) filtered QuickBird PS image

	Rs	Cr	Tm	Sb	Rc	RTot
Rs	183	20	0	0	0	203
Cr	2	249	23	0	4	278
Tm	7	52	332	17	12	420
Sb	0	0	6	20	3	29
Rc	1	25	1	0	10	37
CTot	193	346	362	37	29	967
Producer's (%)	94,8	71,9	91,7	54	34,4	
User's (%)	90,1	89,5	79	68,9	27	
Overall (%) = 82,1	Kappa (%) = 74					

4.3.2.2 5*5 Filtering

Next, the original common bands of each image were filtered using the kernel size of 5*5. For SPOT4, the overall accuracy and overall kappa were computed to be 61,7% and 44,6%, respectively (Table 4.11). In general, except for the class Tm/Pp, the producer's accuracies were found to be low. Although 82,5% of the Tm/Pp fields were correctly classified, only 50,6% of these fields labeled Tm/Pp are actually tomato/pepper on the ground. The lowest user's accuracy of 28,1% was obtained for the class Sb. The producer's accuracy of Sb was also low. On the other hand, the producer's accuracies of the classes Cr and Rc were remarkably low. This is due to the fact that for these classes, a significant number of fields were omitted.

Table 4.11 The error matrix of the (5*5) filtered SPOT 4 XS image

	Cr	Tm/Pp	Rc	Rs	Sb	RTot
Cr	103	20	9	8	1	141
Tm/Pp	147	298	4	124	15	587
Rc	2	0	10	0	1	13
Rs	6	3	0	199	0	209
Sb	4	40	6	1	20	71
CTot	262	361	29	332	37	1021
Producer's (%)	39,3	82,5	34,4	59,9	54	
User's (%)	73	50,6	76,9	95,6	28,1	
Overall (%) = 61,7 Kappa (%) = 44,6						

The results of the classified SPOT 5 image are given in table 4.12. As can be seen in the table, SPOT 5 provided an overall accuracy of 71,8%, and a rather low overall kappa of 59,9% (Table 4.12). The lowest producer's accuracy (27,5%) was obtained for the class Rc. This is because only 8 fields of the total 29 were classified correctly as Rc. The other fields belonging to rice were omitted from this class. On the other hand, Rc exhibited a relatively high accuracy of 72,7%. The lowest user's accuracy of 40.7% was computed for the class Sb although the training representaion was good enough for this field.

Table 4.12 The error matrix results of the 5*5 filtered SPOT 5 XS image

	Cr	Tm/Pp	Rc	Rs	Sb	RTot
Cr	168	42	13	3	0	226
Tm/Pp	88	292	2	81	5	468
Rc	2	0	8	0	1	11
Rs	4	1	0	235	0	240
Sb	0	26	6	13	31	76
CTot	262	361	29	332	37	1021
Producer's (%)	64,1	80,8	27,5	70,7	83,7	
User's (%)	74,3	62,3	72,7	97,9	40,7	
Overall (%) = 71,8	Kappa (%) = 59,9					

For the classified filtered IKONOS image, the overall accuracy and overall kappa were obtained to be 83,1% and 75,9%, respectively (Table 4.13). It can be seen in the table that the accuracies are noticeably high. Both the producer's and user's accuracies of the classes Rs, Tm/Pp and Cr were above 75%. The producer's accuracies of the classes Sb and Rc were computed to be 94,5% and 68,9%, respectively. On the other hand, these classes provided 81,3% and 86,9% user's accuracies.

Table 4.13 The error matrix of the (5*5) filtered IKONOS XS image

	Rs	Tm/Pp	Cr	Sb	Rc	RTot
Rs	280	1	6	0	0	287
Tm/Pp	46	310	49	1	1	407
Cr	6	44	204	1	6	261
Sb	0	6	0	35	2	43
Rc	0	0	3	0	20	23
CTot	332	361	262	37	29	1021
Producer's (%)	84,3	85,8	77,8	94,5	68,9	
User's (%)	97,5	76,1	78,1	81,3	86,9	
Overall (%) = 83,1	Kappa (%) = 75,9					

The results of the filtered QuickBird XS image is given in table 4.14. As can be seen in the table, the overall accuracy and overall kappa were computed

to be 79,2% and 69,6%, respectively. The classes Sb and Rc provided remarkably low accuracies, while the accuracies of the other classes were around 80%. The producer's accuracies of the classes Sb and Rc were 45,9% and 34,4%, respectively and their user's accuracies were 54,8% and 50%. The reason for the low accuracies of these classes is that they exhibit high omission and commission errors.

Table 4.14 The error matrix of the (5*5) filtered QuickBird XS image

	Rs	Cr	Tm/Pp	Sb	Rc	RTot
Rs	179	20	1	0	0	200
Cr	1	223	14	0	4	242
Tm/Pp	13	94	337	20	10	474
Sb	0	0	9	17	5	31
Rc	0	9	1	0	10	20
CTot	193	346	362	37	29	967
Producer's (%)	92,7	64,4	93	45,9	34,4	
User's (%)	89,5	92,1	71	54,8	50	
Overall (%) : 79,2 Kappa (%) : 69,6						

The error matrix of the classified filtered QuickBird PS is given in table 4.15. As can be seen in the table, the overall accuracy and overall kappa were computed to be 82,8% and 75,1%, respectively. It is evident that only 10 fields of the total 29 were correctly classified as Rc. Similarly a significant number of Rc fields were included wrongly into other classes. Therefore, both the producer's and user's accuracies were found to be very low for this class. The accuracies of the other classes were computed to be around 80%, which can be considered high.

Table 4.15 The error matrix of the (5*5) filtered QuickBird PS image

	Rs	Cr	Tm	Sb	Rc	RTot
Rs	179	20	1	0	0	200
Cr	1	223	14	0	4	242
Tm	13	94	337	20	10	474
Sb	0	0	9	17	5	31
Rc	0	9	1	0	10	20
CTot	193	346	362	37	29	967
Producer's (%)	94,8	71,6	92,8	62,1	37,9	
User's (%)	90,1	89,5	80	79,3	27,5	
Overall (%) = 82,8 Kappa (%) = 75,1						

4.3.2.3 7*7 Filtering

Next, the kernel size was increased to 7*7. Similarly, after performing the classification operation, the error matrices were constructed for each classified output. The results of the classified filtered SPOT 4 image are given in table 4.16. As can be seen in the table, the overall accuracy (59,3%) and overall kappa (40,5%) are rather low. When the individual class accuracies are examined, it can be seen that the lowest producer's accuracy of 20,6% was obtained for the class Rc. It appears that the training representation of the class Rc is not good causing a high omission error, therefore.

Table 4.16 The error matrix of the (7*7) filtered SPOT4 XS image

	Cr	Tm/Pp	Rc	Rs	Sb	RTot
Cr	91	19	11	11	2	134
Tm/Pp	152	304	7	131	18	611
Rc	2	0	6	0	1	9
Rs	12	12	0	190	1	216
Sb	5	26	5	0	15	51
CTot	262	361	29	332	37	1021
Producer's (%)	34,7	84,2	20,6	57,2	40,5	
User's (%)	67,9	49,6	66,6	88,3	29,4	
Overall (%) = 59,3 Kappa (%) = 40,5						

For the filtered SPOT 5 image, the overall accuracy and overall kappa were computed to be 66,9% and 52,6% (Table 4.17). The producer's accuracies

of the classes Cr, Tm/Pp and Rs were found to be 59,1%, 81,1% and 34,4%, respectively, while the user's accuracies for these classes were computed to be 72,7%, 56,2% and 71,4%. The classes Rs and Sb provided the producer's accuracies of 59,6% and 75,6% and the user's accuracies of 96,1% and 41,7%, respectively. The class Rc had the lowest producer's accuracy of 34,4% and relatively high user's accuracy of 71,4%. On the other hand, the class Sb exhibited the lowest user's accuracy of 41,7%, and remarkably high producer's accuracy of 75,6%.

Table 4.17 The error matrix of the (7*7) filtered SPOT5 XS image

	Cr	Tm/Pp	Rc	Rs	Sb	RTot
Cr	155	38	13	5	2	213
Tm/Pp	95	293	2	125	6	521
Rc	3	0	10	0	1	14
Rs	5	3	0	198	0	206
Sb	4	27	4	4	28	67
CTot	262	361	29	332	37	1021
Producer's (%)	59,1	81,1	34,4	59,6	75,6	
User's (%)	72,7	56,2	71,4	96,1	41,7	
Overall (%) = 66,9 Kappa (%) = 52,6						

The results of the IKONOS image are given table 4.18. As can be seen in the table, the overall accuracy and overall kappa were computed to be 69,3% and 55,6%, respectively. The lowest producer's accuracy was obtained for the class Rs, which surprisingly provided the highest user's accuracy. On the other hand, the lowest user's accuracy of 56,5% was obtained for the class Tm/Pp.

Table 4.18 The error matrix of the (7*7) filtered IKONOS XS image

	Rs	Tm/Pp	Cr	Sb	Rc	RTot
Rs	157	0	4	0	0	161
Tm/Pp	171	319	66	6	2	564
Cr	3	36	179	1	3	222
Sb	0	4	0	30	1	35
Rc	1	2	13	0	23	39
CTot	332	361	262	37	29	1021
Producer's (%)	47,2	88,3	68,3	81	79,3	
User's (%)	97,5	56,5	80,6	85,7	58,9	
Overall (%) : 69,3% Kappa (%) : 55,9						

Of the two QuickBird images, the XS image provided an overall accuracy of 79,2% and an overall kappa of 69,6% (Table 4.19). For this image, the lowest producer's and user's accuracies of both the producer's and user's were obtained for the class Rc. The class Sb also exhibited a low producer's accuracy of 45,9% and the user's accuracy of 51,5%. On the other hand, the class Rs provided the highest accuracies.

Table 4.19 The error matrix of the (7*7) filtered Quickbird XS image

	Rs	Cr	Tm/Pp	Sb	Rc	RTot
Rs	178	17	1	0	0	196
Cr	1	226	15	0	4	246
Tm/Pp	13	89	335	20	10	467
Sb	0	0	11	17	5	33
Rc	1	14	0	0	10	25
CTot	193	346	362	37	29	967
Producer's (%)	92,2	65,3	92,5	45,9	34,4	
User's (%)	90,8	91,8	71,7	51,5	40	
Overall (%) = 79,2 Kappa (%) = 69,6						

The overall accuracy and overall kappa computed for the QuickBird PS image were 82,9% and 75,3% (Table 4.20). Similar to QuickBird XS image, the class Rs provided the highest producer's and user's accuracies. The accuracies of the class Tm/Pp were also remarkably high. While the class Sb exhibited marginally high accuracies, the class Rc provided significantly

low accuracies for both the producer's and user's. It is evident that the class Rc contains high omission and commission errors. On the other hand, for the class Cr, the producer's and user's accuracies were computed to be 89,8% and 71,6%.

Table 4.20 The error matrix of the (7*7) filtered QuickBird PS image

	Rs	Cr	Tm/Pp	Sb	Rc	RTot
Rs	183	20	1	0	0	204
Cr	2	248	21	0	5	276
Tm/Pp	7	51	336	13	10	417
Sb	0	0	3	24	3	30
Rc	1	27	1	0	11	40
CTot	193	346	362	37	29	967
Producer's (%)	94,8	71,6	92,8	64,8	37,9	
User's (%)	89,7	89,8	80,5	80	27,5	
Overall (%) = 82,9 Kappa (%) = 75,3						

4.3.3 Comparing the results of the unfiltered and filtered images

A significant difference was not observed for the SPOT 4 image between the results of the classified unfiltered and the 3*3 filtered images. When the accuracies of individual class were examined, it was observed that the accuracies of the classes Rs, Sb and Tm/Pp did not significantly change. However a decrease of about 30% was observed for the class Rc when the filtered SPOT4 image was used. On the other hand, the producer`s accuracy of the class Cr decreased by about 15% while it`s user`s accuracy increased by about 5%.

For the SPOT 5 image, an increase of about 8% and 10% were observed for the overall accuracy and overall kappa, respectively. While the producer`s accuracy of the Rc was marginal (about 60%) for the classified unfiltered images, a decrease of about 10% was observed for the producer's accuracy when the filtered image was used. On the other hand, the class Rs did not

exhibit a significant difference between the results of the unfiltered and filtered images.

The overall accuracy (81%) and overall kappa (73%) of the IKONOS image remained the same when the filtered image was used in the classification. In general, the accuracies of the individual classes were high. The highest producer`s accuracy of 97,2% was obtained for the class Sb, which exhibited relatively low user`s accuracy of 70,5%. On the other hand, the class Rs provided the highest user`s accuracy of 97,4% when the filtered image was used in the classification.

For the QuickBird XS image, no change was observed between the filtered and unfiltered images. The lowest producer's (31%) and user's accuracies (47,3%) were observed for the class Rc. For the filtered image, the class Tm/Pp had the highest producer`s accuracy of 93.6% and a relatively low user's accuracy of 70,3%. On the other hand, the highest user's accuracy of 89,1% was computed for the class Rs, which also provided a significantly high user's accuracy of 90%.

For the QuickBird PS image, a decrease of about 3% was observed in the overall accuracy and overall kappa of the classified filtered images. When the accuracies of the individual classes were analyzed, it can be seen that the accuracies of the classes Rc and Tm/Pp did not significantly change. Of these classes, the class Tm/Pp provided the highest producer's accuracy for the filtered image. The highest user's accuracy was obtained for the class Rs (98,7%). On the other hand, the lowest producer`s and user`s accuracies were computed to be 34,4% and 25,6% , respectively.

When the results of the classified unfiltered and 5*5 filtered images are analyzed it can be seen that for the SPOT 4 image, the overall accuracy and overall kappa decreased by about 5% when the classification was performed

using the filtered images. No significant change was observed for the class Rs. On the other hand, a significant decrease was seen in the producer's accuracies of the classes Sb and Cr. The lowest producer`s accuracy of 34,4% was observed for the class Rc, which provided relatively high user`s accuracy of 76,9%. While the class Sb had the lowest user`s accuracy, it`s producer`s accuracy was marginal.

For the SPOT 5 image, no significant change was observed for the overall accuracy of the filtered image, while an increase of about 3% was seen in overall kappa. The classes Rs and Tm/Pp did not exhibit a significant change. While the producer`s accuracy of the class Rc decreased from 62% to 27,5%, an increase of about 10% was seen in the user's accuracy of this class. The producer`s accuracy of the class Cr also increased by about 20% when the filtered bands were classified.

For the IKONOS image, both the overall accuracy and overall kappa were found to be higher for the filtered image than the unfiltered image. For the overall accuracy and overall kappa, an increase of about 2% was observed. While the accuracy of the classes Rs, Rc, Cr and Tm/Pp did not exhibit a significant change, the user`s accuracy of the class Sb increased by about 10% when the classification was carried out using the filtered image.

For the classified filtered QuickBird XS image, an increase of about 1% was observed. Similar to IKONOS image, the accuracies of the classes Rs, Rc. Cr and Tm/Pp did not significantly change when the filtered bands were used. However, the user`s accuracy of the class Sb decreased by about 10%. The lowest accuracies were obtained for the class Rc.

For the QuickBird PS image, a decrease of about 2% was observed for the overall accuracy and overall kappa when the classification was performed using the filtered bands. The accuracies of the classes Rc and Tm/Pp did not

significantly change. The lowest producer's accuracy of 37,9% and the user's accuracy of 27,5% were obtained for the class Rc. For the producer's and user`s accuracies of the class Sb, an increase of about 5% and 10%, respectively, was observed.

When the results of the classified unfiltered and 7*7 filtered images are analyzed it can be seen that for the SPOT 4 image, both the overall accuracy and overall kappa decreased by about 5% and 10%, respectively. When the accuracies of the individual classes were compared, no significant change was observed for the class Rs. On the other hand, for the classes Sb and Cr, a significant difference was seen between the results of the filtered and unfiltered bands. The producer's accuracies of these classes decreased by about 40%. The lowest producer's accuracy was computed as 20,6% for the class Rc while the user's accuracy for this class was marginal. On the other hand, the class Sb provided the lowest user`s accuracy of 29,4%.

For the SPOT 5 image, no change was observed in the overall accuracy and overall kappa between the filtered and unfiltered images. The class Rc provided the lowest producer's accuracy of 34,4% for the filtered image while the producer's accuracy of the unfiltered image was marginal. The lowest user`s accuracy of 41,7% was observed for the class Sb, which provided relatively high user`s accuracy of 75,6%. On the other hand, no significant change was observed for the class Tm/Pp between the results of the filtered and unfiltered images.

For the IKONOS image, the overall accuracy and overall kappa were found to be lower for the filtered image. For both the overall accuracy and overall kappa, a decrease of about 10% was observed. The producer's accuracy of the class Rs decreased significantly (about 40%) but this class provided a remarkably high user's accuracy of 97,5%. This result was the lowest producer`s accuracy for the filtered image.

For the QuickBird XS image, both the producer`s and user's accuracies increased by about 1% when the filtered image was used for the classification. When the accuracies of the individual classes were examined, it was observed that the classes Rs, Sb, Cr and Tm/Pp did not show a significant difference. On the other hand, the lowest accuracies were observed for the class Rc.

The overall accuracies of the QuickBird PS remained unchanged when the filtered image was used for the classification. No significant change was observed for the classes Rs, Rc, Cr and Tm/Pp. On the other hand, for the class Sb, both the producer's and user's accuracies increased by about 10% when the filtered image was used.

For each image, a graphical representation of the overall accuracies for the pre-polygon classifications are provided in figure 4.4.

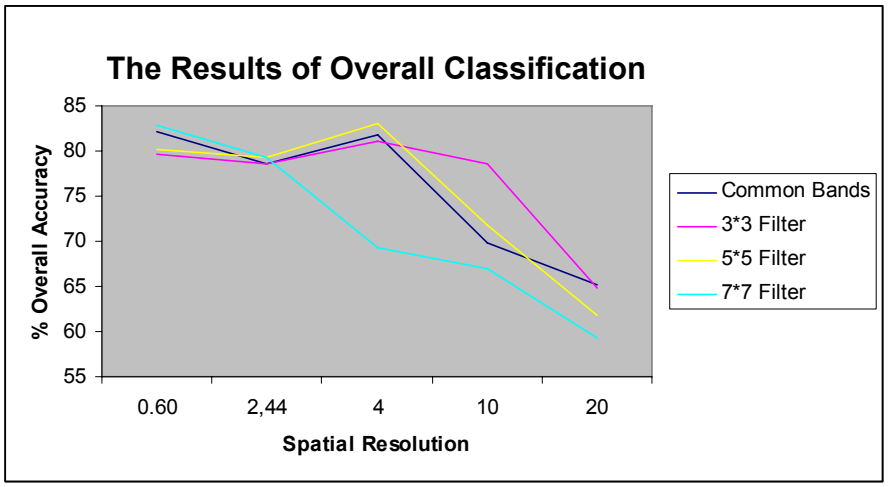

Figure 4.4 The overall accuracies of the pre-polygon classifications of each image

4.4 The results for the median values

For the SPOT 4 image, the overall accuracy and overall kappa were computed to be 42,9% and 21,7%, respectively (Table 4.21). In general, rather low accuracies were obtained for the individiual classes. The lowest producer's accuracy of 9% was observed for the class Rs. However, the user's accuracy of this class (96,7%) was surprisingly the highest one in the matrix. The reason for this is that the omission error was computed to be very high when the median value was used as the statistical measure.

Table 4.21 The error matrix of SPOT 4 XS image

	Cr	Tm	Rc	Rs	Sb	RTot
Cr	207	151	12	290	18	678
Tm	53	184	6	12	5	260
Rc	1	24	10	0	6	41
Rs	1	0	0	30	0	31
Sb	0	2	1	0	8	11
CTot	262	361	29	332	37	1021
Producer's (%)	79	50,9	34,4	9	21,6	
User's (%)	30,5	70,7	24,3	96,7	72,7	
Overall (%) = 42,9	Kappa (%) = 21,7					

The similar results were obtained for the SPOT 5 image. The overall accuracy and overall kappa were computed to be 45,2% and 24,7%, respectively. The lowest producer's accuracy of 6% was obtained for the class Rs. It appears that 302 residue pixels were omitted from this class. On the other hand, 95,2% of the residue fields classified as Rs actually represent the Rs category on the ground.

Table 4.22 The error matrix of SPOT 5 XS image

	Cr	Tm	Rc	Rs	Sb	RTot
Cr	232	171	19	306	17	745
Tm	28	188	1	6	1	224
Rc	1	0	9	0	6	16
Rs	1	0	0	20	0	21
Sb	0	2	0	0	13	15
CTot	262	361	29	332	37	1021
Producer's (%)	88,5	52	31	6	35,1	
User's (%)	31,1	83,9	56,2	95,2	86,6	
Overall (%) = 45,2 Kappa (%) = 24,7						

For the IKONOS image, the overall accuracy, overall kappa and individual class accuracies are given in table 4.23. As can be seen in the table, the overall accuracy and overall kappa were computed to be 80,2% and 71,7%, respectively. The class Rc had the lowest producer's and user's accuracies. The accuracies of the other classes were around 80%.

Table 4.23 The error matrix of IKONOS XS image

	Cr	Tm	Rc	Rs	Sb	RTot
Cr	197	59	8	4	0	268
Tm	50	296	5	51	2	404
Rc	9	0	14	0	0	23
Rs	6	2	0	277	0	285
Sb	0	4	2	0	35	41
CTot	262	361	29	332	37	1021
Producer's (%)	75,1	81,9	48,2	83,4	94,5	
User's (%)	73,5	73,2	60,8	97,1	85,3	
Overall (%) = 80,2 Kappa (%) = 71,7						

The QuickBird XS image provided an overall accuracy of 69,5%, and a rather low overall kappa of 53,9% (Table 4.24). All the Sb fields were classified as Tm and Cr. Therefore, non of the Sb fields were correctly classified providing a producer's accuracy of 0%. The second lowest producer's accuracy (6,8%) was observed for the class Rc, which provided a user's accuracy of 66,6%. On the other hand, the class Cr provided the

highest producer's accuracy of 93,9%, and a rather low user's accuracy of 58,9%.

Table 4.24 The error matrix of QuickBird XS image

	Rs	Cr	Tm	Sb	Rc	RTot
Rs	133	4	0	0	0	137
Cr	57	325	149	4	16	551
Tm	3	16	213	33	11	276
Sb	0	0	0	0	0	0
Rc	0	1	0	0	2	3
CTot	193	346	362	37	29	967
Producer's (%)	68,9	93,9	58,8	0	6,8	
User's (%)	97	58,9	77,1	NaN	66,6	
Overall (%) = 69,5 Kappa (%) = 53,9						

For the QuickBird PS image, the overall accuracy and overall kappa were computed to be 85,2% and 78,8%, respectively. The lowest producer's and user's accuracies were obtained as 31% and 28,1%, respectively, for the class Rc. The reason for this is that only 9 fields out of the total 29 were classified correctly as Rc. It was observed that the accuracies of the classes were around 80%.

Table 4.25 The error matrix of QuickBird PS image

	Rs	Cr	Tm	Sb	Rc	RTot
Rs	185	23	1	0	0	209
Cr	1	263	12	1	7	284
Tm	6	38	335	4	7	390
Sb	0	0	14	32	6	52
Rc	1	22	0	0	9	32
CTot	193	346	362	37	29	967
Producer's (%)	95,8	76	92,5	86,4	31	
User's (%)	88,5	92,6	85,8	61,5	28,1	
Overall (%) = 85,2 Kappa (%) = 78,8						

4.5 The results for the mode values

The overall accuracy and individual class accuracies of the SPOT 4 image are given in table 4.26. As can be seen in the table, the overall accuracy and overall kappa were found to be 48,2% and 28,8%, respectively. The classes Rc, Rs and Sb provided significantly low producer's accuracies of 24,1%, 14,1% and 18,9%, respectively. When the user's accuracies were examined, it was observed that the highest accuracy of 95,9% was obtained for the class Rs. The classes Cr and Rc exhibited low user's accuracies of 34,4% and 12,9%, respectively. The user's accuracies of the classes Tm and Sb were rather high.

Table 4.26 The error matrix of SPOT4 XS image

	Cr	Tm	Rc	Rs	Sb	RTot
Cr	214	110	11	271	15	621
Tm	41	218	11	12	5	287
Rc	6	29	7	2	10	54
Rs	1	1	0	47	0	49
Sb	0	3	0	0	7	10
CTot	262	361	29	332	37	1021
Producer's (%)	81,6	60,3	24,1	14,1	18,9	
User's (%)	34,4	75,9	12,9	95,9	70	
Overall (%) = 48,2 Kappa (%) = 28,8						

For the SPOT 5 image, the overall accuracy and overall kappa were computed to be 81,2% and 73,1%, respectively. While the user's accuracies of the classes Rc and Sb were marginal, the classes Cr, Tm and Rs provided relatively high values. The class Tm provided the highest user's accuracy of 91,6%. On the other hand, the lowest user's accuracy of 44,1% was computed for the class Rc, while the class Cr provided the highest user's accuracy of 86,8%.

Table 4.27 The error matrix of SPOT5 XS image

	Cr	Tm	Rc	Rs	Sb	RTot
Cr	204	19	8	3	1	235
Tm	48	331	2	71	5	457
Rc	6	4	15	0	9	34
Rs	4	0	0	258	0	262
Sb	0	7	4	0	22	33
CTot	262	361	29	332	37	1021
Producer's (%)	77,8	91,6	51,7	77,7	59,4	
User's (%)	86,8	72,4	44,1	98,4	66,6	
Overall (%) = 81,2 Kappa (%) = 73,1						

For the IKONOS image, the overall accuracy, overall kappa and individual class accuracies are given in table 4.28. It can be seen in the table that the overall accuracy and overall kappa were computed to be 81,9% and 74,2%, respectively. Of the producer's accuracies, the class Rc provided the lowest value of 58,6%, while the producer's accuracies of the other classes were around 80%. The highest user's accuracy of 96,7% was provided by the class Rs. On the other hand, the user's accuracies of the other classes were also remarkably high.

Table 4.28 The error matrix of IKONOS XS image

	Rs	Tm	Cr	Sb	Rc	RTot
Rs	297	4	6	0	0	307
Tm	29	289	50	4	5	377
Cr	6	63	202	1	6	278
Sb	0	5	0	32	1	38
Rc	0	0	4	0	17	21
CTot	332	361	262	37	29	1021
Producer's (%)	89,4	80	77	86,4	58,6	
User's (%)	96,7	76,6	72,6	84,2	80,9	
Overall (%) = 81,9 Kappa (%) = 74,2						

The overall accuracy and overall kappa of the Quickbird XS image were nearly identical to that of the IKONOS image (Table 4.29). The overall accuracy and overall kappa were computed to be 80,5% and 71,7%,

respectively. The lowest accuracies were obtained for the class Rc. The reason for this is that only 10 fields of the total 29 were classified correctly as Rc producing therefore, high omission and comission errors. Among the classes, Rs provided the highest producer's accuracy of 96,3% and a significantly high user's accuracy of 88,1%.

Table 4.29 The error matrix of QuickBird XS image

	Rs	Cr	Tm	Sb	Rc	RTot
Rs	186	22	3	0	0	211
Cr	2	238	18	0	5	263
Tm	5	63	331	23	13	435
Sb	0	0	9	14	1	24
Rc	0	23	1	0	10	34
CTot	193	346	362	37	29	967
Producer's (%)	96,3	68,7	91,4	37,8	34,4	
User's (%)	88,1	90,4	76	58,3	29,4	
Overall (%) = 80,5 Kappa (%) = 71,7						

For the QuickBird PS image, the overall accuracy, overall kappa and individual class accuracies are provided in table 4.30. As can be seen in the table, the overall accuracy and overall kappa were computed to be 69,7% and 53,9%, respectively. Of the classes, Cr provided the highest producer's accuracy of 94,5% while the producer's accuracies of Rs and Tm/Pp were marginal. Of the user's accuracies, the highest value of 97,6% was provided by Rs, while the user's accuracies of the Tm/Pp and Cr were computed to be 78,3% and 58,9%, respectively. Surprisingly, both the user's and producer's accuracies of the classes Sb and Rc were found to be 0%. Unfortunately, no logical eplanation could be made for this.

Table 4.30 The error matrix of QuickBird PS image

	Rs	Cr	Tm	Sb	Rc	RTot
Rs	123	3	0	0	0	126
Cr	67	327	138	5	18	555
Tm	3	16	224	32	11	286
Sb	0	0	0	0	0	0
Rc	0	0	0	0	0	0
CTot	193	346	362	37	29	967
Producer's (%)	63,7	94,5	61,8	0	0	
User's (%)	97,6	58,9	78,3	NaN	NaN	
Overall (%) = 69,7 Kappa (%) = 53,9						

4.6 Comparing the results of pre- and post-classification

The results of the post-polygon classification were compared with the results of the pre-polygon classification carried out using the mean bands. For the SPOT4 image, both the overall accuracy and overall kappa are higher for the pre-polygon classification than the post-polygon classification. For both the overall accuracy and overall kappa, a decrease of about %10 is observed. When the accuracies of individual classes are compared, it is seen that for the classes Rs, Rc and Tm\Pp, the producer's accuracies are higher in pre-polygon classification. On the other hand, the classes Sb and Cr provided better accuracies for the post-polygon classification. No change is observed for Rs, while the classes Sb, Cr, and Tm\Pp exhibited better results in the pre-polygon classification.

For the SPOT 5 image, an increase of about 10% was observed for both the overall accuracy and overall kappa when the post-polygon classification was performed. For the class Sb, the producer`s accuracy of the pre-polygon classification was identical to the accuracy computed for the post-polygon classification. On the other hand, the poducer's accuracies of the other classes were better in the post-polygon classification than the pre-polygon

classification. When the user's accuracies were examined, it was seen that the classes Sb, Rc, Cr and Tm/Pp provided more accurate results than the pre-polygon classification. But, the accuracy of the class Rs remained unchanged.

The overall accuracy and overall kappa of the IKONOS image were better by about 7% and 10%, respectively, for the post-polygon classification. For the individual classes, the producer's accuracies of the post-polygon classification were better than the accuracies of the pre-polygon classification. The user`s accuracies of the classes Sb, Rc, Cr and Tm/Pp computed for the post-polygon classification were also better than the accuracies of the pre-polygon classification. On the other hand, the user's accuracies of the class Rs remained unchanged.

For the QuickBird XS image, an increase of about 7% was observed for both the overall accuracy and overall kappa. For all classes, the producer`s accuracies increased in the post-polygon classification and the increase was about 50% for the class Sb. When the user's accuracies were compared, it was found that the classes Rs and Rc provided more accurate results for the pre-polygon classification than the post-polygon classification.

For the QuickBird PS image, the overall accuracy and overall kappa increased by about 3% and 5%, respectively in the post-polygon classification. When the accuracies of the individual classes were examined, it was seen that the producer's accuracies of the classes improved in the post-polygon classification. On the other hand, the user's accuracies of the classes Rs and Sb were higher in the pre-polygon classification.

4.7 Disscussion

It was observed that the post-polygon classification provided more reliable results than the pre-polygon classification. The main reason for this is that the statistical values calculated for the pre-polygon classification may not represent the actual crop information within the fields due to the heterogenity of the fields.

Unfortunately, a logical trend was not observed in the results. The highest accuracies were provided by the high spatial resolution images. The IKONOS image provided the best results (around 85%), which was followed by the QuickBird images (around 80%). Unexpectedly, the lowest accuracies (around 65%) were provided by the SPOT 4 image. One reason for this would be the training pixels. As explained in Chapter 3, the training areas were selected from the 4m resolution IKONOS image. Then, the training areas were transferred to other images so that the same training areas should be used for all the images. After transferring the training areas to other images with different resolutions, the number of training pixels changed. For example, the training pixels dramatically increased for the QuickBird images. On the other hand, it slightly decreased for the SPOT5 and SPOT4 images. Therefore, this caused to a decrease in the number of training pixels for the coarser resolution images and might have resulted in low classification accuracies. The other reason would be that the small fields are better classified using the high resolution images. This is because, for high resolution images, more pixels fall within the fields.

For the post-polygon classification, the inclusion of the blue and SWIR bands did not improve the accuracies. This may be due to the acquisation

dates of the images. In these dates, the blue and SWIR bands may not be effective to differantiate the selected crops in the study area. It was observed that there was no change in the accuracies of the SPOT 4, IKONOS and QuickBird PS images, when the blue and SWIR bands were included in the classification. On the other hand, the accuracies of the SPOT 5 and QuickBird XS images increased by about 3% when all bands were used in the classification.

The images were smoothed using the median filter prior to image classification. However, for the post-polygon classification, the filtering procedure did not increase the classification accuracies. This is unlike the statement made by Cushine (1987), who found that the low pass filtering process carried out before the classification reduced the accuracy. It was observed that increasing the kernel size decreased the accuracies except for the kernel size of 7*7 which improved the results of all images by about 2%. However, the same improvement was not observed in the accuuracies of the classifications carried out using the unfiltered common bands. Whereas the post-polygon classification, a reverse trend was observed for the pre-polygon classification. In general, the accuracies decreased when the kernel size was increased. But, an improvement of about 5% was observed for the SPOT 5 image when the 3*3 kernel was used. The other increase was observed for the IKONOS image when the kernel size was increased to 7*7. The reason for the improvement is that high proportion of internal variability was reduced when the kernel size was increased.

When the individual class accuracies were examined it was found that the best results were obtained for the class Rs. This is due to the fact that the class Rs represented distinct spectral response pattern in the July and August images used in this study. The other reason would be that the majority of the Rs fields are relatively large. Compared with the small

fields, significantly higher number of pixels fall within the larger fields increasing the chance that a higher proportion of the pixels can be correctly classified. For both the QuicBird XS and PAN images, the class Rc provided lower accuracies than the other classes. The QuickBird images were recorded in August ten days later than the other images that were acquired in July. In July the Rc fields still contain water which have low reflectance in the NIR band of the SPOT 4, SPOT 5 and IKONOS images. In August the crop Rc was grown and the fields were covered by the green Rc crop. As mentioned earlier the training areas were selected from the IKONOS image and transfered to other images. Therefore, it is unticipated that the delay of the acquistion date of the QuickBird images might have negative effects on the training areas and the accuracy of Rc.

A summary of the prices and the overall classification accuracies are given in table 4.31. As can be seen in the table, the SPOT4 XS image costs US$ 0,90 km2 and is the cheapest one of the four images used in this study. Although SPOT4 XS imagery appears to be cost effective for crop mapping, it provides an overall accuracy in the order of 65% and 76% for the pre-polygon and post polygon classifications, respectively. The SPOT5 XS image was more than six times as expensive as the SPOT 4 XS image. When the classification accuracies are analyzed, it is seen that SPOT 5 imagery provides about 5% better results than SPOT 4 imagery. Compared with the SPOT images, a significant difference in the price is evident for the IKONOS XS imagery, ehich was more than five times as expensive as the SPOT 5 XS imagery and more than 30 times as expensive as SPOT 4 XS imagery. Although the IKONOS imagery does not appear to be cost effective, it provided the highest overall accuracies for both the pre-polygon and post-polygon classification. The price for the QuickBird Bundle imagery is US$ 32,00km2 and is the most expensive of the images used in this study. When compared with the other images,

QuickBird provided the second highest classification accuracies for both pre- and post polygon classification.

In summary, SPOT 4 XS and SPOT 5 XS images are comparatively much cheaper than the IKONOS and QuickBird images. However, in this study, the IKONOS and QuickBird images provided remarkably higher accuracies than the SPOT 4 and SPOT 5 images. The difference in price between the images raises the question of cost effectiveness, especially for users to purchase images under a fixed budget. To answer this question more applications would need to be carried out at different study sites representing a variety of land cover types.

Table 4.31 The overall accuracies and the costs of the images

	Price/km2 ($)	Pre-Polygon Classf.	Post-Polygon Classf.
SPOT4	0.90	65,2 (%)	76,1 (%)
SPOT5	5.50	69,8 (%)	81,4 (%)
IKONOS	28.00	81,8 (%)	88,6 (%)
QuickBird XS	31.00	78,6 (%)	83,7 (%)
QuickBird PS	32.00	82,1 (%)	85,8 (%)

CHAPTER 5

CONCLUSIONS AND RECOMMENDATIONS

5.1 Conclusions

Based on the results, the following conclusions were drawn for this study:

- For agricultural lands, polygon-based classification was found to be an appropriate way to classify unitemporal images overcoming the problem of misclassification as a result of within field internal spectral variabilities.

- For all the images used, the accuracies of the post-polygon classification was found to be higher than the accuracies of the pre-polygon classification.

- The post-polygon classification of the IKONOS and QuickBird images provides better overall accuracies (around 85%) than the other images. The lowest accuracies of about 70% were computed for the SPOT 4 image, which has the coarsest resolution among the images used in this study.

- For both the pre-polygon and post-polygon classification approaches, the IKONOS image provided the best results.

- When compared with the common bands (Green, Red, and NIR), the use of all bands did not improve the accuracies for both the pre-polygon and post-polygon classification approaches.

- It was found that high spatial resolution images (IKONOS, QuickBird XS and QuickBird PS) provided more accurate results than the coarser resolution images (SPOT 4 and SPOT 5). While the overall accuracies of the high spatial resolution images were around 85%, the coarser resolution images provided overall accuracies of about 75%.

- It was found in this study that performing the classification operation using the median filtered bands reduced the accuracies and the decrease was more for the higher kernel sizes.

- Digitizing the sub-field boundaries was very time consuming. However, it should be recommended that polygon-based classification improves the accuracy by means of classifiying the homogenous fields.

- The use of a database provides storage and access to a range of additional information and allows to make queries .

5.2 Recommendations

The following recommendations were made for the future studies:

- The interpretation of the spectral classes can be made more reliable by the collection of more detailed and realistic ground truth data during the satellite overpass.

- Prior probabilities can be used for discriminating inseparable classes in the classification.

- To decrease the time spent during training area collection, automated training area selection can be used.
- It is recommended that different training strategies should be used for performing polygon-based image classification and to assess the results.

- Crop area estimation through the classification can be valuable information to compute water consumption in large regions.

- To make an accurate discrimination between the classes, highly accurate digital elevation model (DEM) can be included in the classification for using the height information of the crops.

REFERENCES

Aplin, P., Atkinson, P. M. and Curran P. J. 1997, “Fine spatial resolution satellite sensors for the next decade”, *International Journal of Remote Sensing, Vol.18, NO.18, 3873-3881.*

Aplin, P., Atkinson, P. M., and Curran, P.J. 1999, “Fine spatial resolution simulated satellite sensor imagery for land cover mapping in the United Kingdom”, Remote Sensing of Environment, Vol.68, 206-216.

Aplin, P., and Atkinson, P. M., 2001, “Sub-pixel land cover mapping for per-field classification”. *International Journal of Remote Sensing*, Vol.22, 2853-2858.

Aplin, P., and Atkinson, P. M., 2004, “Predicting missing field boundaries to increase per-field classification accuracy”. *Photogrammetric Engineering and Remote Sensing*, Vol.70, 141-149.

Arikan, M., 2003, “A multi-temporal masking classification method for field-based agricultural crop mapping”, Thesis in Geodetic and Geographic Information Technologies, Midde East Technical University, Ankara, Turkey.

Baker, J. R., Briggs, S.A., Gordon, V., Jones A. R., Settle, J. J., J.R.G. and Townshend, Wyatt, B. K. 1991, “Advances in classification for land cover mapping using SPOT HRV imagery”, *International Journal of Remote Sensing, Vol.12, NO. 5, 1071-1085.*

Beltran, C. M. and Belmonte, A. C. 2001, “Irrigated crop area estimation using Landsat TM Imagery in La Mancha, Spain”, *Photogrammetric Engineering and Remote Sensing, Vol. 67, No. 10, pp. 1177-1184.*

Chen, D. and Stow, D. 2002, “The effect of training strategies on supervised classification at different spatial resolutions”, *Photogrammetric Engineering and Remote Sensing, Vol. 68, No. 11, pp. 1155-1161.*

Collins, J. B., and Woodcock, C. E. 1999, “Geostatistical estimation of resolution-dependent variance in remotely sensed images*”, Photogrammetric Engineering and Remote Sensing, Vol. 65, No. 1, pp. 41-50.*

Congalton, R. G., Balogh, M., Bell, C., Green, K., Milliken, J. A., and Ottmann, R. 1998, “Mapping and monitoring agricultural crops and other land cover in the Lower Colorado River Basin”, *Photoggrammetric Engineering and Remote Sensing, pp. 1107-1113.*

Congalton and Green, 1999, “Assessing the accuracy of remotely sensed Data: Principles and Practices”, *pp. 3-4*

Cushine, J. 1987, “The interactive effect of spatial resolution and degree of internal variability within land-cover types on classification accuracies”, *International Journal of Remote Sensing, Vol. 8, NO.1, 15-29.*

Dean, A.M., and Smith, G.M. 2003, “An evaluation of per-parcel land cover mapping using maximum likelihood class probabilities”, *International Journal of Remote Sensing, Vol.24, NO. 14, 2905-2920.*

De Wit A. J. W., and Clevers J. G. P. W. 2004, “Efficiency and accuracy of per-field classification for operational crop mapping”, *International Journal of Remote Sensing.*

DongMei C., and Stow D. 2002 , “The effect of training strategies on supervised classification at different spatial resolutions”, *Photogrammetric Engineering and Remote Sensing, Vol. 68, No.11, pp. 1155-1161.*

Franklin, S. E. 1994, “Discrimination of subalpine forest species and canopy density using digital CASI, SPOT PLA, and Landsat TM data”, *Photogrammetric Engineering and Remote Sensing, Vol. 60, No.10, pp. 1233-1241.*

Gao, J. 1999, “A comparative study on spatial and spectral resolutions of satellite data in mapping mangrove forests”, *International Journal of Remote Sensing, Vol. 20, No. 14, 2823-2833.*

Green, E. P., Clark, C. D., Mumby, P. J., and Ellis, A. C. 1998, “Remote sensing techniques for mangrove mapping”, *International Journal of Remote Sensing, Vol. 19, No. 5, 905-956.*

Hutchinson, C. F. 1982, “Techniques for combining Landsat and ancillary data for digital classification improvement”, *Photogrammetric Engineering and Remote Sensing, Vol. 48, No. 1, pp. 123-130.*

Janssen L. L. F., and Van Amsterdam J. D., 1991 ,”An object based approach to the classification of remotely sensed images”, IEEE transactions on geoscience and remote sensing, *pp. 2191-2195*.

Jewell, N. 1989, “An evaluation of multi-date SPOT data for agriculture and land use mapping in the United Kingdom”, *International Journal of Remote Sensing, Vol.10, NO.6, 939-951.*

Kershaw, C.D.,and Fuller*,R.M. 1992, “Statistical problems in the discrimination of land cover from satellite images: a case study in lowland Britain”, *International Journal of Remote Sensing, Vol.13, No.16, 3085-3140.*

Langley, S. K., Cheshire, H. M., Humes, K. S. 2001, “A comparison of single date and multitemporal satellite image classifications in a semi-arid grassland”, *Journal of Arid Environments,* Vol*.49, 401-411.*

Lillesand, T.M, Kiefer R.W. and Chipman J. W. 2004, “Remote sensing and image interpretation”, 552-572.

Lloyd, C. D, Berberoglu, S., Curran, P. J., and Atkinson, P. M., 2004, “A comparison of texture measures for the per-field classification of Mediterranean land cover”, Vol. 25, 3943-3965.

Lobell, D. B., and Asner G.P. 2003, “Comparison of observing ALI and Landsat ETM+ for crop identification and yield prediction in Mexico”, *IEEE Transactions on Geoscience and Remote Sensing, Vol. 41, No. 6.*

Manual of photogrammetry, Fifth Edition, 2004

Miguel-Ayanz, J.S., and G. S. Biging, 1997, “Comparisn of single-stage and multi-stage classification approaches for cover type mapping with TM and SPOT data, *Remote Sensing of Environment, Vol. 59, 92-104.*

Mukarami, T., Ogawa, Ishitsuka, S., N., Kumagai, K. and Saito, G. 2001,"*Crop* discrimination with multitemporal SPOT/HRV data in the Saga Plains, Japan*"*, *International Journal of Remote Sensing, Vol.22, No. 7, 1335 -1348..*

Mumby, P. J. and Edwards A. J. 2002, "Mapping marine environments with IKONOS imagery: enhanced spatial resolution can deliver greater thematic accuracy", *Remote Sensing of Environment, Vol. 82, 248-257.*

Ortiz, M. J., Formaggio, A. R., and Epiphanio, J. C. N. 1997, "Classification of croplands through integration of Remote Sensing, GIS, and historical database", *International Journal of Remote Sensing, Vol.18, No.1, 95-105.*

Pedley, M. I.,and Curran, P. J. 1991, "Per-field classification: an example using SPOT HRV imagery", *International Journal of Remote Sensing, VOL.12, NO. 11, 2181 – 2192.*

Smith.G.M. AND Fuller R. M. 2001, "An integrated approach to land cover classification: an example in the Island of Jersey", *International Journal of Remote Sensing, Vol.22, No. 16, 3123-3142.*

Stein, A., Meer, F. V.D. and Gorte, B. 2002, "Spatial statistics for remote sensing".

Sun, J. 2000, "Dynamic monitoring and yield estimation of crops by mainly using the Remote Sensing technique in China"*, Photogrammetric Engineering and Remote Sensing, Vol. 66, No. 5, pp. 645-650.*

Turker, M. and Arikan M. (In Press). “Sequential masking classification of multi-temporal Landsat7 ETM+ images for field-based crop mapping in Karacabey, Turkey” *International Journal of Remote Sensing*.

Turker, M., and Derenyi, E., 2000, GIS assisted change detection using remote sensing. *Geocarto International*, 15, 49-54.

Trichon, V., Ducrot, D. And Gastellu-Etchegorry, J. P. 1999, “SPOT4 potential for the monitoring of tropical vegetation. A case study in Sumatra”, *International Journal of Remote Sensing, Vol. 20, No. 14, 2764-2785.*

Url1 Spot Image http://www.spotimage.fr/html/_167_224_555_234_.php

Url2 Info-Terra satellite imagery worldwide http://www.infoterra-global.com/spot.htm.

Vieira, C., Mather, P., and McCullagh, M. 2000, “The spectral-temporal response surface and its use in the multi-sensor, multi-temporal classification of agricultural crops”, *International Archives of Photogrammetry and Remote Sensing, Vol. 33, Part B2.,Amsterdam.*

Wang, L., Sousa, W.P., and Gong, P. 2004, “Integration of object-based and pixel-based classification for mapping mangroves with IKONOS imagery, *International Journal of Remote Sensing”, Vol. 25, No. 24, 5655-5668.*

Wang, L., Sousa W. P., Gong, P., Biging, G. S. 2004, “Comparison of IKONOS and Quickbird images for mapping mangrove species on the

Caribbean coast of Panama", *Remote Sensing of Environment, Vol. , 432-440.*

Name	Rs2	Sb1	Rc2	Rc1	Cr1	Cr2	Cr3	Tm1	Tm2	Sb2	Pp1
Rs2											
Sb1	2.000000										
Rc2	2.000000	1.999988									
Rc1	2.000000	1.474046	1.995396								
Cr1	2.000000	2.000000	1.492039	1.999996							
Cr2	2.000000	2.000000	1.999979	1.999996	1.999834						
Cr3	2.000000	2.000000	1.999996	2.000000	1.999984	2.000000					
Tm1	2.000000	1.915613	2.000000	1.894960	2.000000	2.000000	2.000000				
Tm2	2.000000	1.999985	1.997747	2.000000	1.982694	2.000000	1.998100	2.000000			
Sb2	2.000000	1.805025	2.000000	1.694350	2.000000	2.000000	2.000000	1.873130	2.000000		
Pp1	2.000000	1.999978	2.000000	2.000000	1.999966	2.000000	1.999785	2.000000	1.180998	2.000000	
Pp2	2.000000	1.999920	1.914757	1.999996	1.920677	1.999996	1.999811	2.000000	0.934220	2.000000	1.845770

Figure A.1 The TDI of SPOT4 XS image

Name	Rs1	Rs2	Sb1	Rc2	Rc1	Cr1	Cr2	Cr3	Tm1	Tm2	Sb2	Pp1
Rs2	2.000000											
Sb1	2.000000	2.000000										
Rc2	2.000000	2.000000	1.998741									
Rc1	2.000000	2.000000	1.796739	1.997827								
Cr1	2.000000	2.000000	1.999999	1.622659	2.000000							
Cr2	2.000000	2.000000	2.000000	1.999981	2.000000	1.998776						
Cr3	2.000000	1.999994	2.000000	1.999540	2.000000	1.999769	2.000000					
Tm1	2.000000	2.000000	1.961289	2.000000	1.998347	2.000000	1.999983	2.000000				
Tm2	2.000000	2.000000	1.999999	1.999768	2.000000	1.998881	2.000000	1.989907	2.000000			
Sb2	2.000000	2.000000	1.620348	1.999996	1.642127	2.000000	2.000000	2.000000	1.926253	2.000000		
Pp1	2.000000	1.999998	1.999807	1.999946	2.000000	1.999522	1.999989	1.994850	1.999999	1.579447	2.000000	
Pp2	2.000000	2.000000	2.000000	1.969161	2.000000	1.630913	1.999917	1.999734	2.000000	1.556255	2.000000	1.546310

Figure A.2 The TDI of SPOT5 XS image

Name	Rs1	Rs2	Sb1	Rc2	Rc1	Cr1	Cr2	Cr3	Tm1	Tm2	Sb2	Pp1
Rs2	2.000000											
Sb1	2.000000	2.000000										
Rc2	2.000000	2.000000	1.999998									
Rc1	2.000000	2.000000	1.984062	1.845375								
Cr1	2.000000	2.000000	1.999986	1.850128	1.995286							
Cr2	2.000000	2.000000	1.999999	1.999903	1.996470	1.985049						
Cr3	2.000000	1.991855	2.000000	2.000000	2.000000	1.999472	2.000000					
Tm1	2.000000	2.000000	1.911627	1.999988	1.957528	1.999816	1.999640	2.000000				
Tm2	2.000000	2.000000	1.998981	1.999956	2.000000	1.765159	2.000000	1.997265	1.999988			
Sb2	2.000000	2.000000	1.499630	2.000000	1.950688	2.000000	2.000000	2.000000	1.911405	2.000000		
Pp1	2.000000	2.000000	1.993723	2.000000	2.000000	1.966841	2.000000	1.999805	1.999944	0.618278	2.000000	
Pp2	2.000000	2.000000	1.999722	1.998827	1.999993	1.156790	1.999550	1.999925	1.999804	1.140667	2.000000	1.508377

Figure A.3 The TDI of IKONOS XS image

Name	Rs1	Rs2	Sb1	Rc2	Rc1	Cr1	Cr2	Cr3	Tm1	Tm2	Sb2	Pp1
Rs2	2.000000											
Sb1	2.000000	2.000000										
Rc2	2.000000	2.000000	1.651187									
Rc1	2.000000	2.000000	1.946630	1.585713								
Cr1	2.000000	1.999998	1.983515	1.263953	1.995545							
Cr2	2.000000	2.000000	1.995103	1.576316	1.997165	0.405339						
Cr3	2.000000	1.993187	1.968796	1.194983	1.998538	0.743052	1.360528					
Tm1	2.000000	1.999999	1.746070	1.978266	1.997933	1.996109	1.999847	1.963935				
Tm2	2.000000	1.998112	1.907058	1.981256	1.999877	1.977192	1.999563	1.775330	1.171087			
Sb2	2.000000	2.000000	0.880982	1.997227	1.982872	2.000000	2.000000	2.000000	1.916920	1.996905		
Pp1	2.000000	1.997841	1.798565	1.911569	1.998813	1.872725	1.988767	1.413189	1.126281	0.215635	1.997198	
Pp2	2.000000	1.999800	1.870480	1.705719	1.990593	1.762877	1.913584	1.710387	1.629146	0.478623	1.999330	0.574703

Figure A.4 The TDI of QuickBird XS image

Name	Rs1	Rs2	Sb1	Rc2	Rc1	Cr1	Cr2	Cr3	Tm1	Tm2	Sb2	Pp1
Rs2	1.999997											
Sb1	2.000000	2.000000										
Rc2	2.000000	1.999999	1.370349									
Rc1	2.000000	2.000000	1.887280	1.352744								
Cr1	2.000000	1.999643	1.935654	1.199773	1.979268							
Cr2	2.000000	1.999997	1.957056	1.505688	1.992467	0.225152						
Cr3	2.000000	1.961381	1.899743	1.115680	1.991267	0.629812	1.096563					
Tm1	2.000000	1.999909	1.663917	1.843552	1.988502	1.942579	1.984037	1.773831				
Tm2	2.000000	1.982986	1.826389	1.876839	1.998981	1.852620	1.955443	1.403663	0.829085			
Sb2	2.000000	2.000000	0.377938	1.727267	1.825925	1.996085	1.997476	1.992891	1.806924	1.958624		
Pp1	2.000000	1.989645	1.685611	1.723343	1.995616	1.665795	1.849171	1.135279	0.790811	0.145789	1.924002	
Pp2	2.000000	1.995978	1.633422	1.388837	1.968131	1.349957	1.583417	1.046754	0.977499	0.294074	1.912450	0.304744

Figure A.5 The TDI of QuickBird PS image

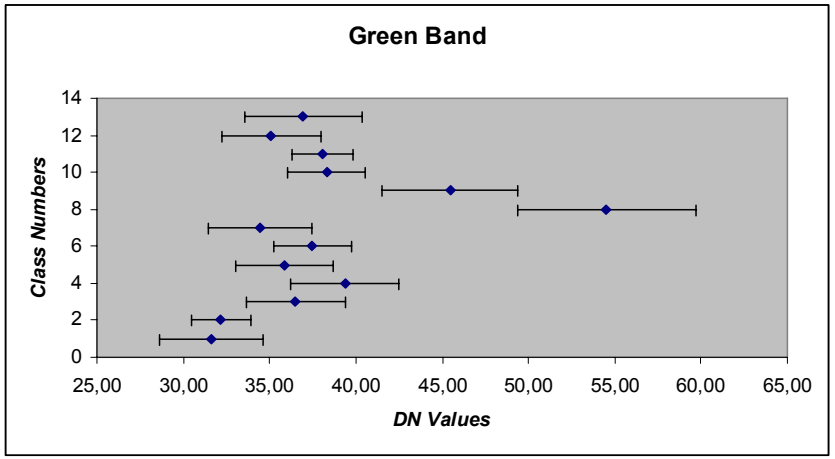

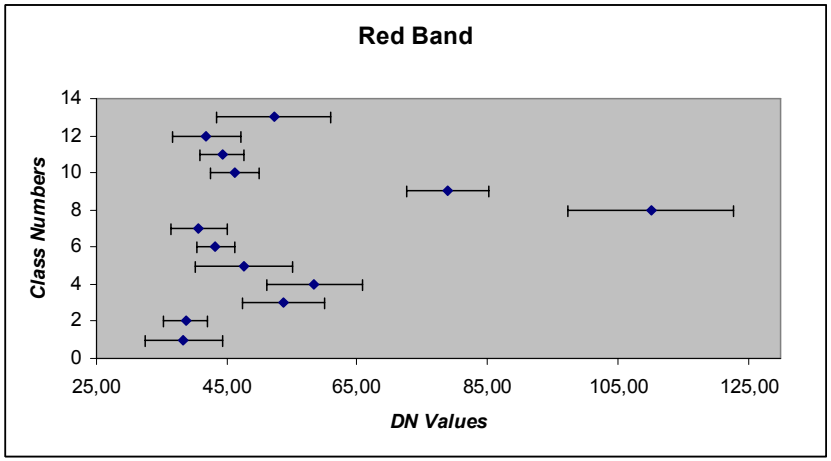

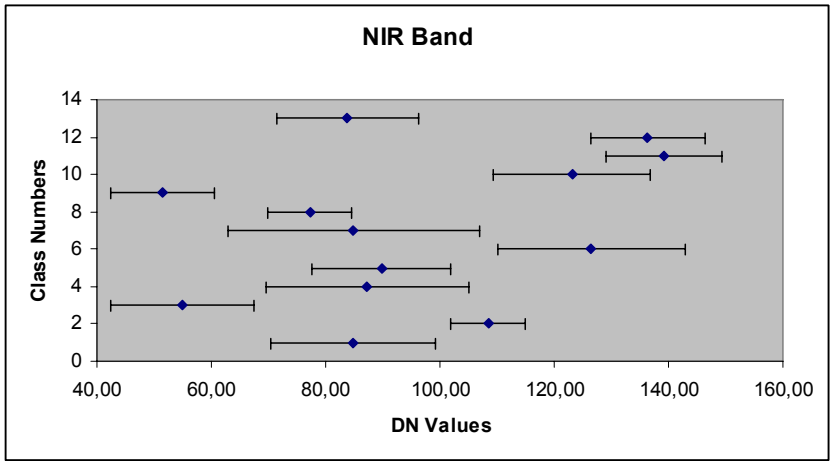

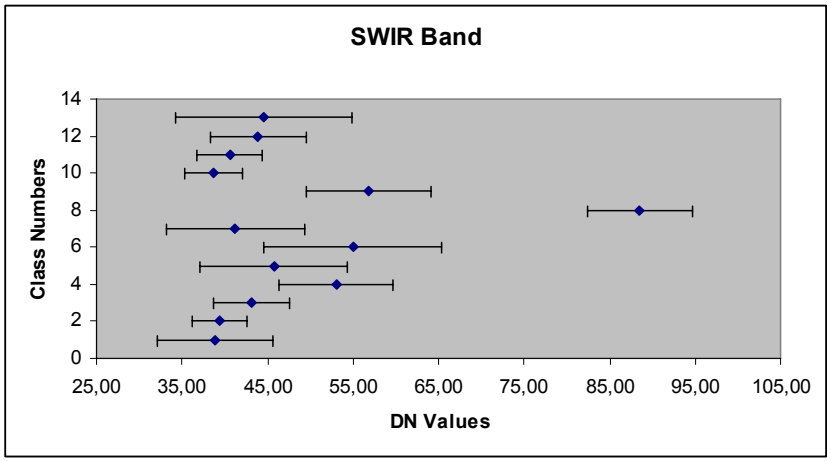

Figure B.1 Coincidence spectral plots of SPOT4 XS image

Figure B.2 Coincidence spectral plots of SPOT5 XS image

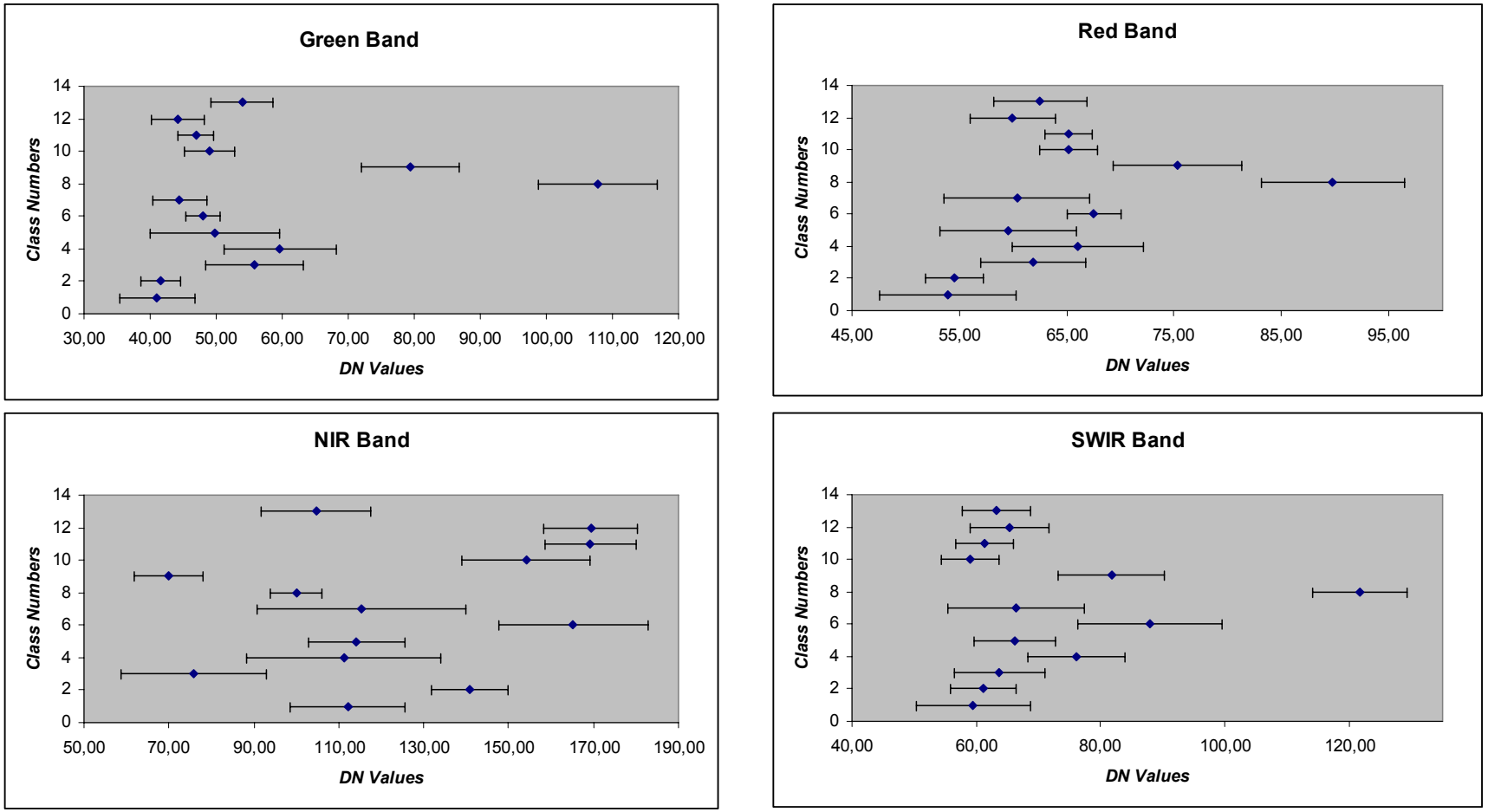

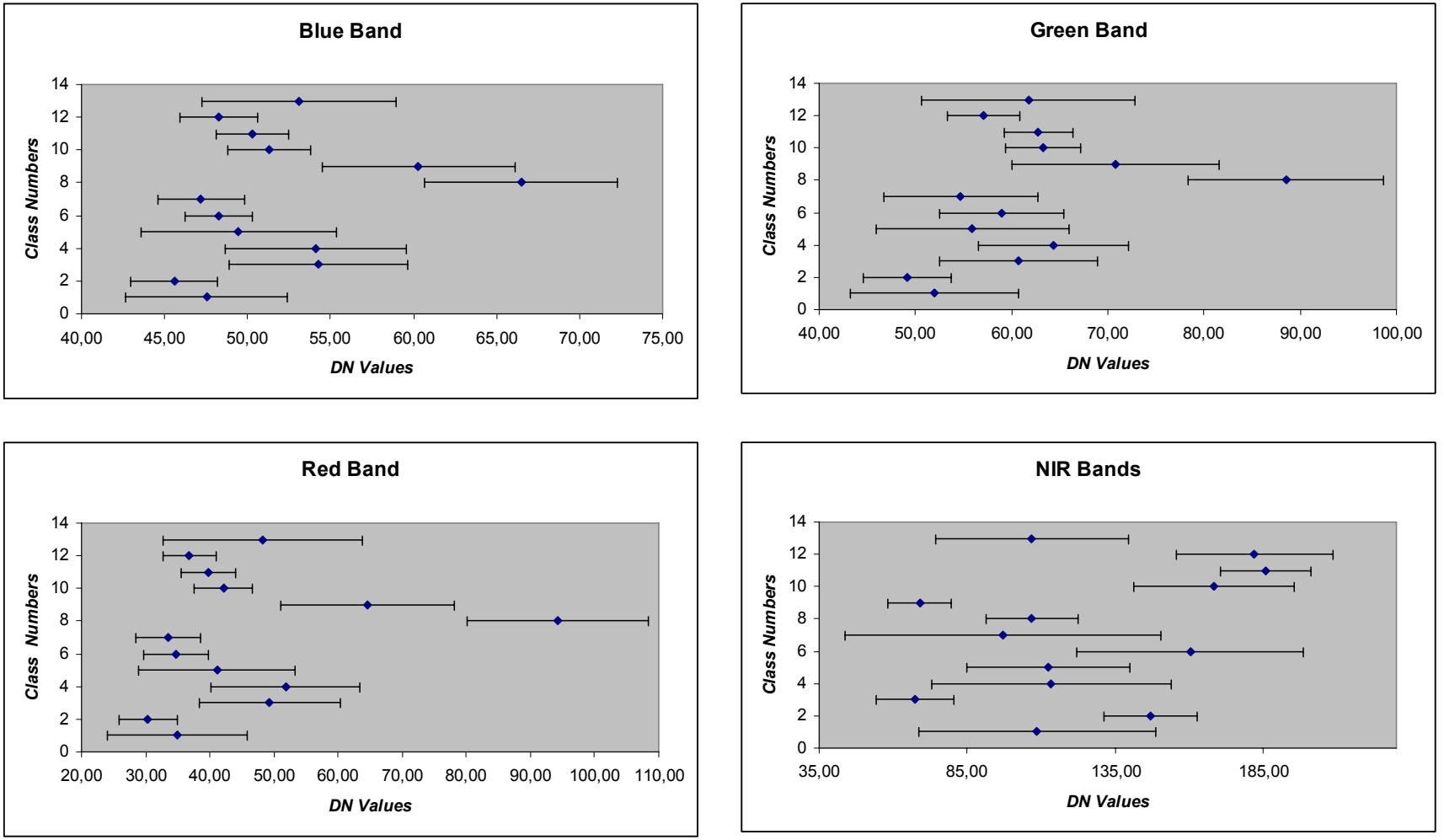

Figure B.3 Coincidence spectral plots of IKONOS XS image

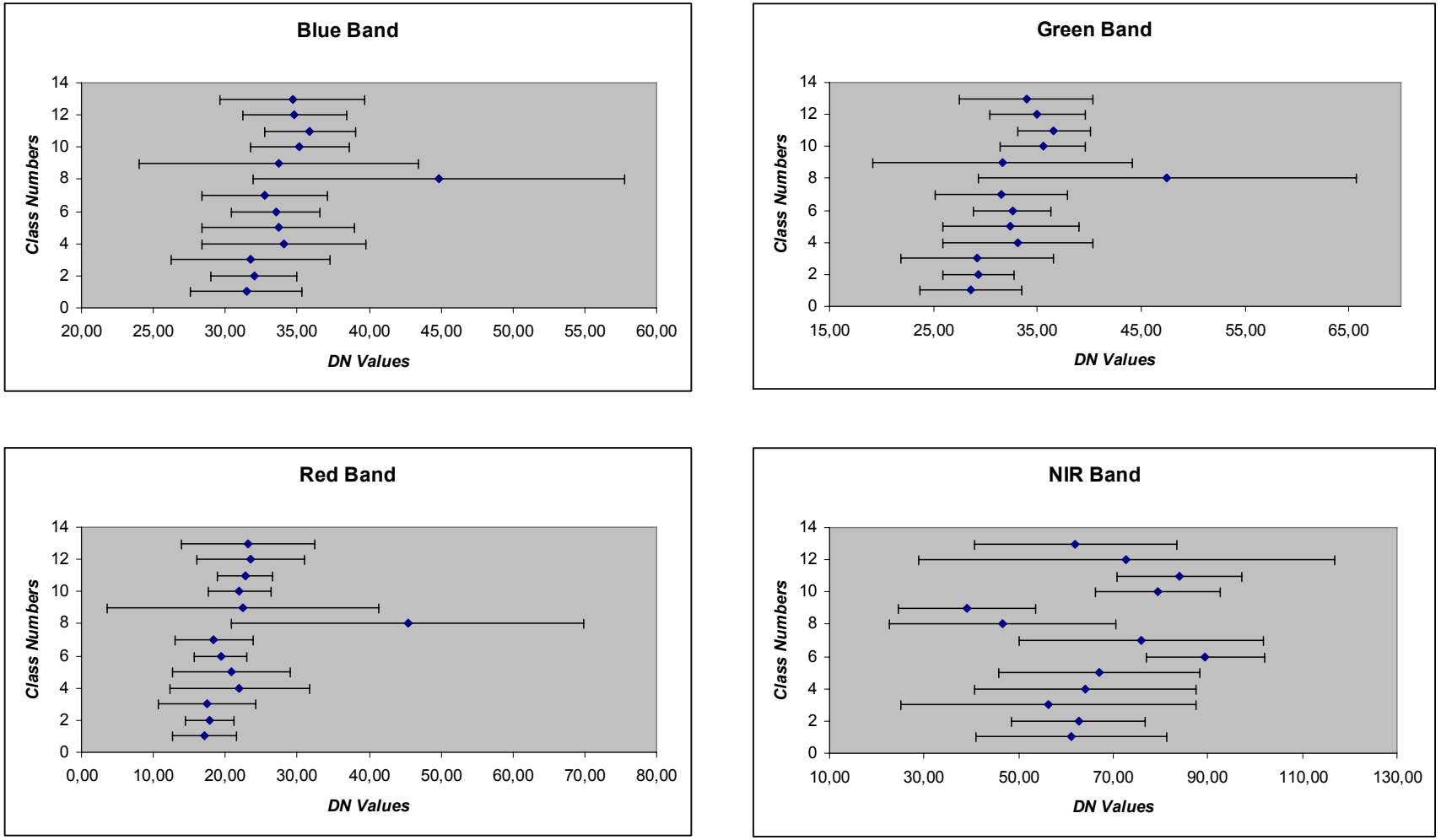

Figure B.4 Coincidence spectral plots of QuickBird XS image

APPENDIX C

Training Statistics of Each Image

Table C.1 Training statistics of the subclasses for SPOT4 XS image

	B1 (G)		B2 (R)		B3 (NIR)		B4 (SWIR)		
Subclass	Mean	Std. Dev.	Mean	Std. Dev.	Mean	Std. Dev.	Mean	Std. Dev.	Sample
Cr1	31,60	1,01	38,40	2,00	84,77	4,78	38,89	2,24	199
Cr2	32,18	0,57	38,67	1,13	108,46	2,18	39,40	1,07	216
Cr3	36,50	0,96	53,67	2,11	54,88	4,18	43,14	1,51	220
Pp1	39,36	1,04	58,46	2,48	87,30	5,92	53,03	2,20	160
Pp2	35,84	0,94	47,63	2,52	89,75	4,06	45,72	2,89	32
Rc1	37,49	0,76	43,26	0,99	126,46	5,45	54,97	3,49	117
Rc2	34,43	1,00	40,72	1,44	84,91	7,36	41,20	2,69	148
Rs1	54,51	1,72	110,13	4,25	77,26	2,46	88,55	2,07	241
Rs2	45,46	1,31	78,94	2,12	51,52	3,04	56,86	2,43	69
Sb1	38,32	0,75	46,26	1,24	123,13	4,59	38,73	1,13	140
Sb2	38,06	0,58	44,34	1,12	139,21	3,34	40,62	1,28	120
Tm1	35,09	0,95	41,88	1,73	136,39	3,31	43,91	1,85	186
Tm2	36,96	1,14	52,20	2,95	83,85	4,13	44,52	3,45	110

Table C.2 Training statistics of the subclasses for SPOT5 XS image

	B2 (G)		B3 (R)		B1 (NIR)		B4 (SWIR)		
Subclass	Mean	Std. Dev.	Mean	Std. Dev.	Mean	Std. Dev.	Mean	Std. Dev.	Sample
Cr1	41,06	1,89	53,89	2,12	112,10	4,49	59,50	3,07	824
Cr2	41,64	1,00	54,51	0,89	140,77	3,01	61,08	1,77	876
Cr3	55,82	2,45	61,89	1,64	75,77	5,70	63,69	2,42	915
Pp1	59,66	2,84	66,01	2,05	111,15	7,65	76,10	2,64	673
Pp2	49,83	3,26	59,49	2,12	114,19	3,82	66,18	2,19	126
Rc1	48,02	0,85	67,53	0,83	165,18	5,85	88,00	3,87	496
Rc2	44,47	1,38	60,35	2,25	115,27	8,17	66,48	3,66	607
Rs1	107,79	2,98	89,79	2,22	99,95	2,06	121,68	2,54	965
Rs2	79,39	2,47	75,29	2,00	69,88	2,73	81,70	2,86	273
Sb1	48,98	1,27	65,14	0,90	154,16	5,05	58,94	1,56	570
Sb2	46,90	0,92	65,15	0,74	169,27	3,61	61,33	1,58	535
Tm1	44,13	1,33	59,93	1,32	169,31	3,69	65,32	2,11	738
Tm2	53,91	1,56	62,51	1,45	104,69	4,32	63,21	1,85	457

Table C.3 Training statistics of the subclasses for IKONOS XS image

	B1 (B)		B 2 (G)		B3 (R)		B4 (NIR)		
Subclass	**Mean**	**Std. Dev.**	**Mean**	**Std. Dev.**	**Mean**	**Std. Dev.**	**Mean**	**Std. Dev.**	**Sample**
Cr1	47,53	1,62	51,94	2,92	34,88	3,64	108,60	13,33	5147
Cr2	45,60	0,87	49,20	1,52	30,32	1,52	146,91	5,25	5493
Cr3	54,27	1,80	60,70	2,74	49,32	3,68	67,38	4,35	5739
Pp1	54,08	1,82	64,41	2,60	51,80	3,85	113,47	13,52	4212
Pp2	49,46	1,97	55,91	3,35	41,13	4,09	112,24	9,17	811
Rc1	48,27	0,69	58,93	2,15	34,66	1,67	160,32	12,79	3103
Rc2	47,20	0,88	54,72	2,67	33,51	1,71	97,07	17,77	3837
Rs1	66,49	1,94	88,54	3,39	94,26	4,70	106,83	5,15	6081
Rs2	60,31	1,93	70,86	3,58	64,62	4,50	68,96	3,61	1703
Sb1	51,31	0,82	63,21	1,30	42,14	1,52	168,37	9,10	3558
Sb2	50,28	0,73	62,76	1,19	39,75	1,42	185,84	5,11	3334
Tm1	48,27	0,77	57,04	1,26	36,78	1,39	182,00	8,85	4615
Tm2	53,08	1,95	61,74	3,72	48,27	5,19	106,72	10,86	2859

Table C.4 Training statistics of the subclasses for QuickBird XS image

	B1 (B)		B2 (G)		B3 (R)		B4 (NIR)		
Subclass	**Mean**	**Std. Dev.**	**Mean**	**Std. Dev.**	**Mean**	**Std. Dev.**	**Mean**	**Std. Dev.**	**Sample**
Cr1	35,50	0,94	34,68	1,56	18,59	1,15	98,52	10,77	14244
Cr2	36,15	0,62	35,62	0,94	19,28	0,75	100,61	7,34	15241
Cr3	36,20	1,40	35,87	2,43	19,31	2,07	90,10	16,66	15931
Pp1	38,10	1,62	40,21	2,52	23,82	3,67	101,35	11,96	11758
Pp2	37,40	1,45	38,93	2,37	22,18	2,99	106,08	11,16	2209
Rc1	36,08	0,55	37,88	1,00	19,02	0,78	143,69	5,74	8557
Rc2	36,13	0,79	37,54	1,95	18,96	1,25	122,14	12,95	10613
Rs1	52,14	4,06	60,71	6,98	54,44	8,93	68,93	11,08	16908
Rs2	39,67	4,06	40,44	5,78	26,94	8,06	60,42	8,70	4762
Sb1	38,53	0,94	42,51	1,32	22,78	1,27	126,16	6,51	9844
Sb2	39,09	0,81	43,49	0,98	23,23	1,03	133,58	6,63	9187
Tm1	38,27	0,95	41,99	1,75	25,03	3,68	114,88	24,01	12795
Tm2	39,07	1,62	41,58	2,55	25,60	3,77	98,10	11,17	7937

Table C.5 Training statistics of the subclasses for QuickBird PS image

	B1 (B)		B2 (G)		B3 (R)		B4 (NIR)		
Subclass	**Mean**	**Std. Dev.**	**Mean**	**Std. Dev.**	**Mean**	**Std. Dev.**	**Mean**	**Std. Dev.**	**Sample**
Cr1	31,45	1,28	28,58	1,62	17,14	1,47	61,23	6,72	227752
Cr2	32,02	1,00	29,34	1,15	17,79	1,12	62,60	4,69	243808
Cr3	31,75	1,84	29,18	2,45	17,44	2,26	56,27	10,42	254896
Pp1	34,08	1,89	33,14	2,40	21,93	3,23	64,14	7,81	188128
Pp2	33,68	1,75	32,43	2,19	20,85	2,75	66,98	7,10	35344
Rc1	33,50	1,03	32,62	1,24	19,33	1,22	89,50	4,17	136912
Rc2	32,75	1,45	31,52	2,11	18,40	1,80	75,95	8,64	169808
Rs1	44,84	4,31	47,47	6,07	45,38	8,15	46,60	7,99	270528
Rs2	33,73	3,25	31,64	4,16	22,47	6,29	39,07	4,81	76192
Sb1	35,17	1,14	35,55	1,37	22,00	1,43	79,36	4,39	157504
Sb2	35,88	1,05	36,59	1,17	22,73	1,29	84,04	4,39	146992
Tm1	34,80	1,20	34,99	1,53	23,53	2,49	72,75	14,68	204720
Tm2	34,66	1,67	33,93	2,14	23,10	3,09	62,02	7,16	126960

APPENDIX D

Mean Value Differences

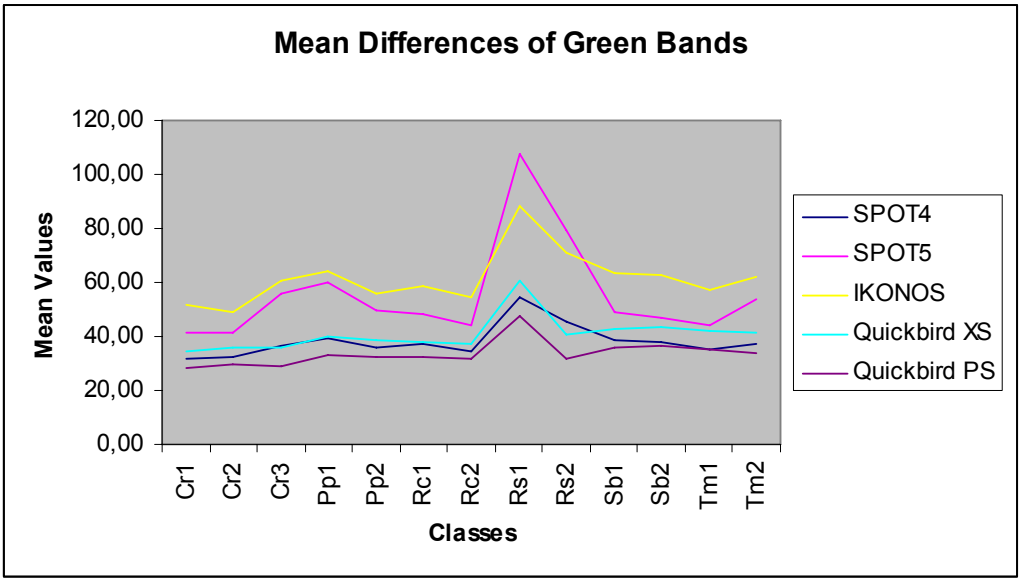

Figure D.1 The mean difference of green bands for each satellite

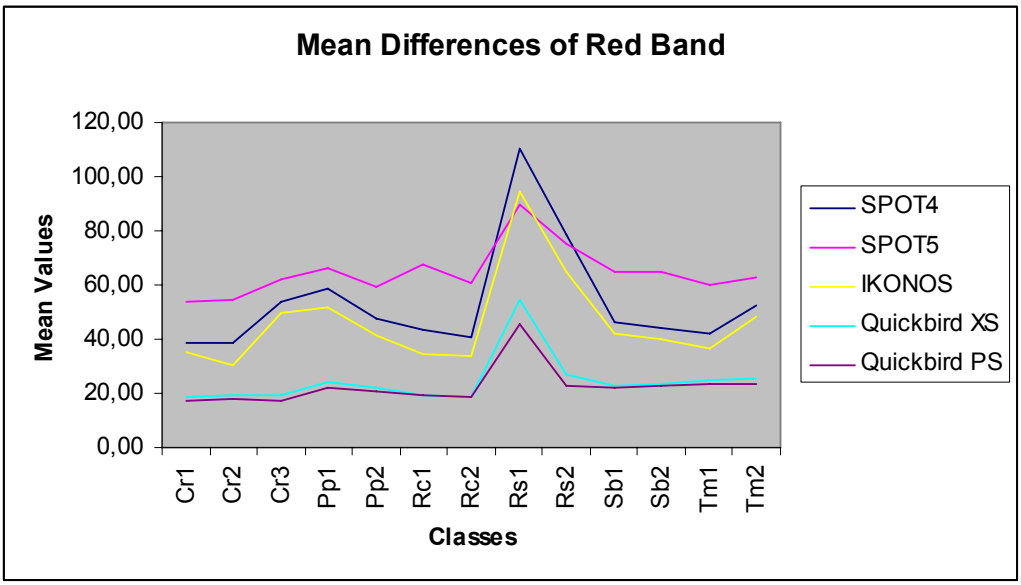

Figure D.2 The mean difference of red bands for each satellitE

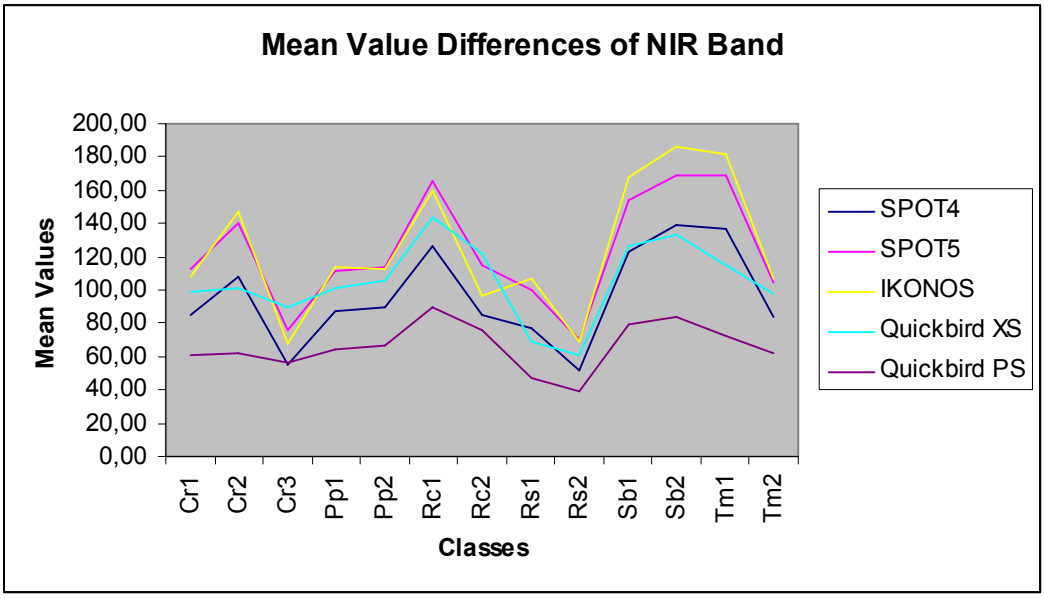

Figure D.3 The mean difference of NIR bands for each satellite

APPENDIX E

Accuracies of the Post-Polygon Classification

Table E.1 The classification accuracies of the common bands

	SPOT4		SPOT5		IKONOS		QUICKBIRD XS		QUICKBIRD PS	
	OA(%)	OK(%)	OA	OK	OA	OK	OA	OK	OA	OK
	76,1	**65,7**	**81,4**	**73,3**	**88,6**	**83,7**	**83,7**	**77,0**	**85,8**	**79,9**
Class	*PA(%)*	*UA(%)*	*PA*	*UA*	*PA*	*UA*	*PA*	*UA*	*PA*	*UA*
Rs	*83,4*	*97,5*	*84,6*	*97,5*	*90*	*97,3*	*96,3*	*87,3*	*96,3*	*86,1*
Sb	*78,3*	*48,3*	*81*	*63,8*	*100*	*75,5*	*91,8*	*66,6*	*89,1*	*64,7*
Rc	*72,4*	*63,6*	*72,4*	*67,7*	*79,3*	*85,1*	*58,6*	*30,3*	*58,6*	*29,8*
Cr	*48,8*	*88,8*	*59,9*	*94*	*78,6*	*91,9*	*68,7*	*94,8*	*75,1*	*95,9*
Tm/Pp	*89,1*	*64,4*	*95*	*70,2*	*94,1*	*82,1*	*92,5*	*84,5*	*92,2*	*89,7*

PA: Producer's Accuracy, UA: User's Accuracy, OA: Overall Accuracy, OK: Overall Kappa

Table E.2 The classification accuracies of the (3*3) filtered bands

	SPOT4		SPOT5		IKONOS		QUICKBIRD XS		QUICKBIRD PS	
	OA(%)	OK(%)	OA	OK	OA	OK	OA	OK	OA	OK
	71,8	**59,6**	**80,2**	**71,4**	**87,9**	**82,7**	**83,5**	**76,6**	**85,4**	**79,3**
Class	*PA(%)*	*UA(%)*	*PA*	*UA*	*PA*	*UA*	*PA*	*UA*	*PA*	*UA*
Rs	*73,4*	*96,8*	*82,8*	*97,8*	*88,5*	*97,3*	*96,3*	*87,3*	*96,3*	*86,9*
Sb	*72,9*	*45*	*78,3*	*64,4*	*100*	*74*	*89,1*	*68,7*	*89,1*	*61,1*
Rc	*75,8*	*62,8*	*72,4*	*77,7*	*79,3*	*88,4*	*58,6*	*34,0*	*58,6*	*30,9*
Cr	*46,9*	*87,8*	*56,4*	*93,6*	*79*	*91,5*	*66,1*	*95,8*	*74,5*	*95,5*
Tm/Pp	*88*	*59,5*	*95,8*	*67,8*	*93,3*	*80,8*	*94,7*	*82,2*	*91,7*	*88,7*

Table E.3 The classification accuracies of the (5*5) filtered bands

	SPOT4		SPOT5		IKONOS		QUICKBIRD XS		QUICKBIRD PS	
	OA(%)	OK(%)	OA	OK	OA	OK	OA	OK	OA	OK
	66,6	**51,3**	**78**	**68,2**	**86,9**	**81,3**	**82,5**	**75,0**	**86,2**	**80,5**
Class	*PA(%)*	*UA(%)*	*PA*	*UA*	*PA*	*UA*	*PA*	*UA*	*PA*	*UA*
Rs	68,3	95,3	77,7	97,7	87,6	97,3	96,3	87,3	96,3	87,3
Sb	51,3	44,1	81	63,8	100	72,5	78,3	65,9	91,8	66,6
Rc	72,4	70	72,4	87,5	79,3	88,4	55,1	32,0	58,6	31,4
Cr	32	90,3	55,7	92,4	77,8	90,2	64,4	95,7	74,5	95,9
Tm/Pp	91,4	53,4	94,7	64,7	92,2	79,4	95,0	80,5	93,6	89,2

Table E.4 The classification accuracies of the (7*7) filtered bands

	SPOT4		SPOT5		IKONOS		QUICKBIRD XS		QUICKBIRD PS	
	OA(%)	OK(%)	OA	OK	OA	OK	OA	OK	OA	OK
	62,3	**44,7**	**73,1**	**60,8**	**86,6**	**80,9**	**82,7**	**75,3**	**86,2**	**80,5**
Class	*PA(%)*	*UA(%)*	*PA*	*UA*	*PA*	*UA*	*PA*	*UA*	*PA*	*UA*
Rs	69,2	86,1	73,4	97,2	87	97,6	95,8	87,6	96,3	87,7
Sb	48,6	40,9	78,3	64,4	100	72,5	78,3	69,0	91,8	66,6
Rc	58,6	77,2	65,5	86,3	79,3	88,4	55,1	32,6	58,6	31,4
Cr	23,2	85,9	42,3	91,7	77,8	89,4	65,0	95,7	74,2	95,5
Tm/Pp	86,1	50,4	95,2	59,1	91,9	79	95,3	80,2	93,9	89,2

Table E.5 The classification accuracies of the all bands

	SPOT4		SPOT5		IKONOS		QUICKBIRD XS		QUICKBIRD PS	
	OA	OK	OA	OK	OA	OK	OA	OK	OA	OK
	76,3	**65,6**	**77,9**	**67,8**	**88,9**	**84,1**	**85,0**	**78,7**	**85,5**	**79,5**
Class	*PA*	*UA*	*PA*	*UA*	*PA*	*UA*	*PA*	*UA*	*PA*	*UA*
Rs	*79,8*	*97,4*	*86,1*	*97,2*	*90*	*97,3*	*96,8*	*85,7*	*96,8*	*85,7*
Sb	*72,9*	*81,8*	*75,6*	*82,3*	*100*	*75,5*	*91,8*	*65,3*	*89,1*	*61,1*
Rc	*68,9*	*66,6*	*79,3*	*82,1*	*79,3*	*85,1*	*62,0*	*35,2*	*58,6*	*30,3*
Cr	*47,3*	*88,5*	*41,2*	*94,7*	*79,3*	*92,4*	*71,9*	*95,4*	*75,7*	*95,2*
Tm/Pp	*95,2*	*63*	*97,2*	*63,7*	*94,4*	*82,5*	*92,2*	*86,7*	*90,6*	*90,1*

APPENDIX F

Accuracies of the Pre-Polygon Classification

Table F.1 The classification accuracies of the common bands using mean values

	SPOT4		SPOT5		IKONOS		QUICKBIRD XS		QUICKBIRD PS	
	OA(%)	OK(%)	OA	OK	OA	OK	OA	OK	OA	OK
	65,2	**50,8**	**69,8**	**56,5**	**81,8**	**74,2**	**78,6**	**68,6**	**82,1**	**74**
Class	*PA(%)*	*UA(%)*	*PA*	*UA*	*PA*	*UA*	*PA*	*UA*	*PA*	*UA*
Rs	*56,3*	*96,3*	*72,8*	*97,1*	*84,9*	*97,9*	*93,2*	*89,1*	*94,8*	*90,1*
Sb	*81*	*36,1*	*81*	*56,6*	*97,2*	*69,2*	*43,2*	*64*	*54*	*68,9*
Rc	*13,7*	*100*	*62*	*60*	*65,5*	*82,6*	*27,5*	*53,3*	*34,4*	*27*
Cr	*78,2*	*69*	*45*	*75,1*	*77*	*76,2*	*62,4*	*91,5*	*71,9*	*89,5*
Tm/Pp	*66,4*	*54,1*	*84,4*	*57,3*	*82,2*	*75,5*	*94,1*	*69,7*	*91,7*	*79*

PA: Producer's Accuracy, **UA**: User's Accuracy, **OA**: Overall Accuracy, **OK**: Overall Kappa

Table F.2 The classification accuracies of the (3*3) filtered bands using mean values

	SPOT4		SPOT5		IKONOS		QUICKBIRD XS		QUICKBIRD PS	
	OA(%)	OK(%)	OA	OK	OA	OK	OA	OK	OA	OK
	64,8	**49,9**	**78,6**	**69,4**	**81**	**73**	**78,5**	**68,6**	**79,7**	**71,1**
Class	*PA(%)*	*UA(%)*	*PA*	*UA*	*PA*	*UA*	*PA*	*UA*	*PA*	*UA*
Rs	*57,5*	*95,9*	*79,8*	*97*	*81*	*97,4*	*93,2*	*89,1*	*72,5*	*98,7*
Sb	*78,3*	*32,5*	*83,7*	*70,4*	*97,2*	*70,5*	*45,9*	*60,7*	*62,1*	*74,1*
Rc	*17,2*	*71,4*	*48,2*	*82,3*	*65,5*	*86,3*	*31*	*47,3*	*34,4*	*25,6*
Cr	*62,2*	*74,4*	*78,2*	*72,6*	*77,4*	*77,1*	*62,1*	*91,1*	*79,3*	*74,5*
Tm/Pp	*75,9*	*54*	*79,7*	*71,1*	*83,3*	*73,5*	*93,6*	*70,3*	*91,9*	*77,5*

Table F.3 The classification accuracies of the (5*5) filtered bands using mean values

	SPOT4		SPOT5		IKONOS		QUICKBIRD XS		QUICKBIRD PS	
	OA(%)	OK(%)	OA	OK	OA	OK	OA	OK	OA	OK
	61,7	**44,6**	**71,8**	**59,9**	**83,1**	**75,9**	**79,2**	**69,6**	**80,2**	**71,7**
Class	*PA(%)*	*UA(%)*	*PA*	*UA*	*PA*	*UA*	*PA*	*UA*	*PA*	*UA*
Rs	*59,9*	*95,6*	*70,7*	*97,9*	*84,3*	*97,5*	*92,7*	*89,5*	*72,5*	*98,7*
Sb	*54*	*28,1*	*83,7*	*40,7*	*94,5*	*81,3*	*45,9*	*54,8*	*62,1*	*79,3*
Rc	*34,4*	*76,9*	*27,5*	*72,7*	*68,9*	*86,9*	*34,4*	*50*	*37,9*	*27,5*
Cr	*39,3*	*73*	*64,1*	*74,3*	*77,8*	*78,1*	*64,4*	*92,1*	*79,7*	*74,9*
Tm/Pp	*82,5*	*50,6*	*80,8*	*62,3*	*85,8*	*76,1*	*93*	*71*	*92,7*	*78*

Table F.4 The classification accuracies of the (7*7) filtered bands using mean values

	SPOT4		SPOT5		IKONOS		QUICKBIRD XS		QUICKBIRD PS	
	OA(%)	OK(%)	OA	OK	OA	OK	OA	OK	OA	OK
	59,3	**40,5**	**66,9**	**52,6**	**69,3**	**55,9**	**79,2**	**69,6**	**82,9**	**75,3**
Class	*PA(%)*	*UA(%)*	*PA*	*UA*	*PA*	*UA*	*PA*	*UA*	*PA*	*UA*
Rs	*57,2*	*88,3*	*59,6*	*96,1*	*47,2*	*97,5*	*92,2*	*90,8*	*94,8*	*89,7*
Sb	*40,5*	*29,4*	*75,6*	*41,7*	*81*	*85,7*	*45,9*	*51,5*	*64,8*	*80*
Rc	*20,6*	*66,6*	*34,4*	*71,4*	*79,3*	*58,9*	*34,4*	*40*	*37,9*	*27,5*
Cr	*34,7*	*67,9*	*59,1*	*72,7*	*68,3*	*80,6*	*65,3*	*91,8*	*71,6*	*89,8*
Tm/Pp	*84,2*	*49,6*	*81,1*	*56,2*	*88,3*	*56,5*	*92,5*	*71,7*	*92,8*	*80,5*

Table F.5 The classification accuracies of the unfiltered bands using median values

	SPOT4		SPOT5		IKONOS		QUICKBIRD XS		QUICKBIRD PS	
	OA(%)	OK(%)	OA	OK	OA	OK	OA	OK	OA	OK
	42,9	**21,7**	**45,2**	**24,7**	**80,2**	**71,7**	**69,5**	**53,9**	**85,2**	**78,8**
Class	*PA(%)*	*UA(%)*	*PA*	*UA*	*PA*	*UA*	*PA*	*UA*	*PA*	*UA*
Rs	*9*	*96,7*	*6*	*95,2*	*83,4*	*97,1*	*68,9*	*97*	*95,8*	*88,5*
Sb	*21,6*	*72,7*	*35,1*	*86,6*	*94,5*	*85,3*	*0*	*NaN*	*86,4*	*61,5*
Rc	*34,4*	*24,3*	*31*	*56,2*	*48,2*	*60,8*	*6*	*66,6*	*31*	*28,1*
Cr	*79*	*30,5*	*88,5*	*31,1*	*75,1*	*73,5*	*93,9*	*58,9*	*76*	*92,6*
Tm/Pp	*50,9*	*70,7*	*52*	*83,9*	*81,9*	*73,2*	*58,8*	*77,1*	*92,5*	*85,8*

Table F.6 The classification accuracies of the unfiltered bands using mode values

	SPOT4		SPOT5		IKONOS		QUICKBIRD XS		QUICKBIRD PS	
	OA(%)	OK(%)	OA	OK	OA	OK	OA	OK	OA	OK
	48,2	**28,8**	**81,2**	**73,1**	**81,9**	**74,2**	**80,5**	**71,7**	**69,7**	**53,9**
Class	*PA(%)*	*UA(%)*	*PA*	*UA*	*PA*	*UA*	*PA*	*UA*	*PA*	*UA*
Rs	*14,1*	*95,9*	*77,7*	*98,4*	*89,4*	*96,7*	*96,3*	*88,1*	*63,7*	*97,6*
Sb	*18,9*	*70*	*59,4*	*66,6*	*86,4*	*84,2*	*37,8*	*58,3*	*0*	*NaN*
Rc	*24,1*	*12,9*	*51,7*	*44,1*	*58,6*	*80,9*	*34,4*	*29,4*	*0*	*NaN*
Cr	*81,6*	*34,4*	*77,8*	*86,8*	*77*	*72,6*	*68,7*	*90,4*	*94,5*	*58,9*
Tm/Pp	*60,3*	*75,9*	*91,6*	*72,4*	*80*	*76,6*	*91,4*	*76*	*61,8*	*78,3*

APPENDIX G

Results of the Post-Polygon Classification Using Common Bands

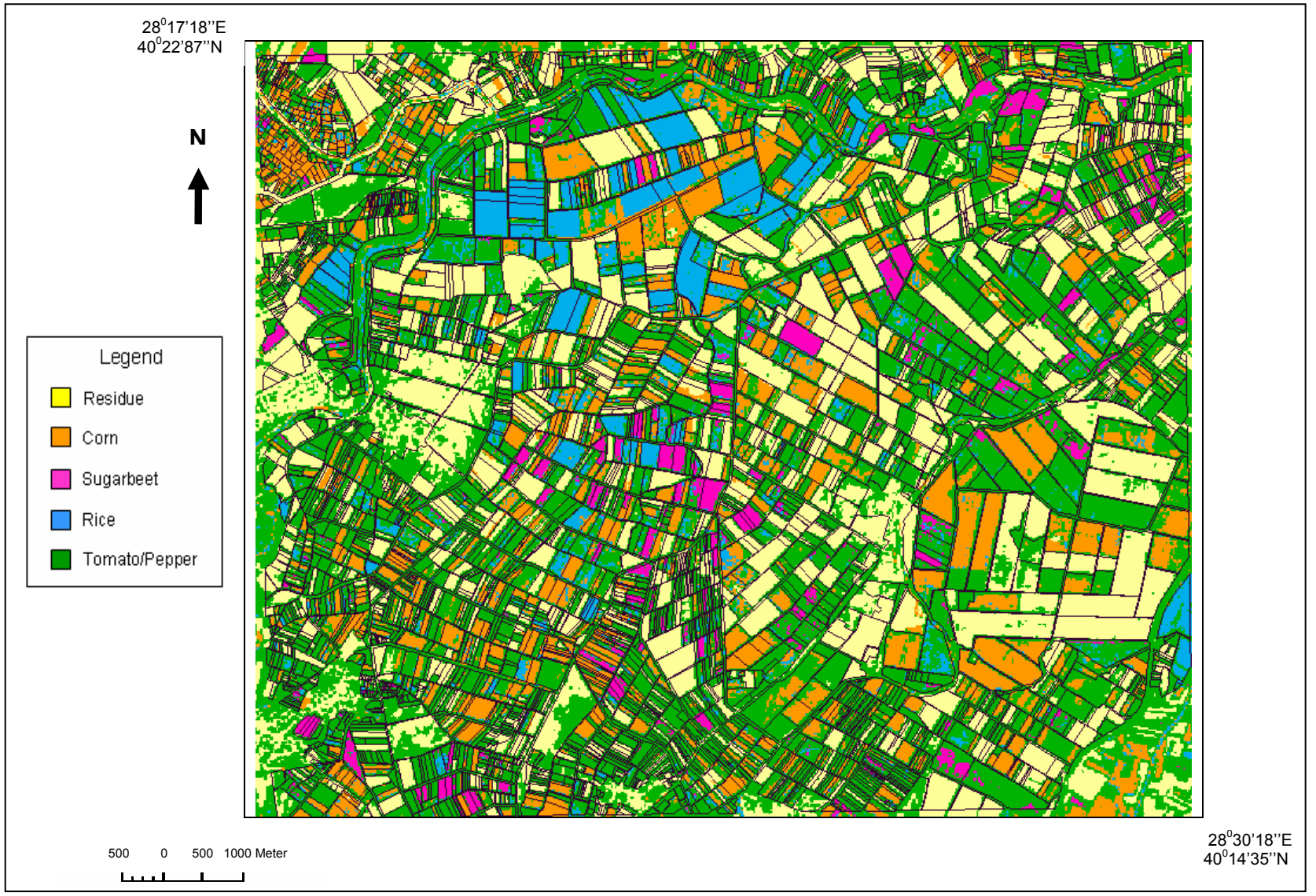

Figure G.1 The output of the post-polygon classification for the SPOT 4 XS image using common bands

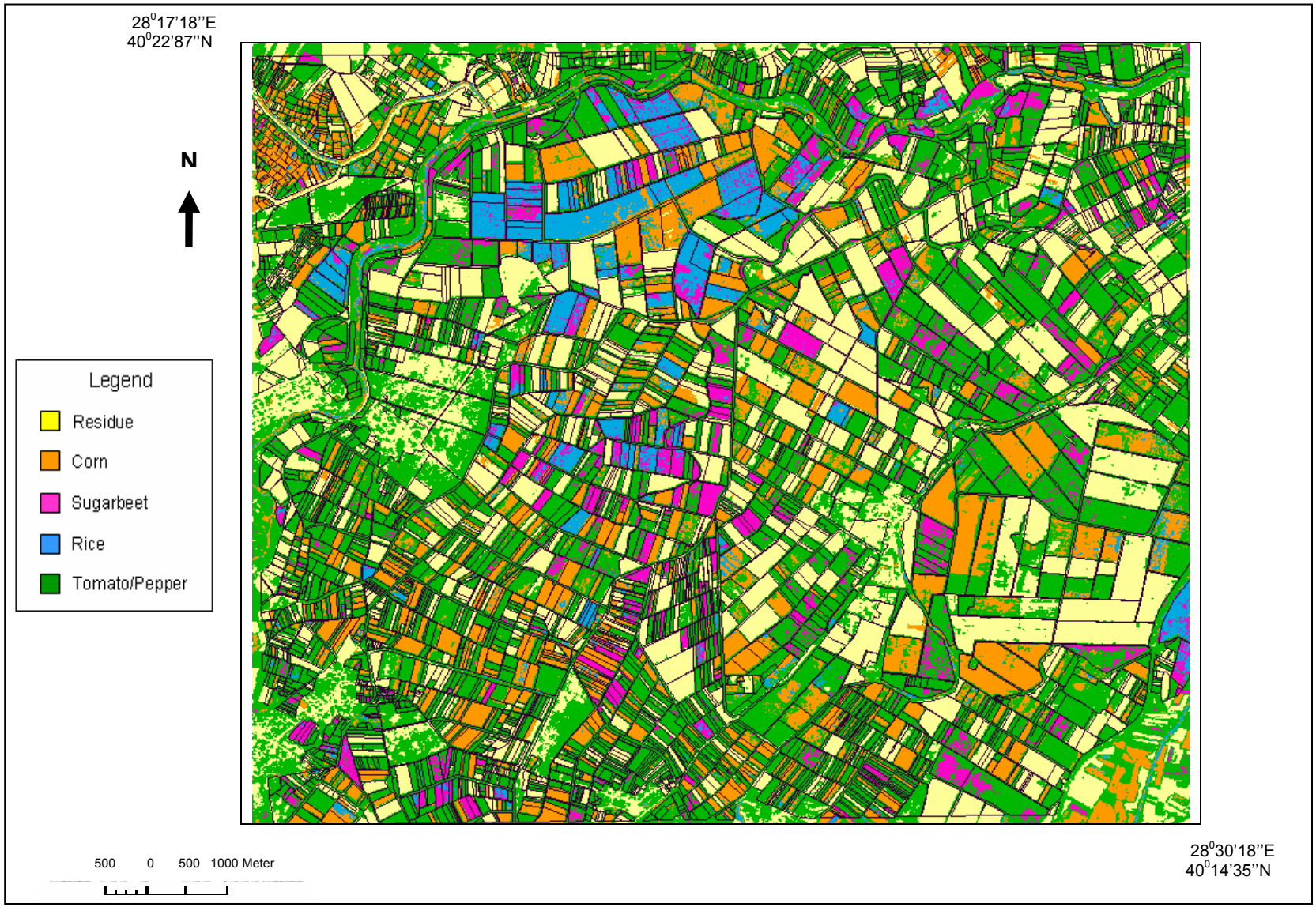

Figure G.2 The output of the post-polygon classification for the SPOT 5 XS image using common bands

Figure G.3 The output of the post-polygon classification for the IKONOS XS image using common bands

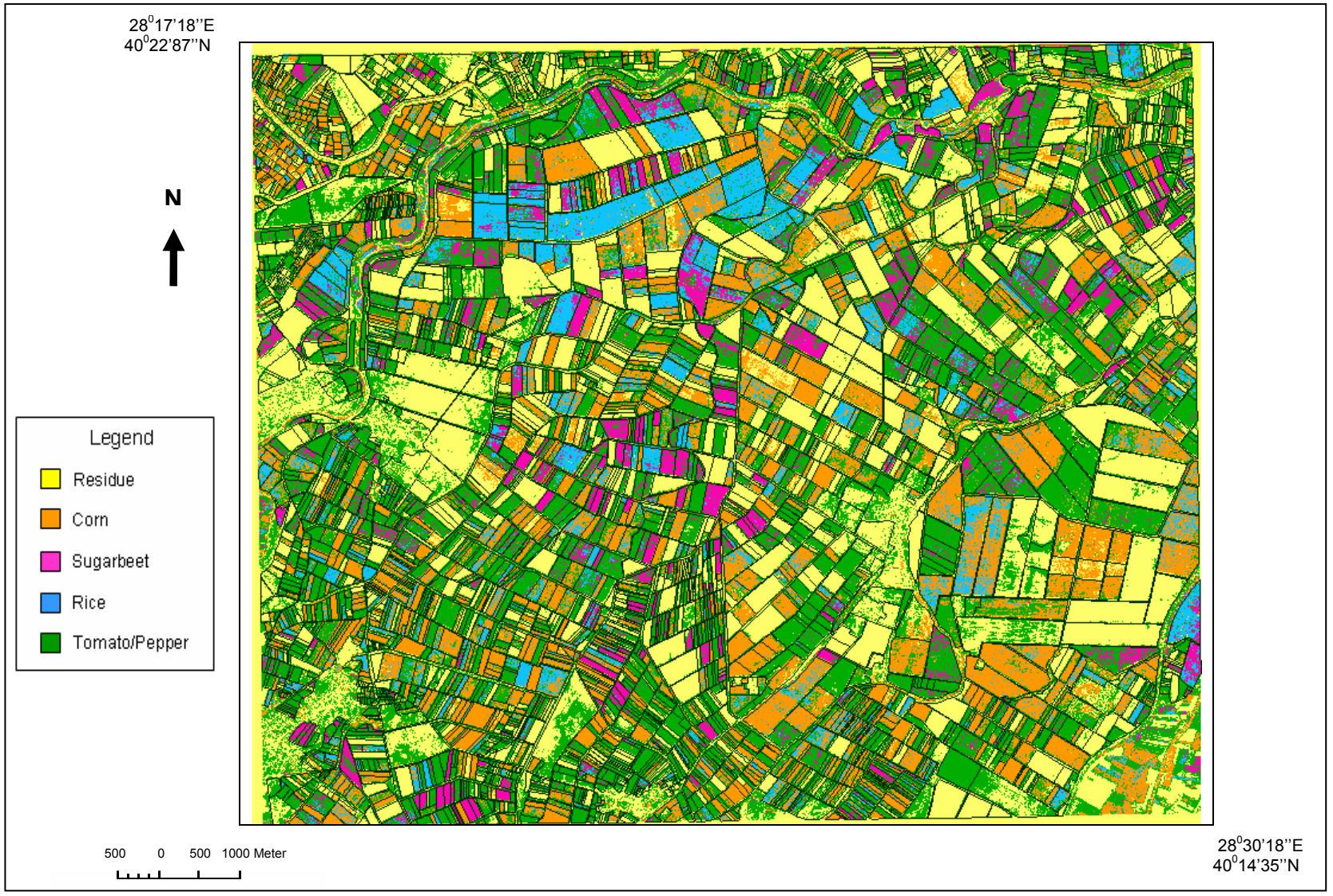

Figure G.4 The output of the post-polygon classification for the QuickBird PS image using common bands

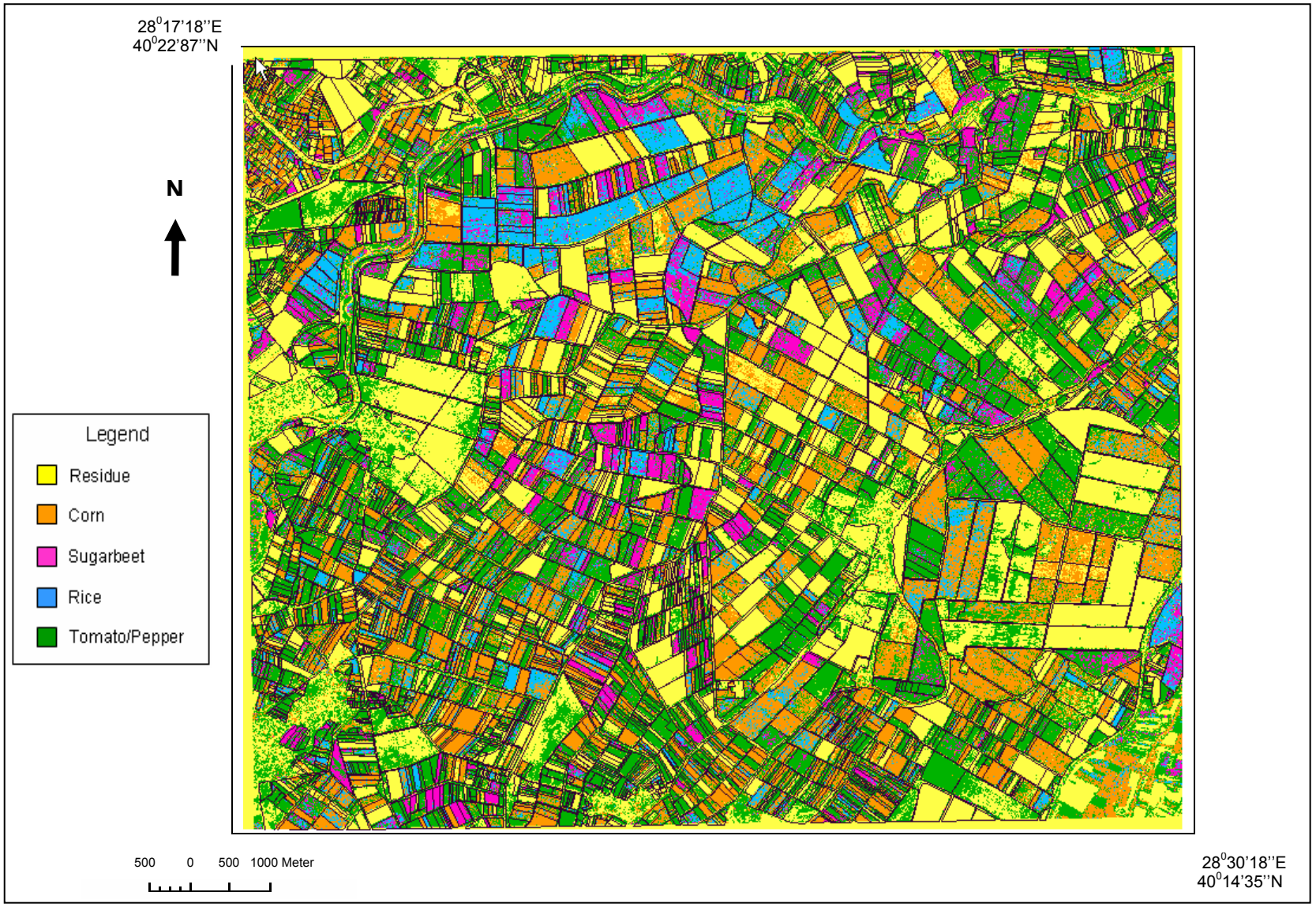

Figure G.5 The output of the post-polygon classification for the QuickBird PS image using common bands

APPENDIX H

Results of the Pre-Polygon Classification Using Common Bands

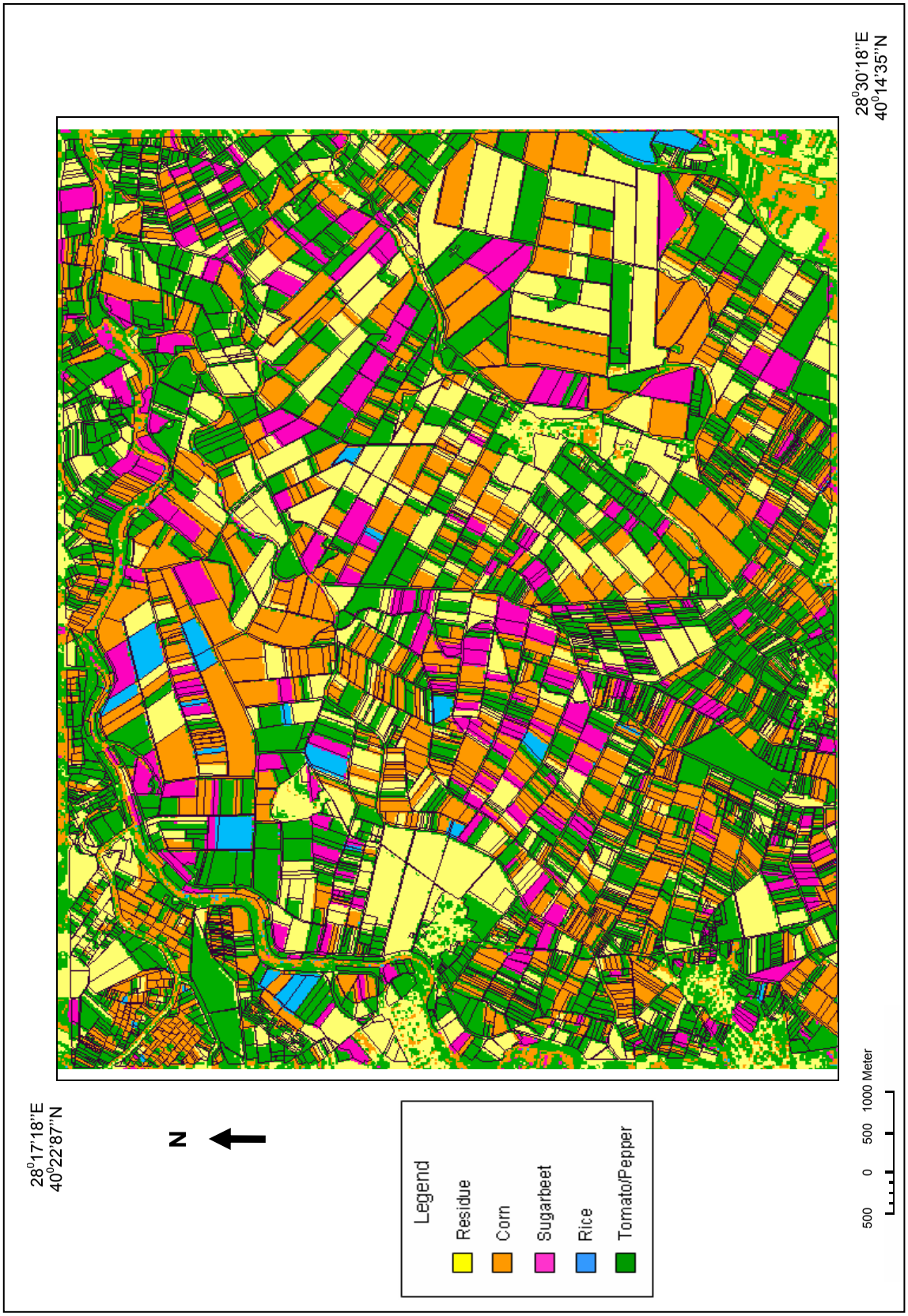

Figure H.1 The output of the pre-polygon classification for the SPOT4 XS image using common bands

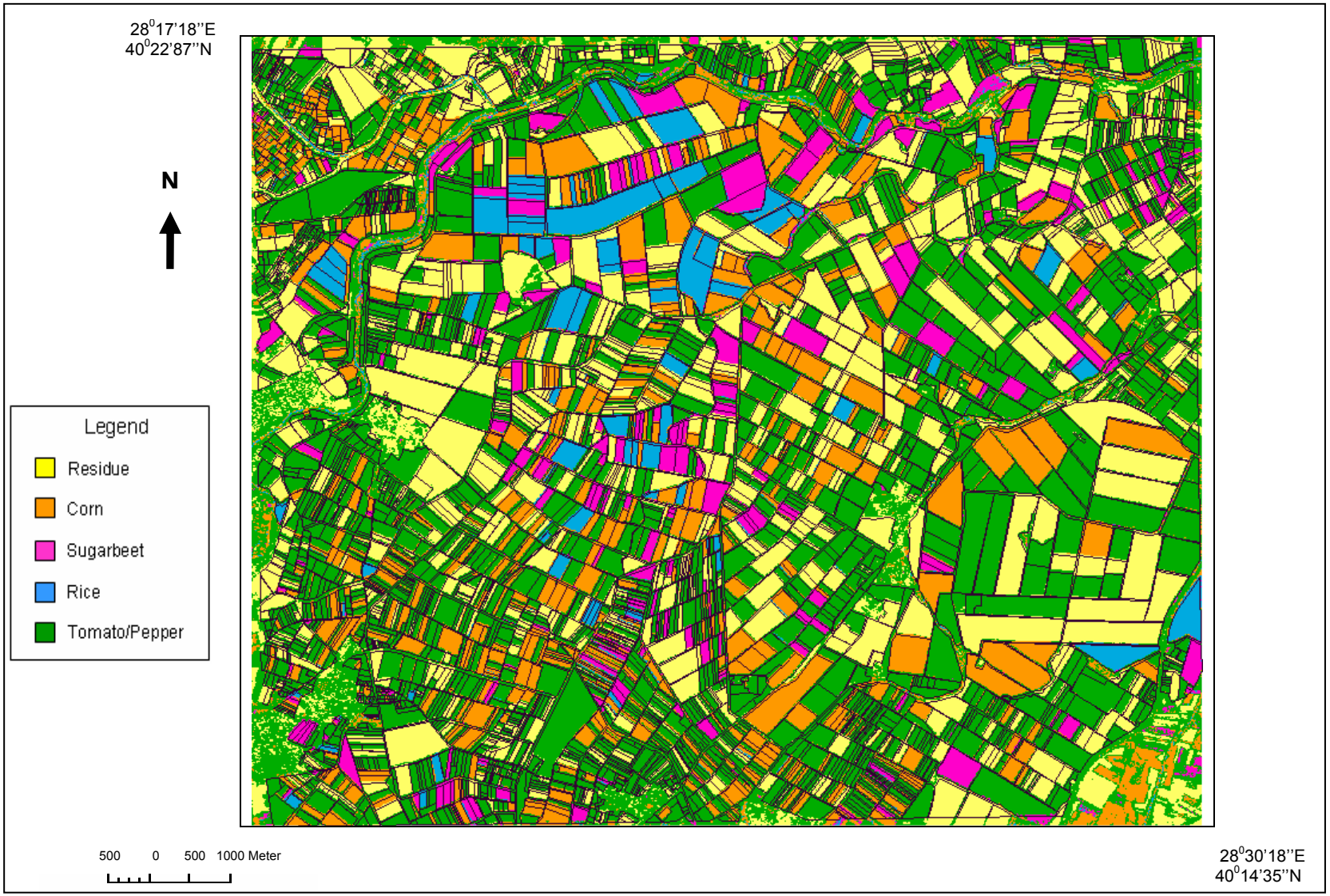

Figure H.2 The output of the pre-polygon classification for the SPOT5 XS image using common bands

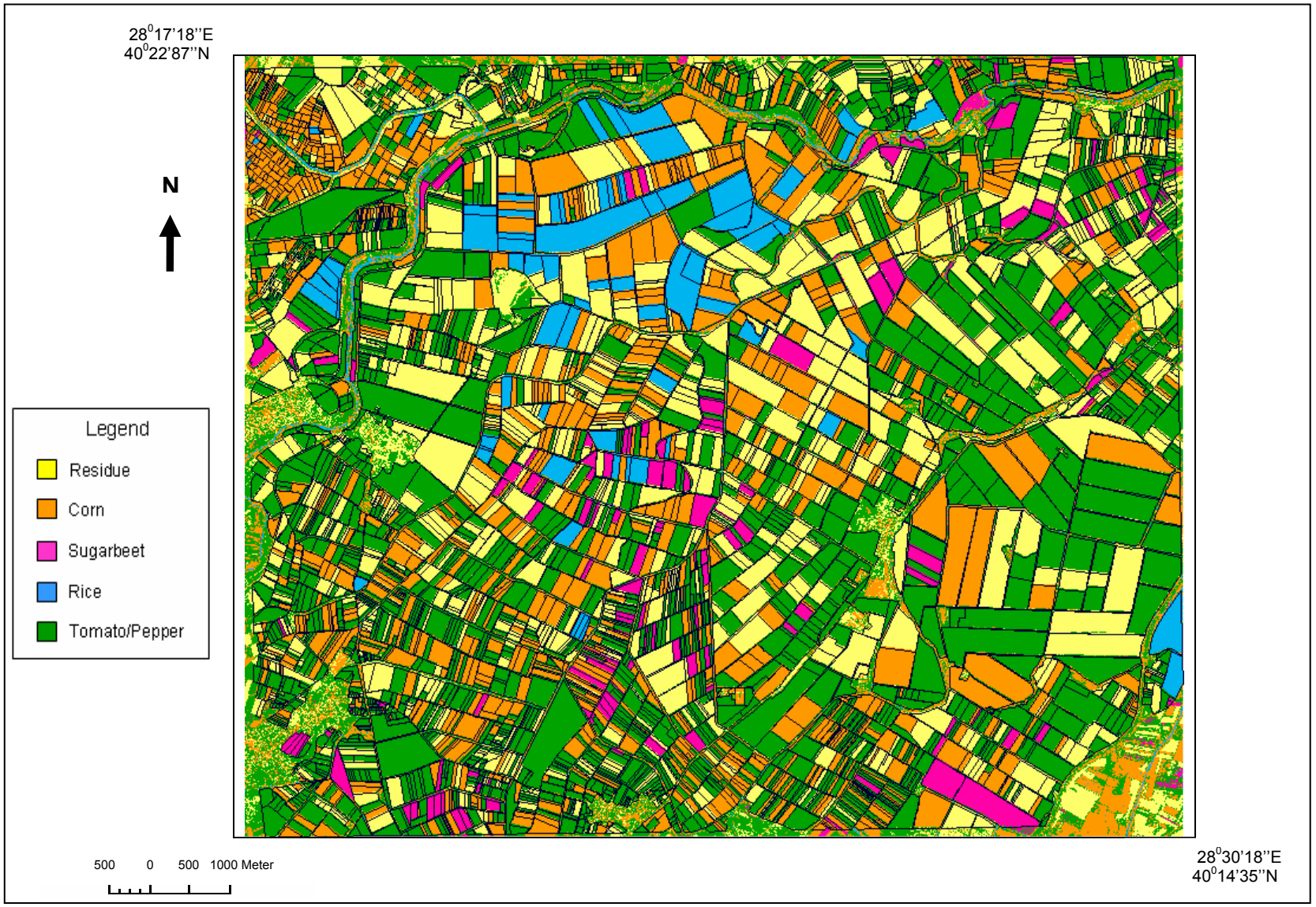

Figure H.3 The output of the pre-polygon classification for the IKONOS XS image using common bands

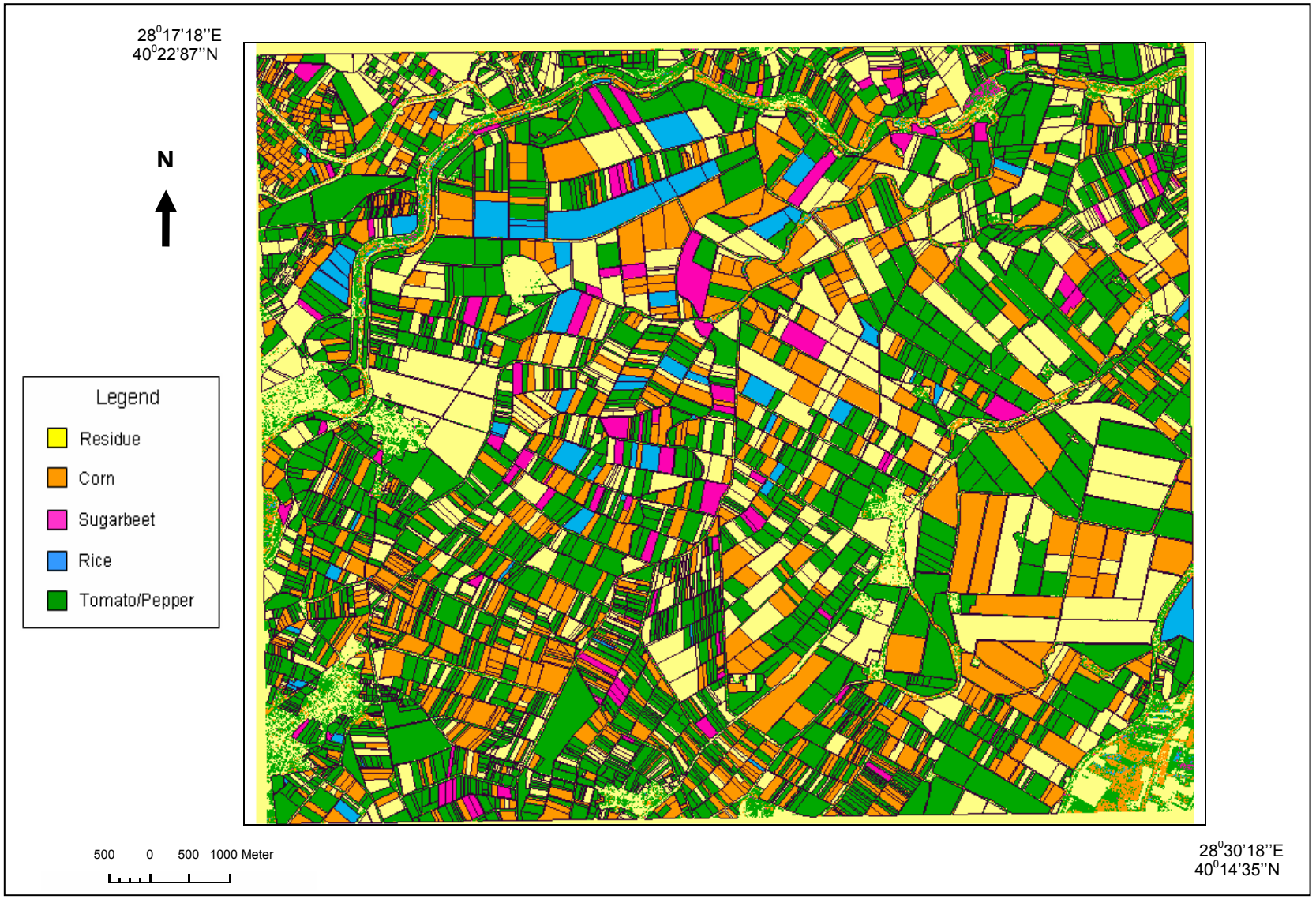

Figure H.4 The output of the pre-polygon classification for the QuickBird XS image using common bands

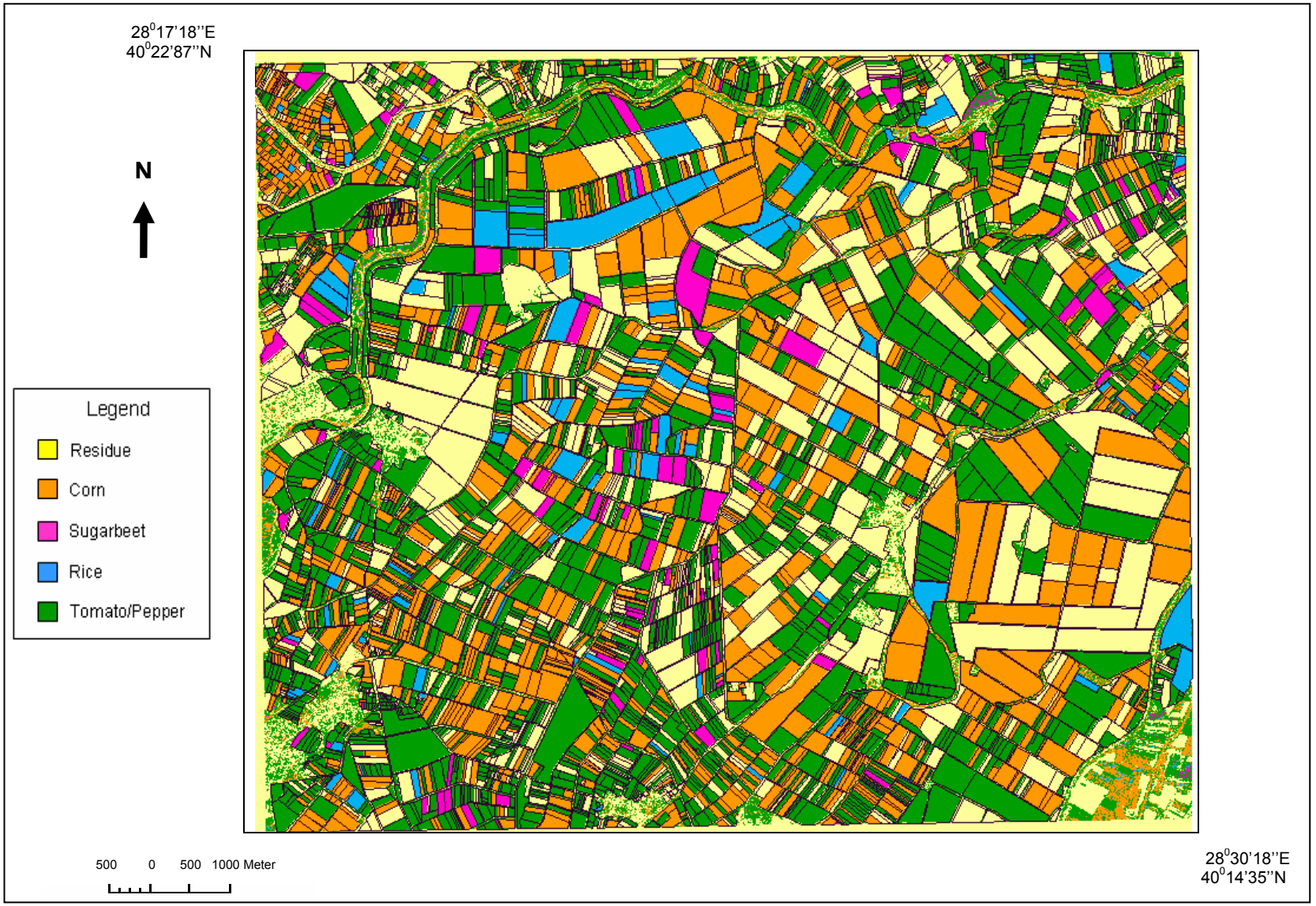

Figure H.5 The output of the pre-polygon classification for the QuickBird PS image using common bands